A Preliminary Study of A Novel and Simple Redox Battery For Load Levelling

By

Ahmed A. Hazza

A thesis submitted for the degree of

MASTER OF PHILOSOPHY

July 2001

Department of Chemistry

University of Southampton

List of contents

UNIVERSITY OF SOUTHAMPTON

ABSTRACT

FACULTY OF SCIENCE

CHEMISTRY

MASTER OF PHILOSOPHY

A Preliminary Study of A Novel and Simple Redox Battery For Load Levelling

by Ahmed A Hazza

The electrochemical deposition of lead and lead dioxide from solutions of Pb(II) and methanesulfonic acid solution have been studied using cyclic voltammetry, rotating disc electrode and plating techniques together with the SEM. Vitreous carbon and nickel have been used as base materials for the deposition of lead. The latter was found to be more suitable in all conditions. Thick, compact and smooth deposits have been obtained from solution containing 0.4 M Pb(II) in 2 M methanesulfonic acid. Lignin sulfonate has been used in low concentrations as an additive to improve the characteristics of the deposit and good quality deposits can be achieved with current densities as high as 256 mA cm^{-2} and the current efficiency for deposition and dissolution is close to 100 %. Lead dioxide has been plated onto gold and vitreous carbon electrodes from the same solutions. The conditions for deposition must be carefully controlled in order to minimise interference from oxygen evolution and adhesion to the substrate is always a problem. However, it is possible to deposit layers of PbO_2 at high rate with a good current efficiency. The thesis considers how the two electrode processes can be combined to give a novel rechargeable battery..

Acknowledgement

I would like to take this chance to thank my supervisor Prof. D. Pletcher for giving me the opportunity to work within his research group and for his excellent supervision and continuous support. I will never forget his charming inspiration and help during all stages of this project. His generosity of advice, time and social support will never be forgotten. Prof. Pletcher has a unique way of supervising which has directed me towards the modern research. Without his tips, hints and directions I would never grasp the skill and talent to understand modern electrochemistry.

Special thanks to friends in Saudi Arabia for their assistance and concerns. Thanks also due to all individuals in the Southampton Electrochemistry Group for their support and useful chats.

Finally, I wish to express my grateful and appreciation to my beloved mother for her unlimited love and support. Also gratefulness and gratitude are directed to my dearest wife Maha and my sweetheart daughters Etessam, Hajer and Lojain.

To my family, friends and colleagues.

CHAPTER (I)

Introduction

1-1 Batteries; a general overview

A battery can be defined as "a device that can store chemical energy and, on demand, convert it into electric energy to drive an external circuit" [1].

Batteries are accepted as a normal part of modern life throughout the world. Their manufacture and sale is a business with an annual turnover amounting to 10's of billions of pounds and this figure is growing every year [1,2]. Batteries have many applications. Perhaps the most familiar are associated with portable electronics, games and toys, torches, watches, reserve power supplies and as starting batteries in cars. Moreover, new opportunities arise continuously and present R & D is focused on the miniaturisation of portable power sources and batteries to power vehicles and for load levelling.

Each application requires a different size of battery and, indeed, batteries with quite different characteristics and performance. It is therefore not surprising that batteries have been developed based on very different chemistries. In this thesis, the objective was to carry out a fundamental study of the electrode reactions in a possible, new load levelling battery.

1-2 Load levelling and storage

Without the facility to store power, the electricity generation industry faces the need to balance electric power production and consumption at all times of day. This is a difficult problem since the demand for electricity varies greatly over a 24 hour cycle; figure (1) shows the variation of demand in the UK and it can be seen that in early evening, the demand is some 5 times that in the night [3].

On the other hand, the industry is committed to the supply of electricity on demand and hence it must have generating capacity ready to switch on at all times. An alternative and more economic scenario employs the cheaper power stations operating continuously and a facility to store power during periods of low demand and feed the power back to the grid at times of peak demand.

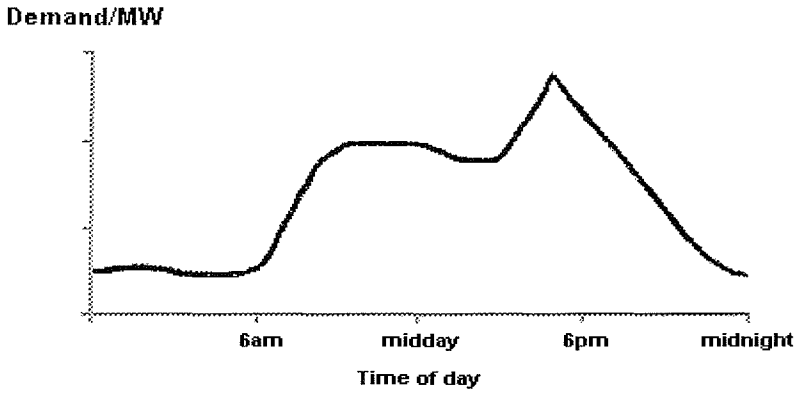

Figure (1) Electricity demand in the UK during the day time [3]

One approach to load levelling is based on pumping water uphill during periods of low demand and hydroelectric power generation to recover the electric power. This is not very efficient and requires sites with appropriate geology. Batteries clearly offer another approach [4].

It is widely recognised that power generation from coal, oil and nuclear sources are all harmful to the environment. In the long term, we must aim to obtain our power from renewable sources and solar, wind and tidal sources are all under investigation. However, the availability of sun and wind do not match the demand for power and hence such renewable energy sources all need to be supported by energy storage for them to be used on any scale.

In both load levelling and power storage associated with the electricity generation industry, the interest is in large batteries. For example, a pilot plant is presently being built at Little Barford in Cambridgeshire and it is equivalent to a 15

MW battery and a commercial facility would be in excess of a 100 MW battery. Clearly, the characteristics and requirements of such a battery will be quite different even from commercial reserve supplies at the present time [3].

1-3 Battery systems for energy storage and load levelling

Present reserve power supplies are Pb/acid or Ni/Cd batteries. These are not considered ideal for load levelling and most recent research programmes for this application has focused on redox batteries [5]. The chemistry of these systems is summarised below.

1-3-1 Lead acid batteries

Reactions taking place at the two electrodes can be envisaged as :

At the positive electrode

$$PbO_2 + 4H^+ + SO_4^{2-} + 2e^- \underset{\text{charge}}{\overset{\text{discharge}}{\rightleftharpoons}} PbSO_4 + 2H_2O$$

At the negative electrode

$$Pb + SO_4^{2-} \underset{\text{charge}}{\overset{\text{discharge}}{\rightleftharpoons}} PbSO_4 + 2e^-$$

The overall cell reaction characterising the battery is

$$PbO_2 + Pb + 4H^+ + 2SO_4^{2-} \underset{\text{charge}}{\overset{\text{discharge}}{\rightleftharpoons}} 2PbSO_4 + 2H_2O$$

Nevertheless, the mechanisms of such reactions are still not fully understood. It should be noted that both the electrode reactions involve the interconversion of two solid phases and such reactions will always be complex. In fact, this is the reason why after more than 150 years of lead-acid batteries development, papers continue to occur [2,6-8].

1-3-2 Nickel-cadmium

The nickel-cadmium battery is another type of widely used system. The following half-cell reactions are involved in the nickel-cadmium battery:

At the positive electrode

$$2\ NiO(OH) + H_2O + 2e^- \underset{\text{charge}}{\overset{\text{discharge}}{\rightleftharpoons}} Ni(OH)_2 + OH^-$$

At the negative electrode

$$Cd + 2OH^- - 2e^- \underset{\text{charge}}{\overset{\text{discharge}}{\rightleftharpoons}} Cd(OH)_2$$

The overall cell reaction which takes place in aqueous KOH solution is

$$2\ NiO(OH) + Cd + 2H_2O \underset{\text{charge}}{\overset{\text{discharge}}{\rightleftharpoons}} 2Ni(OH)_2 + Cd(OH)_2$$

Nickel-cadmium batteries have the advantage of high cycle and long shelf life compared to lead-acid batteries, but they have lower power densities and are more expensive [1].

1-3-3 Redox flow cell batteries

Another important type of power storage system is the redox flow cell battery. In a redox cell, the dissolved species change their oxidation state at the electrodes. The unit of this kind of cells consists of two half-cells, positive and negative separated by a suitable membrane. Inert electrodes are provided in order to transfer the electrical charge to and from the system. Electrolytes are pumped continuously through the cell passing the electrodes and finally into separate storage tanks [4,5].

Unlike the conventional battery systems where solid state electrode reactions are employed, redox flow cells, a term coined from the reduction and oxidation

circulated electrolytes, store the energy in the two-half cell electrolytes. In some cases one of the active materials in the fully charged state is stored externally into the circulated electrolyte, while the other active material produced from the charging process is stored on the stack as a solid material. Zinc-Chlorine, Zinc-Bromine, Iron-Ferric/Ferrous, and Quinone batteries are examples of such systems. Vanadium-Vanadium, Iron-Chromium and Polysulphide/ Bromine systems on the other hand, store the energy from both electrodes in the electrolytes without the need to deposit any solid materials on the stacks. Figure (2) shows an outline design of the flow cell [9,10].

Some of the advantages of these systems are the ability of recharge instantaneously by replacing the discharged electrolytes which are stored in the separated tanks, the flexibility of the capacity by changing the volume of solution and, most importantly the absence of any solid active materials which usually cause the failure in other batteries [5,11,12].

Current collectors are usually made of inert materials like carbons. Graphite, glassy carbon, reticulated vitreous carbon (RVC) and polypropylene filled with carbon black (RPP; 25 carbon black- 75 polypropylene composite) have been used widely in batteries [5,13,14]. The advantage of carbon electrodes is based on their low prices, long life services, their mechanical strength and their high resistance to most corrosive media.

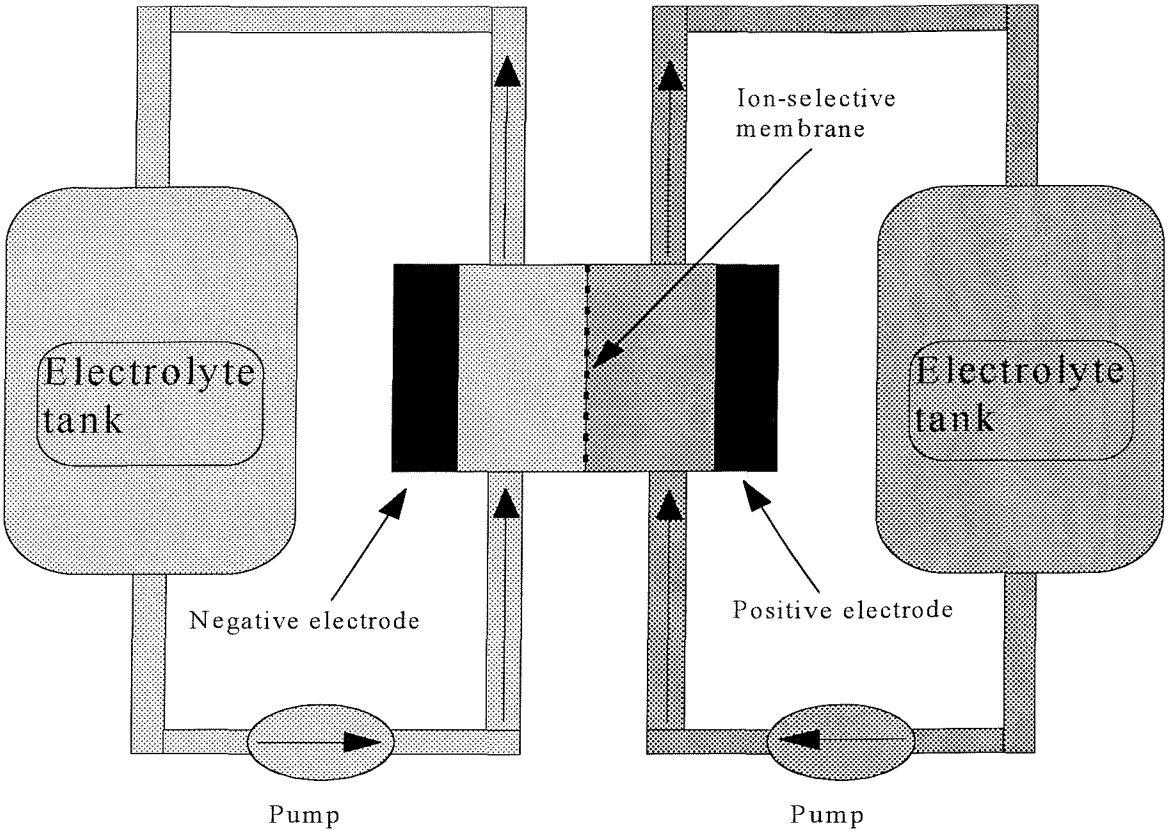

Figure (2) Outline design of flow cell battery

1-3-4 National Power storage system

A new system called "Regenesys[R]" has been developed by National Power plc. as a load levelling battery in power plants. Regenesys[R] is redox flow cell battery using concentrated solutions of sodium bromide and sodium polysulphide as soluble electrolytes [3].

During the charge process, the bromide is oxidised to bromine at the positive electrode and immediately complexed as tribromide to avoid the toxic and hazardous material, free bromine. At the same time sulphur, which is dissolved as the polysulphide anion in the negative electrolyte, is converted at the negative electrode into sulphide. Both products are readily soluble and separated by an ion-selective membrane that can allow sodium to pass in order to maintain charge balance. The two electrolytes are stored in separate tanks. The half-cell reactions taking place in the battery are usually written:

At the positive electrode

$$3\,NaBr \;-\; 2e^- \underset{\text{discharge}}{\overset{\text{charge}}{\rightleftharpoons}} NaBr_3 \;+\; 2Na^+$$

At the negative electrode

$$2Na^+ \;+\; Na_2S_4 \;+\; 2e^- \underset{\text{discharge}}{\overset{\text{charge}}{\rightleftharpoons}} 2Na_2S_2$$

The total reaction in the cell is

$$3NaBr \;+\; Na_2S_4 \underset{\text{discharge}}{\overset{\text{charge}}{\rightleftharpoons}} 2Na_2S_2 \;+\; NaBr_3$$

In order to collect the electricity back from the cell, discharge is allowed to occur by allowing the contents of the two tanks to react at both electrodes in the same cell. This can be done by reducing the tribromide into bromide at the positive electrode and at the same time the sulphide ion is oxidised at the negative electrode into sulphur which is readily dissolved in the polysulphide.

Apparently each tank contains a mixture of the charged and discharged species that flows continuously through the cell during charge/discharge processes while a small portion of the material in the solution is converted electrochemically whenever the electrolytes pass through the cell. In this particular cell there is no need for any other complexing agents and hence the electrochemistry of this system is straightforward. Materials for electrodes are available and can be chosen from wide variety of cheap materials such as carbon, stainless steel, nickel, titanium and steel.

As with most electrochemical systems, Regenesys^R has its own problems. The internal current is carried by sodium ions that pass through the ion selective membrane. At the same time, traces of anions like sulphide pass through the membrane in the reverse direction. Then reaction between sulphide and bromine takes place causing self-discharge and hence, lowering the efficiency of the system. The loss is small

(0.1%), however after many cycles an imbalance of the charged species is observed which causes a defect in the system. Solving this problem requires an electrochemical unit to balance and reset the system. Clearly any auxiliary equipment added to the system means more complexity and hence expense [3].

In general, flow cell batteries are promising as both car and load levelling batteries. However, they are still expensive and considered complex systems as compared to conventional battery systems. Widespread applications of flow cells will depend upon the cost of auxiliaries, maintenance, energy efficiency and life of the battery which determined by the durability of its components (electrodes and membrane) [5,9].

Development is in progress in many countries, including the UK, to improve the energy efficiency and to improve the existing load levelling batteries and even to discover new simple reactions that can be applied in a battery system which requires no expensive materials [5].

1-4 The proposed battery

1-4-1 General development

Ever since it has been invented, lead acid battery has received a great deal of effort in order to fulfil the increasing demands for power storage. Development has included all aspects of the battery such as electrode design, improved components, paste formulation and additives. The aim has been to develop a battery that can operate under severe conditions and remains fully charged for long periods. Furthermore, plenty of work have been carried out to overcome the problems usually associated with lead-acid batteries such as self discharge caused by the contact of the two electrodes materials, cracks in the lead sulfate layers and limited performance at certain temperature ranges [6].

1-4-2 A new and novel development for the lead-acid battery

1-4-2-1 Overview

In the ordinary lead-acid batteries the product of the charging process is lead sulfate. Solubility of this material in sulphuric acid is very low therefore the charge/ discharge processes involve the interconversion of solid materials at both electrodes. Some attempts to use dissolved negative electrodes such as zinc and cadmium have been published but the findings were not totally successful in sulphuric acid solutions [15]. N.E. Bagshaw [16] used a lead-acid system in perchloric acid as a primary reserve cell for military applications. This cell was to be used only for "one shot" application as it was designed to be destroyed at the target. According to Bagshaw, cells with soluble discharge products are well known. Nitric, fluoroboric, flourosilicic and perchloric were the available acids at that time, where Pb(II) would be soluble. All have disadvantages in a lead acid battery. Some are hazardous and nitrate could be reduced at the negative electrode.

Methanesulfonic acid and its derivatives, on the other hand were not commercially available till mid 70s because of the difficulties of large scale manufacture of such acids [17]. Moreover, the cost of methanesulfonic acid is declining since it is in a great demand from many industries such as electronics, oil recovery, organic syntheses and the plating industries. A reason for its expanding use is that it is benign in the environment compared with other acids. In addition, many metal ions are highly soluble in methanesulfonic acid.

1-4-2-2 Methanesulfonic acid (MSA)

Methanesulfonic acid is a strong, non-oxidising acid. It is strong electrolyte and stable under 498 K. It has industrial applications. In the field of electroplating, it has been used since the 1940s [17-19].

Although it was more expensive than fluoroboric acid, methanesulfonic acid has easily replaced it in plating industries for many reasons. It improves the throwing power, gives higher quality deposits, is less corrosive, gives uniform alloy composition over a wide current densities and is simpler in waste treatment. Those characteristics offset the higher cost of the acid and made it the successor of fluoroboric and fluorosilicic acids in electronic and plating industries. Another important feature of methanesulfonic acid and its derivatives is that they are not toxic and hence, will not cause any detrimental effects on the environment. Moreover, the acid can be recovered from the waste by a diffusion dialysis process, which is an efficient, relatively cheap and easy process [20,21].

1-4-2-3 Description of the new battery system

The basic concept of the envisaged battery is that lead methanesulfonate is very soluble in water [17]. Hence the product of the discharge process is a soluble salt which can be deposited again on the electrodes during charge as shown in the reactions:

At the positive electrode

$$PbO_2 + 4H^+ + 2e^- \underset{\text{charge}}{\overset{\text{discharge}}{\rightleftharpoons}} Pb^{2+} + 2H_2O$$

At the negative electrode

$$Pb \underset{\text{charge}}{\overset{\text{discharge}}{\rightleftharpoons}} Pb^{2+} + 2e^-$$

The overall cell reaction characterising the battery is

$$PbO_2 + Pb + 4H^+ \underset{\text{charge}}{\overset{\text{discharge}}{\rightleftharpoons}} 2Pb^{2+} + 2H_2O$$

In this envisaged battery, methanesulfonic acid is used as an electrolyte. The solution is stored in one tank and there is no need for any separator since the solution has the same contents in both halves of the cell. Two electrodes are immersed in the

solution as electron transfer surfaces and as current collectors that hold lead and lead dioxide deposits resulting from the charge process. Materials are chosen to be stable in acid solutions and mechanically strong to hold the heavy deposits. Some additives might be necessary to modify the deposit morphology, prevent dendrite deposits on both electrodes and to improve the deposits properties.

1-4-2-4 Comparison between the envisaged and the traditional lead-acid batteries.

As can be seen in the traditional lead-acid battery reactions, the products are solid in both charge and discharge processes. The solid lead sulfate, is the main cause of the failure in this kind of batteries whereas in the envisaged battery there is no insoluble salt from discharge. It is expected then, that there will be no problems with regards to cracking or loss in the active materials on the electrodes. During the discharge process in the ordinary lead-acid batteries, the volume of the electrodes is increased because of the less dense lead sulfate. The expansion causes loss of active material. To prevent such a problem, it is common to use expensive separators. Clearly there is no need to use such separators in absence of solid lead sulfate and it is expected to save energy that would have been spent otherwise to overcome the separator resistance [6].

1-5 Deposition of conducting materials

In the context of the battery under development, both electrodes involve deposition and dissolution of electron conductive phases. Success required deposition of thick, uniform layers of Pb and PbO_2 and it is important that all electrode reactions are fast, ie. occur without significant overpotential.

1-5-1 General mechanism of electrodeposition

Although it seems to be a simple process, electrocrystallisation is far more complex process involving different steps that can be summarised in the sequence [22]:

1- diffusion of ions in solution to the electrode surface.

2- electron transfer.

3- formation of ad-atoms, by losing some or all the solvation sheath.

4- surface diffusion of ad-atoms.

5- nucleation by clustering of ad-atoms.

6- combining of the ad-atoms at lattice sites.

7- development of crystals and morphology of the surfaces.

8- growth of the small centres in a continuous layers.

9- thickening of the layers. See figure (3).

As can be seen from figure (3), the first step to form the deposit requires the ions to move towards the electrode surface. Mass transfer of ions to the electrode surface can be achieved by means of convection, diffusion and migration. When ad-atoms formed by electron transfer, they diffuse over the surface of the electrode in order to find the most stable position. This will depend on different factors such as crystal defects, inclusions, adsorbed molecules, oxide layers, grain boundary regions and crystallographic orientations. Moreover, the texture and the surface morphology of the deposit are strongly affected by the properties of the ionic solution. Clearly, understanding the process of electrocrystallisation is necessary in order to control the deposition and dissolution process as well as to control the morphology and texture of the deposit [23-27].

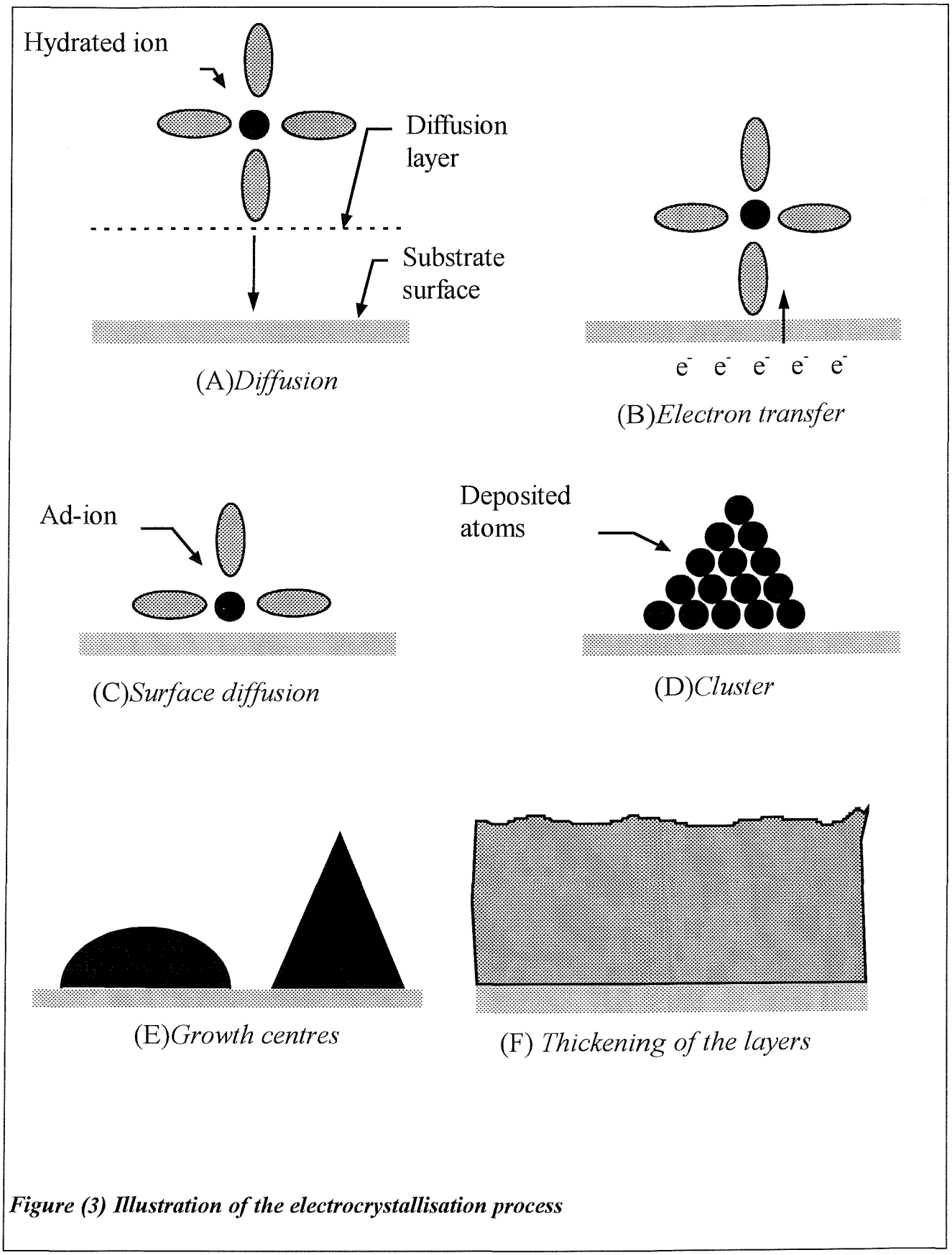

Figure (3) Illustration of the electrocrystallisation process

Figure (4) shows the major components of the electroplating tank. In a commercial electroplating facility, a highly optimised bath composition will be used. This contains the metal to be plated in a soluble form, conducting salt, pH buffer and perhaps some additives.

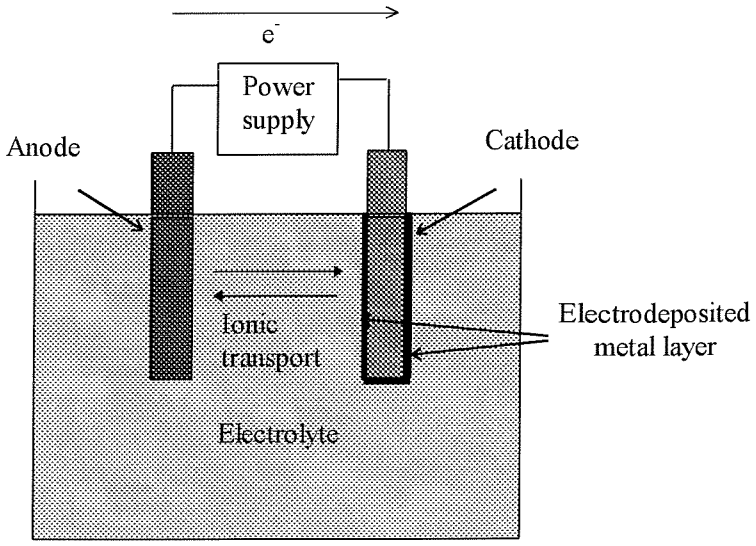

Figure (4) Schematic diagram of an electroplating tank with its components

1-5-2 Equilibrium; Nernst equation

In general, the equilibrium situation for an inert electrode in a solution containing both oxidised and reduced species is discussed in terms of the Nernst equation

$$\mathbf{E = E^{o} + (RT/nF) \ln [(a_{OX})/(a_{RED})]} \qquad \mathbf{eq.\ (1)}$$

where E is the electrode potential at any time, E^{o} is the standard potential for the couple, R is the universal gas constant, T is the absolute temperature, n is the charge number of the electrode reaction (i.e. number of moles of electrons involved in the reaction) and F is the Faraday constant. a_{RED} represents the chemical activities of the species which appear on the reduced side of the electrode reaction and the a_{OX}

represents the chemical activities of the species which appear on the oxidised side of the electrode reaction.

For metal deposition reaction this may be simplified to

$$\mathbf{E = E^{o}_{M^{z+}/M} + (RT/zF) \ln a_{M^{z+}}} \qquad \textbf{eq. (2)}$$

where $E^{o}_{Mz+/M}$ is the standard potential of the couple and z is the charge on the metal cation.

1-5-3 Rate of Deposition

On the other hand, the rate of deposition can be expressed using Faraday's laws of electrolysis as follows. :

$$\mathbf{w = \phi I M t / z F} \qquad \textbf{eq. (3)}$$

where w is the mass of electrodeposited metal, I is the cell current, M is the molar mass of metal, t is the electrodeposition time and ϕ is the cathode current efficiency which in turn depends mainly upon the deposition conditions. Since the metal deposition is performed under constant current density for a certain period of time, the following formula gives the average rate mass deposited per unit area:

$$\mathbf{w / At = \phi j M / n F} \qquad \textbf{eq. (4)}$$

where j is the current density, A is the area of the electrode and t is the time for deposition. Moreover, to calculate the average thickness of the deposit it is useful to use an equation of the form:

$$\mathbf{h = \phi j t M / \rho n F} \qquad \textbf{eq. (5)}$$

where ρ is the density of the deposited metal. The later equation is very useful to estimate the thickness of the deposit provided that there is no competitive reactions such as hydrogen evolution and the deposit is compact and free of dendrites [28].

1-5-4 Kinetics of electron transfer

1-5-4 Kinetics of electron transfer

Sometimes it is necessary to drive electron transfer with an overpotential, η. This can be quantified in terms of the Butler-Volmer equation.

$$j = j_o \left[\exp\left(\alpha_A nF / RT \right) \eta - \exp\left(-\alpha_C nF / RT \right) \eta \right] \qquad \text{eq. (6)}$$

Equation (6) is the well known Butler-Volmer equation which describes the current as a function of overpotential, the displacement from equilibrium. Clearly, the Butler-Volmer equation has two exponential terms. Therefore at high positive overpotential the second term would be very small, hence can be ignored. The current can be described as :

$$\ln j = \ln j_o + \left(\alpha_A nF / RT \right) \eta \qquad \text{eq. (7)}$$

On the other hand, at high negative overpotential the first term can be ignored and the current would be expressed as :

$$\ln -j = \ln j_o - \left(\alpha_C nF / RT \right) \eta \qquad \text{eq. (8)}$$

Equations (7) and (8) are Tafel equations which are used to calculate the exchange current density and transfer coefficient [29].

1-5-5 Nucleation process

Nucleation is a heterogeneous process since it occurs at the boundary between the electrode surface and the solution. It is an essential step in electrocrystallisation which can take place at both the cathode during metal deposition and at the anode during oxide deposition. The process can be represented by the general equation

$$M^{n+} + ne^- = M$$

For a very small spherical nucleus, the Gibbs free energy is composed of two main contributions. First is the contribution of the surface between the sphere and the surrounding liquid. This interfacial free energy (ΔG_{inter})can take a form of :

$$\Delta G_{inter} = 4 \pi r^2 \gamma_{SL} \qquad \text{eq. (9)}$$

where r is radius of the sphere and γ_{SL} is the average value of the free energy over all directions which depends on the exact shape of the nucleus.

The second contribution of the free energy comes from the volume of the spherical nucleus. Again the free energy ($\Delta G_{vol.}$)can be described as:

$$\Delta G_{vol.} = -n F \rho \eta / M \qquad \text{eq. (10)}$$

where η is the overpotential, M is the molecular weight and ρ is the density of the deposit.

Hence, the total free energy for the spherical nucleus is given by :

$$\Delta G_{total} = \Delta G_{inter.} + \Delta G_{vol.} \qquad \text{eq. (11)}$$

Therefore the total free energy change associated with the formation of a spherical nucleus on an electrode surface is given by

$$\Delta G_{total} = [4 \pi r^3 \rho n F \eta / 3M] + 4 \pi r^2 \gamma \qquad \text{eq. (12)}$$

where γ is the molar surface free energy (surface tension).

The two contributions are shown in figure(5). It is clear that the free energy has a maximum value which corresponds to a critical radius r*. Spherical nuclei having radii of less than r* tend to re-dissolve in the solution, whereas those with radii greater than r* rapidly grow to form a solid phase on the substrate. Further deposition will result in a continuous growth of the solid as can be seen in figure (5) [22].

The nucleation process is particularly favourable at some active sites on the surface where the free energy of deposition is at its minimum value. For most solid materials the surface is inhomogeneous and active sites exist where the volume of the deposited metal cluster can overcome its surface area. The number of nuclei formed can be given by equation of the form

$$N = N_O [1 - \exp(-k_N t)] \qquad \text{eq. (13)}$$

where N_O is the total number of active sites and k_N is the rate constant of nuclei formation. Two cases are expected

1) when $k_N t \gg 1$, then $N = N_O$ which means that the creation of growth sites is very fast and nucleation is instantaneous.

2) when $k_N t << 1$, then $N = k_N (N_O t)$ which means that the number of growing nuclei is smaller than the active sites hence, nucleation is in progressive.

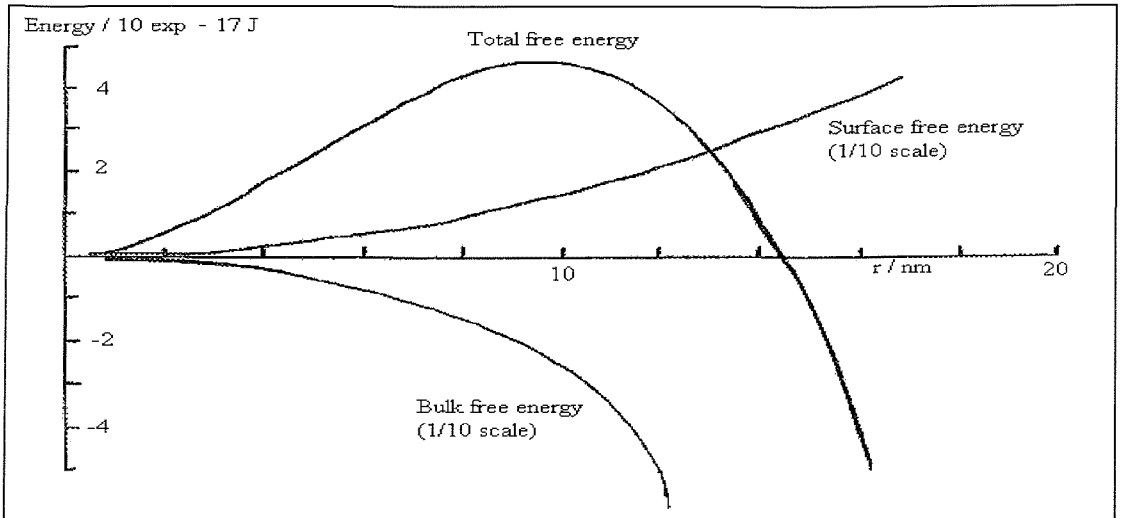

Figure 5 The surface and volume contributions to the free energy as well as the overall free energy of a spherical nucleus as a function of its radius [22].

1-5-6 Growth of individual nuclei

After the electron transfer from the substrate surface to the hydrated ion an ad-ion or ad-atom is formed as can be seen in figure (3). The ad-atom at this stage can be envisaged in an intermediate state where two processes are possible; deposition and dissolution. As discussed above, the total free energy of the newly formed phase has contributions from the surface and the volume of the new solid phase. While it is in equilibrium state, the ad-atom is moving freely on top of the substrate surface which usually has defects such as steps, holes or kinks. Such defects are useful for deposition process since they have a lower free energy for inclusion of the ad-atom see figure (6) below. When the ad-atom finds the stable site it loses the water molecules and enters the crystal lattice [23, 24, 26].

Commonly, nucleation and growth of an electrodeposit is studied using a potential step technique where current is recorded as a function of time. Early in the

response, the current increases with time because (a) the number of nuclei increases with time and / or (b) the surface area of each nuclei increases with time. The exact form of the transient depends on the precise nature of the process.

- two or three dimensional growth of nuclei.
- whether nucleation is progressive or instantaneous
- the rate determining step in growth, i.e. electron transfer or mass transport control.

As a result, I vs. t^n responses can be observed where n= 0.5, 1, 1.5, 2 or 3.0. Moreover, such simple reactions are only observed while the undivided nuclei grow independently (early in the transient).

Eventually, the nuclei overlap and coalesce and thereafter the deposition will thicken under electron transfer or mass transport control and generally a constant current will be observed during this stage in the process.

Different factors affect the choice of the most favourable bath for an electrodeposition process. Among such factors are current density, overpotential, adsorbed species, pH and concentrations of the components. In general, any parameter that causes an increase of the nucleation sites would be in favour of two-dimensional mode and vice versa. However care should be taken while doing such theoretical analysis. In practice, it is not easy to distinguish the power of t in the I-t^n relationship because of competing processes and experimental problems. Hence, techniques such as SEM, should be used to confirm the conclusions [30-32].

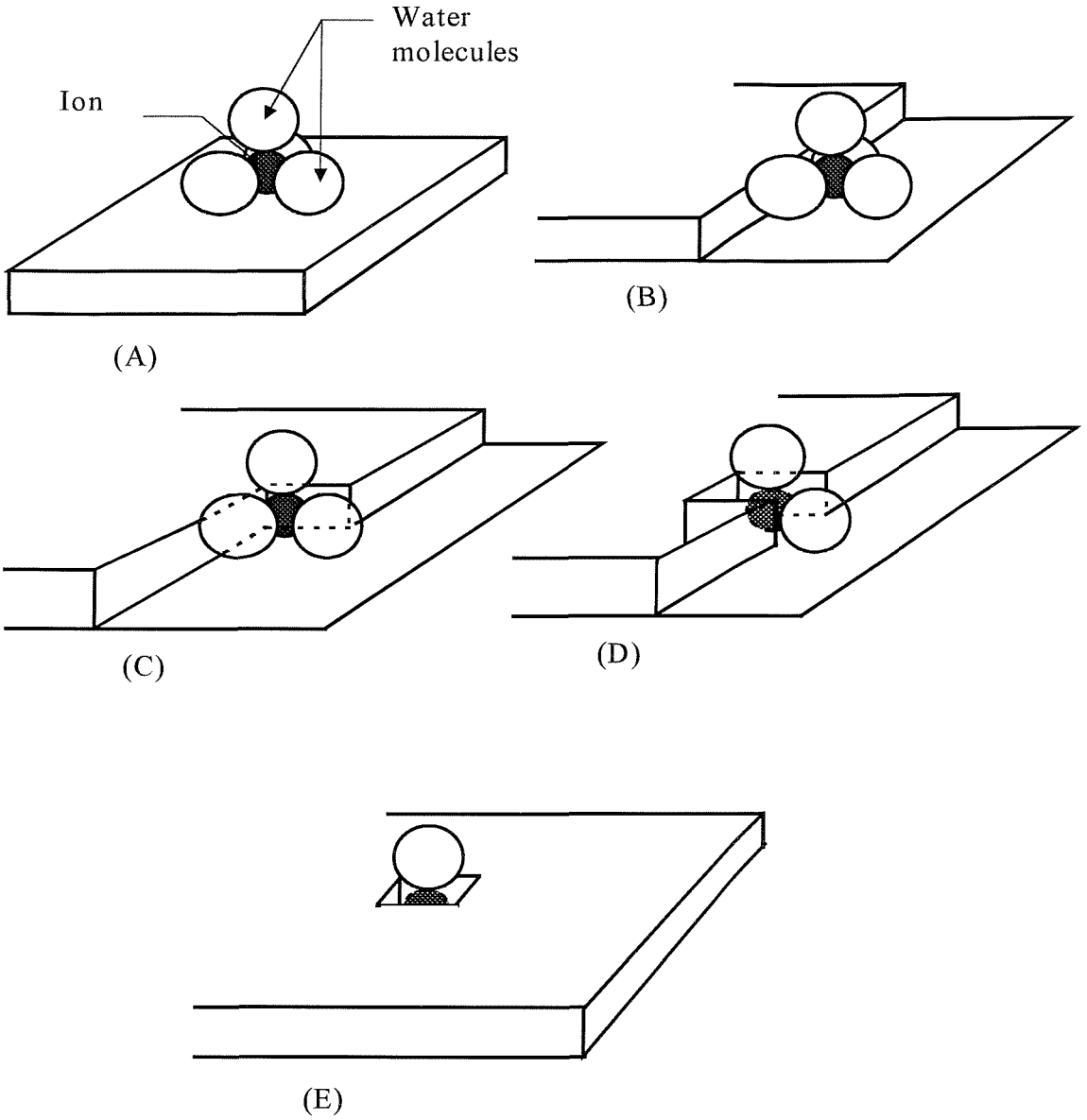

Figure (6) Possible sites for hydrated metal on the substrate surface. (A) perfect surface, (B) step , (C) kink, (D) vacancy, (E) hole [26].

Thickening of the plated film is subject to different factors. Most importantly, it is effected by the rate of deposition or more particularly the relative rates of electron transfer and mass transport, see figure (7) [27,33].

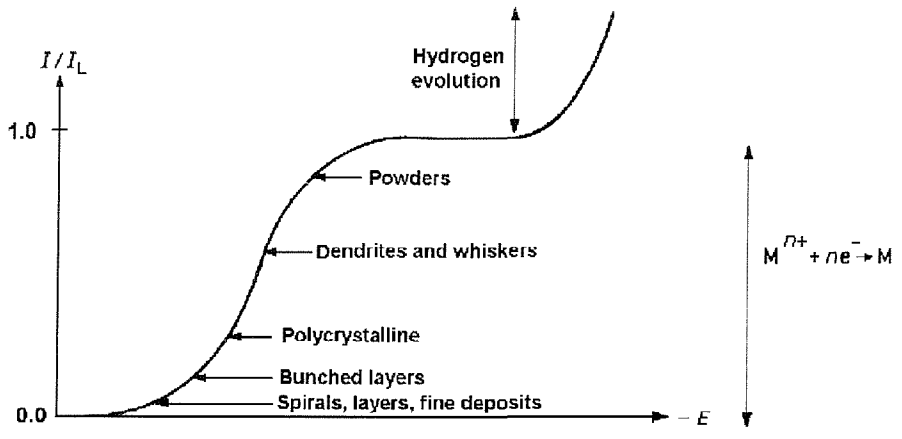

Figure (7) Dependence of growth modes on current density [1]

It has also been found that the texture of the deposited metal is affected by the epitaxy of the substrate material. This effect disappears after a certain thickness of the deposit that depends on both the substrate and the deposited metal [27].

1-5-7 Quality of the deposit

In most applications including batteries, the deposit must be uniform, smooth, coherent and adhere to the surface. In order to obtain such a deposit, it is generally necessary that $I < I_L$ but all plating parameters influence the deposit quality. Additives have an important role and normally the optimum conditions are developed empirically [31,32].

1-5-8 Adhesion

Adhesion can be defined as " *the attraction between substances which, when they are brought into contact, makes it necessary to do work to separate them*" [35]. Many theories have been suggested to explain the adhesion phenomena. However, it is universally agreed that mechanical factors such as substrate surface irregularities aid adhesion. Figure (8) shows a schematic diagram of the surface microstructure. The

roughness of the surface support the adhesion of the deposited metal when the particles accumulate inside the holes that existed in the surface, provided that the substrate metal is hard enough.

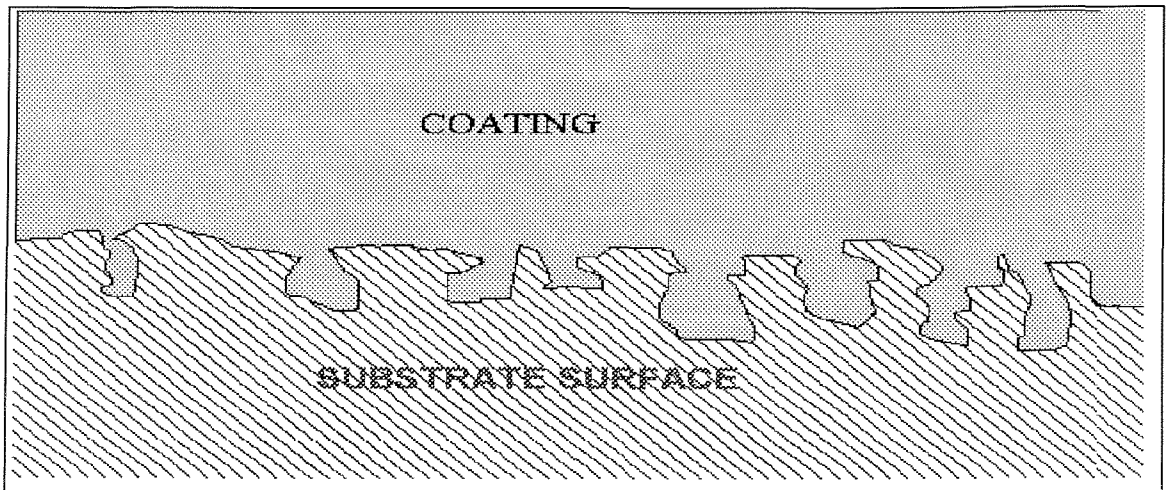

Figure (8) A sketch of the substrate surface in an atomic scale. The caves inside the surface of the substrate helps to improve the adhesion between the deposited metal and the substrate.

Clearly the roughness of the substrate is very important factor in adhesion between the deposited metal and the substrate material. However it is not only the roughness that influence and control the adhesion since there are other factors such as the cleanness of the substrate surface, compatibility of the two materials and the deposition conditions [34-36].

1-6 Negative electrode

1-6-1 Lead deposition

Lead electrodeposition has limited applications in electroplating and finishing industries because of its dull appearance, softness, malleability and toxicity. Moreover, because of its low melting point, 600 K, a hot-dip process can be more attractive for providing lead coatings for corrosion protection and mechanical lubrication. Lead electrodeposition is applied in the mining industries. Two processes are applied therein; electrowinning and electrorefining. The former is a process where lead is extracted

from its ores by electrolysis (Betts process) whereas the latter is a process for purifying lead, or any metal in general, by selective anodic dissolution and electrodeposition. On the other hand, it has been found that lead plated parts are superior to dipped coatings because the deposit is more compact, less porous and has less stress [37,38].

It is possible to deposit lead and its alloys from acidic, alkaline and neutral solutions, however fluoroborate and fluorosilicate are the most widely used solutions for lead deposition in industry. Other solutions, for instance perchlorate, pyrophosphate, acetate and alkaline electrolytes, are less common and probably not used in the plating industry. The morphology, coherence, adherence, and mechanical properties of the deposit are some criteria that influence the selection of the bath. Recently, methanesulfonic acid and its derivatives have been used to deposit lead, tin and lead-tin alloys in electronics industries for contacts on printed circuit boards as well as providing a protective coating for steel parts in the corrosive environments. It has been found that methanesulfonic acid has less destructive effects on the environment than fluoroborate or fluorosilicate [20].

Simple solutions are not practically appropriate, and addition agents are necessary to obtain smooth, compact, coherent and adherent deposit. Among the common agents widely used in lead plating solutions are hydroquinone, quinone, quinhydrone, coumarin, glue, glycerol and gelatine and even some plant extracts such as horse chestnut and aloe extracts [31,39]. Many other additives are proprietary reagents that have been protected by patents. Nevertheless, in most cases a mixture of more than one additive is required to enhance a specific property of the deposit or to prolong the service life of the solution [37,40-42].

1-7 Positive electrode PbO_2

1-7-1 Structure of α and β-PbO_2

Lead dioxide is polymorphous with different crystallographic structural forms. The most important is the orthorhombic form (columbite type), which is called α-

PbO_2, and the naturally occurring tetragonal form (rutile type), which called β-PbO_2 [7,40]. A transition between the two forms is possible under specific conditions [6].

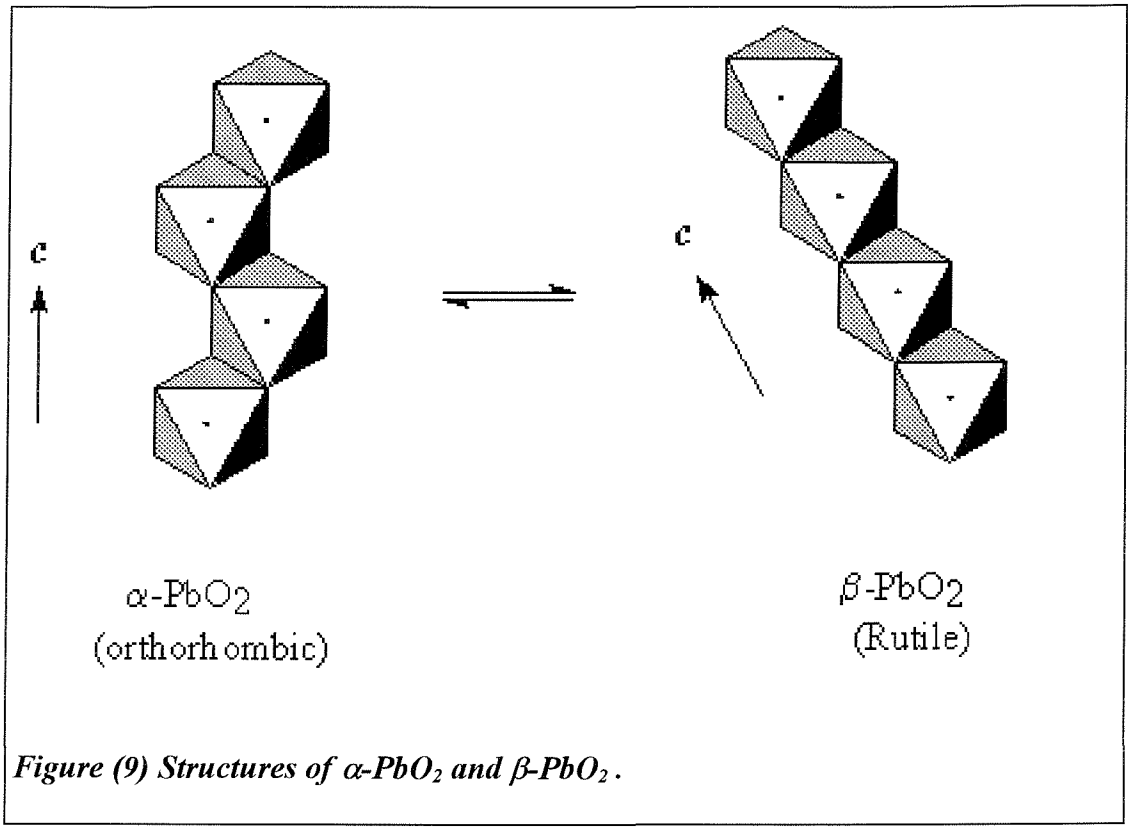

Figure (9) Structures of α-PbO_2 and β-PbO_2.

A general trend is that the α-PbO_2 form has a more compact structure compared to the more porous β-PbO_2 resulting in a better contact between the particles [43].

1-7-2 Physical and chemical properties

Lead dioxide is an oxidising agent, inert in acidic and alkaline solutions and stable at high temperatures. Furthermore it is known to have an extensive defect structure with a non-stoichiometric ratio (i.e., PbO_x, $1.80<x<2.0$). Hence, the PbO_2 matrix is tolerant to the incorporation of foreign ionic and neutral species. A lot of ions have been doped into the dioxide film in order to improve its properties in industrial applications. D.C. Johenson and co-workers reactions [44-51]have been investigating the preparation, characterisation and applications of pure and doped lead-dioxide. The

majority of their work has been devoted to electrocatalysis of anodic oxygen-transfer. It has relatively high electrical conductivity and has large O_2-evolution overpotential [7].

1-7-3 Applications

Lead dioxide anodes are of special interest to industry because of their low price compared to the noble metals such as gold and platinum together with their physical and chemical properties mentioned above. Moreover, chemical inertness and stability during chemical processes are of great importance. The applications of lead dioxide includes energy conversion especially in lead-acid batteries, as anodes in electrosynthesis, process recycling and environmental treatment, ozone production, and protective coating [52,53].

It has been found that doped lead dioxide is more efficient for catalysis processes than pure lead dioxide. The reason could be ascribed to the generation of surface defect sites which enhanced the anodic discharge of water molecules to produce intermediates responsible for oxygen transfer reactions [48,49].

1-7-4 Deposition of lead dioxide

Both forms of lead dioxide can be electrodeposited during battery charging at the positive electrode, however, β-PbO_2 is said to be electrodeposited in acidic media and high current density. α-PbO_2 is electrodeposited in neutral and slightly alkaline solutions and low current density [50,54]. However, it is possible to deposit both α-PbO_2 and β-PbO_2 pure and as mixtures from the same solution. There are claims that different factors influence the nature of the deposit including pH, additives, temperature, solution composition, stirring, current density and substrates [55].

Different solutions have been used to electrodeposit pure and doped lead dioxide such as perchlorate, acetate, nitrate, fluoroborate and flourosilicic as well as

sulphuric acid solutions. Platinum, titanium, gold, glassy carbon, stainless steel and lead have been used as substrates [52].

1-7-5 Mechanism of the lead dioxide electrodeposition

According to A. B. Velichenko et. al [56] and D. C. Johnson [44] the mechanism of lead dioxide electrodeposition is that first suggested by Fleischmann and his co-workers. The proposed scheme is :

$$H_2O - e^- \longrightarrow OH_{ads} + H^+$$

$$Pb^{2+} + OH_{ad} \longrightarrow Pb(OH)^{2+}$$

$$Pb(OH)^{2+} + H_2O - e^- \longrightarrow PbO_2 + 3H^+$$

On the other hand, the mechanism of lead dioxide stripping in acetic, nitric and perchloric acids is given by the following scheme [65]:

$$PbO_2 + 2H^+ \rightleftharpoons PbO_2(H^+)_2 ,$$

$$PbO_2(H^+)_2 + e^- \rightleftharpoons Pb(OH)_2^+$$

$$Pb(OH)_2^+ + e^- \rightleftharpoons Pb(OH)_2$$

$$Pb(OH)_2 + 2H^+ \rightleftharpoons Pb^{2+} + 2H_2O$$

It has been concluded that lead dioxide is not stripped totally during the cathodic scan of cyclic voltammograms in many conditions. The remaining residue was

suggested to be PbO [48]. This may explain why the responses in repetitive cyclic voltammograms are not identical.
Some soluble materials have also been detected in the solution [46,57].

1-8 Parameters affecting the deposition process

1-8-1 Additives

1-8-1-1 General view

Addition agents are substances which, when added to the plating bath in small concentrations with respect to the deposited material, produce useful effects on the character and appearance of the deposit. One useful effect is the reduction of the grain size of the deposit improving the smoothness and brightness of the deposit. Otherwise the deposit without any additives (lead for instance) would deposit at low overpotential and tend to be a rough, porous and dendritic deposit. In addition, additives are added for the attainment of adherent, non-dendritic deposit as well as to decrease the rate of growth at sharp edges. A large number of additive agents are known in the plating industries usually with a high molecular weight. Selection of the additive hence, depend on the specific application of the deposit. They may be either organic or inorganic. These materials do not have a common structure and hence they probably have different working mechanisms. Examples of some groups of additive agents for lead include gelatine, proteins and plant extracts [58,59].

Although it is more common to use additives to achieve better quality of the deposit at the cathode, additives have also been used to improve the deposit at the anode. As an example, additives have been used in lead dioxide depositing bath to control the ration between α -and β -PbO_2, to improve the surface grain morphology as well as to have compact, less porous and stable deposit [49,60,61].

Because of their low concentration in the solution, additives usually do not affect the properties of the solution such as viscosity, conductivity, pH or metal concentration. On the other hand, additives usually increase the deposition overpotential and are often thought to operate by adsorption [62].

The remarkable effects of additives on the quality of the deposit might be attributed to the inclusion of the additives or some of their decomposition products into the deposit during electrodeposition. It should be noted that this inclusion might affect the deposit properties. It is common practice to analyse the deposit to look for traces of the additive agents. Radioactive isotopes are used in some cases to detect such traces and to study the levelling mechanism caused by additives [58].

Although the mechanism of the levelling effect of additives on the deposition process is not yet totally understood, it seems to be that adsorption of the additives on top of the substrate surface is the widely accepted mechanism. Part of the problem is that the additives do not have common properties or similar functional groups in their structures. It should be noted as well that certain additives have different effects on the quality of different metals which requires, of course, more effort to explain the reasons. According to the adsorption hypothesis, the polarisation in the deposition potential can then be attributed to the effect of the additives on the electrode surface kinetics. By using ultraviolet spectroscopy techniques, it has been found that effect of lignin sulfonate additive to lead deposition bath is acting through the adsorption of lignin sulfonate onto lead surface [40,62].

It is common practice in plating industries, that a mixture of more than one additive is added in order to pertain the desired properties. It has been found , for example, that the lead deposit becomes levelled, compact, smooth and has microcrystalline structure when a combination of sodium lignin sulfonate and horse chestnut extract is used in the plating bath. The synergetic effect of the additives has proven that a better deposit resulted when two or more additives were mixed rather than if each additive was used alone [38,42].

Brightening, on the other hand, is not favourable for lead since this metal is not used for a decorative purposes. Nevertheless, brightening can be defined as the ability to produce a smooth deposit which contains crystals smaller than the wavelength of visible light. It is important to note that small grain size is not sufficient for brightness since the crystals morphology must be in the same plane. This in turn adds more complexity to the role of additives and hence more difficulty to explain the mechanism.

Furthermore, all the attempts to correlate the nature and structure of the additive to the nature and structure of the deposited metal is restricted to a specific additive with a specific metal. Otherwise it is impossible, up to the present, to make generalisations which account for every metal deposition process [62].

When using additives in electrodeposition, it is essential to monitor the additive concentration and the organic impurities which are usually generated by the decomposition of the additives. On one hand, controlling the quantity of the additives is essential in order to control the properties of the deposit [20]. On the other hand, additives undergoes some decomposition during electrolysis producing organic materials that incorporate into the deposited metal. Organics, when present in excessive amounts into the deposited metal can cause a change in the properties or even defects in the deposit.

1-8-1-2 Types of additives

There are different types of additives according to their effects on the electroplating. They include

- levellers

Levellers are substances usually added in small quantity to improve the throwing power and hence to smooth the surface of the deposit.

- brighteners

Brighteners are materials that causes the deposited metal to have a pleasing appearance by reflecting the visible part of the spectrum. It has a wide application in the decorative devices but less importance in the industrial applications.

- wetting agents

When hydrogen is incorporated within the deposit at the cathode, the deposit some times becomes brittle and hence this process is called hydrogen embrittlement. This process causes crack in the deposit and weakens the mechanical properties of the

deposit. Wetting agents are used to repel the hydrogen bubbles away from the electrode surface [31].

1-8-2 Uniform deposition

The deposit should be smooth, compact and uniform in order to perform well in the battery application. This is not always the case since the deposit can grow non-uniformly even as powder or in a tree like shape. Treeing in the deposit growth is called dendritic growth. It is believed that the growth of dendrites depends primarily upon the ratio between the current density and the concentration of the solute. Accordingly when the ratio is in favour of the dendrite growth, a critical overpotential is essential as well as an initial induction time before the dendritic growth take place. The rate of occurrence of the dendrites increase with increasing the overall current. Finally it has been found that dendrite growth occurs at the tip points of the electrode surface. Levellers and brighteners are thought to operate by adsorbing on the tip sites and retarding electron transfer there [26,63].

1-8-3 Solution components

An electroplating bath usually consists of the following components

■ Electrolyte

The electrolyte is added to the bath in a high concentrations in order to increase the conductivity and hence minimise the IR drop, making the deposit over the entire electrode surface more uniform.

■ Metal ion for deposition

The deposited metal has to present in a high concentration so as to prevent depletion of ions at the electrode surface. The metal may exist as a simple ion or as a complex depending on the nature of the plating process.

■ Additives

A simple plating solution is rarely used and additives are of a great importance in most of the plating processes. The different kinds of additives used in the plating process are mentioned above.

■ Buffer

A buffer is needed when the pH of the solution has to be stable. A wide variety of buffers can be used and the choice depends upon the condition of the specific bath.

1-8-4 Temperature

Temperature is one of the parameters of the plating bath. In most plating processes, a certain range of temperatures are required in order to have good deposit. Assigning the range of temperature therefore is essential when choosing the bath conditions. Although it is not applicable in every plating bath, elevated temperatures favour of coarse grained and loose deposits. On the other hand, increasing the temperature causes the movement of the ions towards the electrodes to increase and this enhances the plating quality to some extent. Many systems in plating industries operate at 313 - 333 K [64].

1-8-5 pH

The hydrogen discharge potential, the deposition of solid materials at electrodes, adsorption of the additives and the ratio of the complexes are all affected by the pH of the solution. For these reasons, the pH of the bath ought to be controlled within certain working limits. Stress and strain of the deposited solid materials are also affected by pH level. Besides the electrode materials may corrode in some environments associated with the pH range. Moreover, during deposition/dissolution processes in our envisaged battery it is very important to control the pH levels otherwise the deposition or the dissolution processes will not be completed and consequently a loss of power may occur either by the collapse of the deposit during

dissolution or the occurrence of some competitive reactions during deposition process [31].

1-9 Purpose of this thesis

This thesis describes a preliminary study of the deposition of Pb and PbO_2 in methanesulfonic acid to define whether the proposed battery should be built and tested.

Chapter (II)

Experimental work

2-1 Chemicals

The following table contains the chemicals which have been used in this project. The chemicals were used as received.

Chemical	Supplier	Purity %
Methanesulfonic acid	Aldrich	99.5 +
Lead (II) carbonate	Aldrich	99.99 +
Lignosulfonic acid, sodium salt	Aldrich	----
Iron	Goodfellow	99.5
Lead nitrate	Aldrich	98 +

Table (1) Chemicals used in the study

The lead methanesulfonate solutions were prepared using the reaction

$$PbCO_3 + 2\ CH_3SO_3H \longrightarrow Pb(CH_3SO_3)_2 + CO_2 + H_2O$$

Hence, to prepare the electrolyte solutions, different exact amounts of lead(II) carbonate and the additive, if any, were added to an appropriate concentration of methanesulfonic acid in order to give the derived final concentrations of Pb(II) and CH_3SO_3H. Where the concentration of Pb(II) was required with accuracy, it was determined using a RDE and standards prepared from $Pb(NO_3)_2$ .The solution was kept covered until the reaction was completed then was poured into the electrochemical cell.

To remove the dissolved oxygen from the solution, a fast stream of nitrogen was passed through the electrochemical cell for at least 10 minutes before each experiment and a N_2 atmosphere was maintained during the experiment.

Some experiments were carried out in a commercial fluoroboric acid solution supplied by BASF (UK) plc. in order to compare the quality of the deposits. The commercial solution contains the following ingredients :

Bath contents and condition	Value
Lead g/l	200
Free fluoroboric acid, g/l	20
Excess boric acid, g/l	--
Animal glue, g/l	--
Iron, g/l	7
Temperature, °C.	18
Current density, (-j) mA/ cm^2	15
Deposit thickness, μm	50

Table (2) Commercial bath contents and conditions. Supplied by BASF

This solution was used to deposit lead on flat mild steel plates (also supplied by BASF). All solutions were prepared with de-ionised water, produced by Whatman system (Whatman International LTD).

2-2 Instrumentation

All experiments were carried out using an electrochemical system consisting of a potentiostat model DT 2101 controlled by a waveform generator model PP R1. The electrode was controlled by EG&G PARC 616 RDE.

Results were recorded on a x-y chart recorder (BRYANS Instruments). The resulted voltammograms were converted to a word document using a scanner, model

AGFA DUOSCAN T1200. Corel Photo-Paint software was used to prepare and label the voltammograms.

A three compartment glass electrochemical cell fabricated in the Department's Glass Workshop with a volume of 50 cm^3 was used for voltammetric and plating experiments as shown in figure(1).

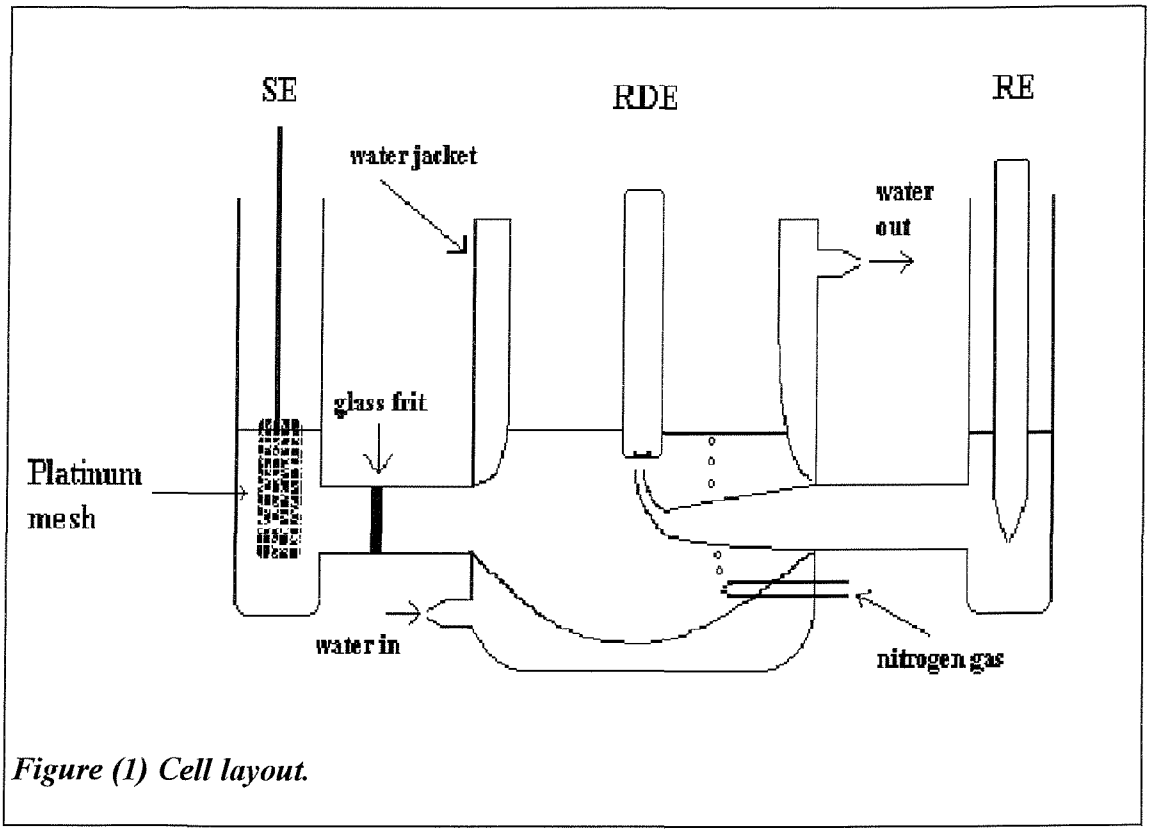

Figure (1) Cell layout.

A platinum mesh was used as a secondary electrode (SE) and a commercial saturated calomel electrode (SCE) served as the reference electrode (RE). The reference electrode was mounted in a luggin capillary whose tip was placed approximately 1 mm from the surface of disc working electrode in order to minimise the IR drop. The cell is surrounded by a jacket filled with water so that the temperature could be controlled or varied. The water temperature is adjusted by a water bath (Grant Instruments W14). All experiments were carried out at room temperature unless otherwise mentioned.

Electrode	Diameter / cm*[1]	Area / cm^2
Vitreous carbon, RDE	0.396	0.123
stainless steel, RDE	0.408	0.131
steel, RDE	0.41	0.132
Mild steel, RDE (BASF)*[2]		
Nickel, RDE (thick)	0.496	0.193
Nickel, RDE (thin)	0.510	0.204
Gold, RDE	0.204	0.033
Graphite, RDE	0.296	0.069
Ti, RDE	0.570	0.255

Table (3) Electrode diameters.

*[1] ***determined with traveling microscope***

*[2] ***the sample was provided by BASF company.***

Different rotating disc electrodes have been used as substrates to deposit lead and lead dioxide from different solutions. Information about these electrodes is summarised in the above table. It should be noted that some of these electrode have been used for lead deposition and others have been used for lead dioxide and some have been used for both as will be seen in details in the results section. All these electrodes have been made locally in the Department's Mechanical Workshop.

All the electrodes were pressed into Teflon, with only a disc of metal /carbon exposed to the electrolyte. The exception was the rotating gold disc electrode, which was surrounded by glass.

2-3 Electrode preparation

The electrodes were polished first by fine emery paper, followed by polishing with decreasing size alumina particles (1.0 , 0.3, and 0.05 μm) in an aqueous suspension on a Buehler micropolish cloth until a mirror like surface was obtained.

After polishing the electrodes were washed thoroughly with de-ionised water. The electrodes were not touched by hand after polishing in order to protect them from any grease. Care must be taken during cleaning process since slight changes in the electrode surface changes the shape of the voltammogram hence, affecting the reproducibility of the voltammetry.

2-4 Electrochemical techniques

The following electrochemical techniques have been employed to study the deposition of lead and lead dioxide.

2-4-1 Cyclic voltammetry

This technique was used to characterise the Pb/Pb^{2+} and PbO_2/Pb^{2+} systems. Cyclic voltammogram sweeps for deposition of Pb or PbO_2 , and the corresponding dissolution of the respective deposits, were recorded as a function of scan rate, switching potentials and rotation rates. The cyclic voltammogram of a specific solution was obtained by initiating the potential scan from a starting potential where the current is zero and scanning in the negative direction for Pb deposition or positive direction for PbO_2 deposition. The potential scan was reversed at a conventional value, that was often varied.

The technique has been employed to study the kinetics and thermodynamics of the envisaged battery system. The electrical charge under the cathodic and anodic areas was calculated using the cut and weight method. The piece of paper representing the process is cut and weighed to four digital figures. A factor of mC to g is calculated then used to calculate the cathodic and anodic charges as well as the charge ratio. It has been found that this method is comparable to the other method which uses the visual calculation of the area under the cathodic and anodic regions

2-4-2 *Potential step experiments.*

Chronoamperometry was used to study the nucleation mechanism of the electrodeposited lead and lead dioxide particularly the deposit growth processes. Potentiostatic I-t transients were recorded as a function of potential. The transients were then analysed in order to detect the relationship between current and time according to the equation:

$$I = \text{constant x. } t^n .$$

2-4-3 *Rotating disc experiments*

A series of steady state measurements was made to investigate the kinetics. Rotating disk voltammograms were recorded with a sweep rate of 20 mV s^{-1} and a rotation speed of 400, 900, 1600 and 2500 rpm in most of the experiments. The resulting voltammograms were analysed and the diffusion coefficient was calculated using Levich equation:

$$I_L = 0.62nF\pi r_1^2 D^{2/3} \nu^{-1/6} \omega^{1/2} c^b$$

2-5 *SEM*

A scanning electron microscope, PHILIPS model XL 30 ESEM, has been used to study topographical views of the electrode surfaces. The effects of additives on the deposits were compared by viewing the surfaces before and after the addition of the organic agents.

2-6 *Photographs*

Some images of the lead deposits were photographed using a SONY digital MAVECA camera model MVC-FD91. The photos then transferred to , and manipulated by, Microsoft (R) Paint. The images were used to illustrate the morphologies and features of the deposits.

2-7 Adhesion

The quality of adhesion between the deposits and the substrates was checked by transparent adhesive tape and/or gentle scraping with a fingernail according to [49, 66]. The adhesive tape was pressed onto the deposit then removed by rapid pull. The adhesion was considered weak if the deposit went off with the adhesive tape.

Results and discussion

Chapter (III) Lead deposition

3 Introduction

The approach has been to use a combination of voltammetry and lead deposition experiments to develop and understand the conditions for the plating of uniform and adherent deposits of lead on various substrates. The emphasis has been on selecting the conditions for high rate deposition appropriate to a load levelling battery. The quality of the deposit has been judged by visual observation and an adhesive tape test together with a simple scratching. In some cases, these experiments have been supported by digital photography and SEM. By necessity, the voltammetry and plating experiments have sometimes used slightly different conditions, e.g. Pb^{2+} concentration.

3-1 Preliminary studies of Pb deposition from methanesulfonic acid solutions

Cyclic voltammetry has been used to study the thermodynamics and kinetics of the deposition behaviour of the Pb/Pb^{2+} system in methanesulfonic acid solutions using different kinds of rotating and stationary electrodes under various conditions.

A typical voltammogram is shown in figure (1) where a voltammogram was recorded at a rotating vitreous carbon disc electrode for a solution of 40 mM Pb(II) in 2 M methanesulfonic acid with a rotation rate of 400 rpm. A potential scan rate of 20 mV s^{-1} was used in this experiment. The potential limits were -0.30 V and -0.65 V and the experiment was performed at room temperature (301 K).

The forward scan shows a reduction wave with $E_{1/2}$ = -0.51 V and the wave has a well defined plateau. On the reverse scan deposition continues until -0.45 V. The difference between the forward and reverse scans results from nucleation phenomena.

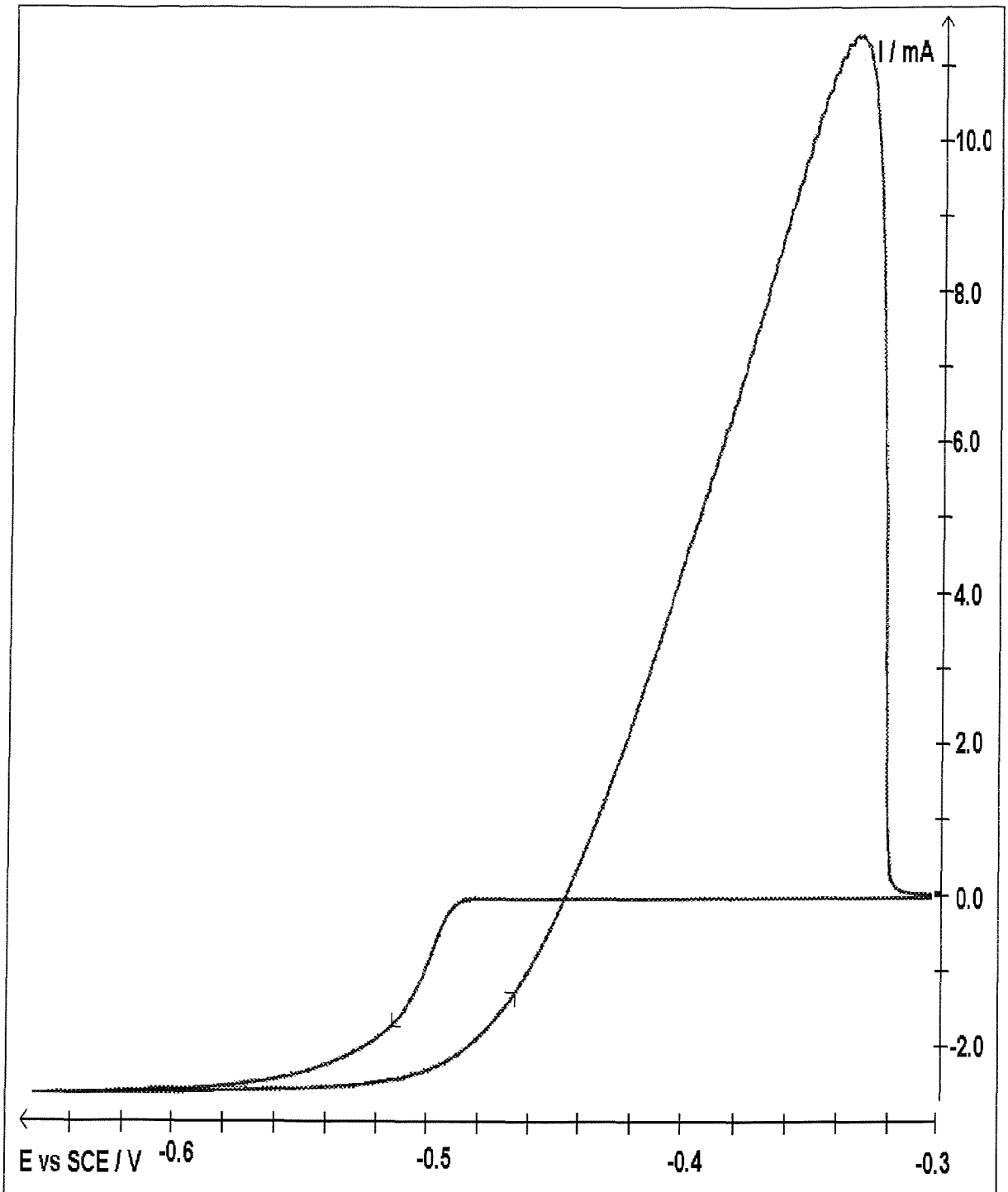

Figure (1) Cyclic voltammogram of rotating vitreous carbon electrode (0.126 cm^2) at 400 rpm in 40 mM Pb(II) in 2M CH_3SO_3H. Potential scan rate 20 mV/s.

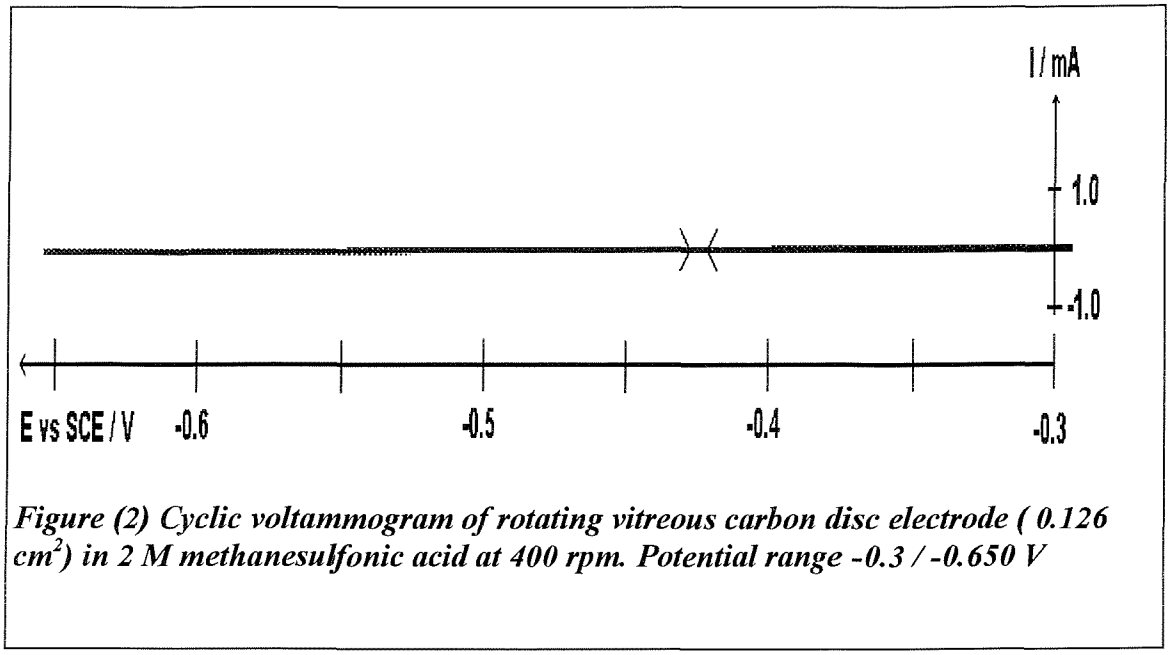

Figure (2) Cyclic voltammogram of rotating vitreous carbon disc electrode (0.126 cm^2) in 2 M methanesulfonic acid at 400 rpm. Potential range -0.3 / -0.650 V

Positive of -0.45 V, there is a large anodic peak with E_p = -0.36 V. This is due to the stripping of the lead metal from the electrode. In this experiment the charge under the anodic peak (302 mC cm^{-2}) is almost the same as the total cathodic charge passed (310 mC cm^{-2}). However, this is not the typical behaviour with a vitreous carbon electrode since the charge ratio, Q_A/Q_C is less than one in most experiments as will be seen in a later section. A charge ratio less than one can be attributed to a competing cathodic reaction, not all the lead dissolving or simply detachment of the lead from the substrate.

To confirm that all the features in figure (1) are associated with Pb deposition and dissolution a cyclic voltammogram has been recorded for rotating vitreous carbon disc electrode in 2 M methanesulfonic acid at a scan speed of 20 mV/s. The potential range was the same as that used in the experiment of figure (1). The forward and reverse scans are identical and the current is effectively zero throughout. It is clear from figure (2) that no competing reactions are taking place in the potential range under study. Also it can be inferred that methanesulfonic acid is very stable to reduction and can be used in the proposed battery. The stability of methanesulfonic acid has been reported in the literature[31].

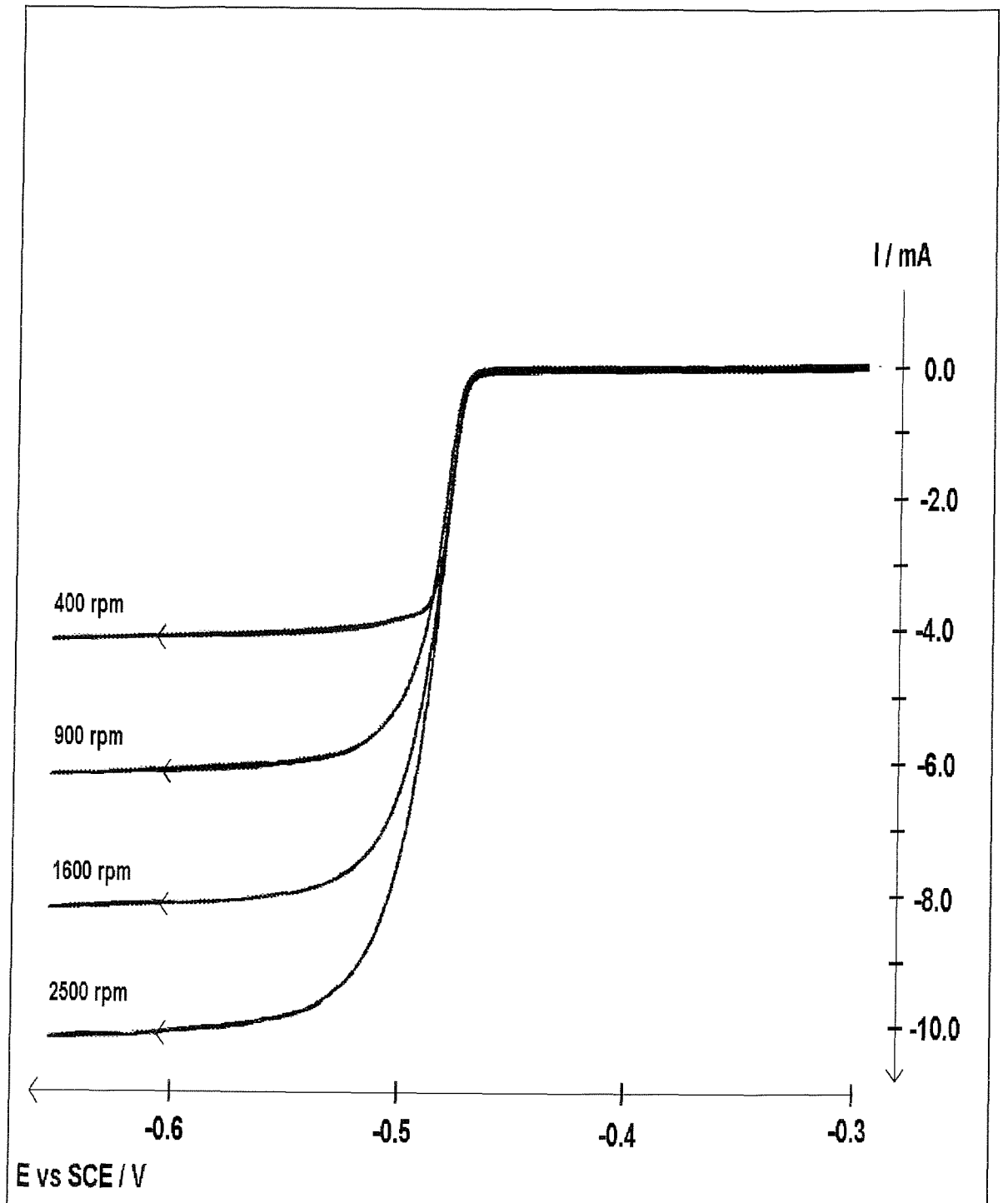

Figure (3) Voltammograms of a rotating nickel electrode (0.2 cm^2) at various rotation rates in 40 mM Pb(II) in 1.8 M CH_3SO_3H. Potential scan rate 20 mV/s.

Voltammograms for the solution containing 40 mM Pb(II) in 2 M methanesulfonic acid were recorded at a nickel disc electrode at a series of rotation rates and the results are shown in figure (3). At all rotation rates, a well formed reduction wave is observed with $E_{1/2}$ = -0.49 V and all waves have very flat plateaux. At the beginning of the reduction wave it is clear that the current is independent of the rotation rate. Therefore, it can be inferred that the current is kinetically controlled during this part of the curve. On the other hand, the limiting current is proportional to the square rout of the rotation speed, $I_L \alpha \omega^{1/2}$. In the plateaux region of the curves mass transport is the predominant control at this part of the response. However, between these limits it can be seen that the current changes with rotation speed but not as rapidly indicating that there is a mixed control of electron transfer and mass transport at this region. Furthermore, this result is in agreement with the theoretical treatment as explained in chapter one. The diffusion coefficient was calculated to be $5.45 \pm 0.15 \times 10^{-10}$ m^2 s^{-1} for Pb(II) using the Levich equation

$$I_L = 0.62\, n\, F\, A\, D^{2/3}\, \nu^{-1/6}\, C\, \omega^{1/2}$$

where: D = diffusion coefficient; ν = kinematic viscosity ($\sim 10^{-6}$ m^2 s^{-1}); C = bulk concentration(mol. m^{-3}); ω = rotation rate (radians s^{-1}); I_L = limiting current (A m^{-2}); F = Faraday constant(96485 C); A = 2 x 10^{-5} m and n = 2. The diffusion coefficient for lead (II) in 0.01 M Pb(II) in 1 M HBF4 solution was reported in the literature to be 6.1 $\pm$ 0.2 x 10^{-10} m^2 s^{-1} [62].

Cyclic voltammograms were recorded on stationary vitreous carbon electrode from 5 mM Pb(II) in 2 M methanesulfonic acid solution in order to study the effect on the voltammogram features. Figure (4) shows a reduction peak at -0.57. The current decreases to a steady state but without a well defined plateau. During the reverse scan, the deposition continues while the current is still decreasing until it reaches -0.50 V. The decrease in current is due to the consumption of the Pb(II) at the surface of the electrode since there is not enough supply from the bulk. An anodic peak is seen at -0.44 V.

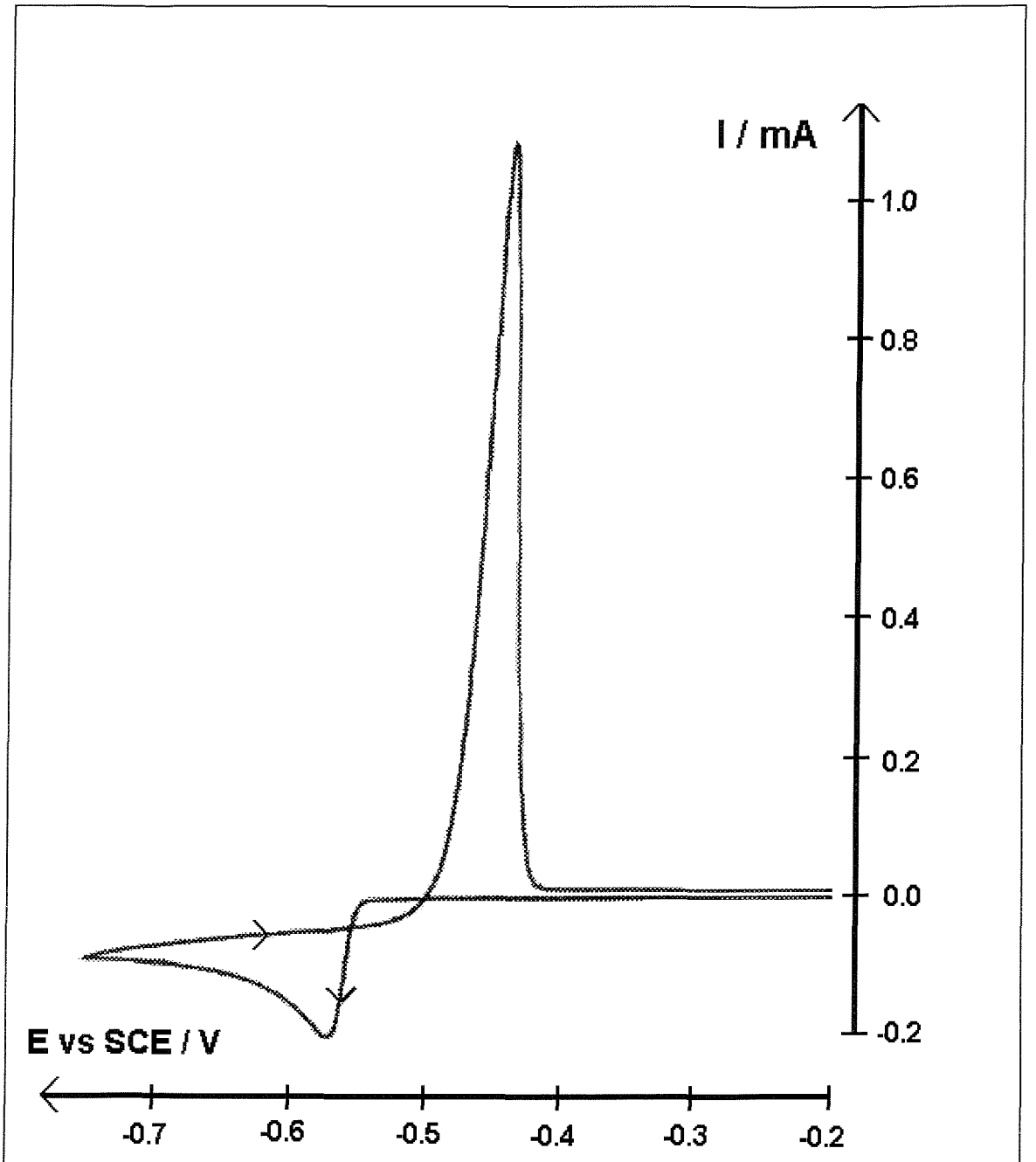

Figure (4) Cyclic voltammogram recorded on stationary vitreous carbon (0.126 cm^2) from 5 mM Pb(II) in 2 M methanesulfonic acid Potential scan rate 20 mV/s.

Lead was deposited from 40mM Pb(II) in 2M methanesulfonic acid onto a stationary vitreous carbon electrode using a constant potential of -0.6 V vs SCE for 40 s (the charge passed was 144 mC cm^{-2}). Figure (5) shows four SEMS with increasing magnification A to D. On the lowest magnification shows a number of uniform sized Pb centres distributed uniformly over the surface. This is a clear indication that instantaneous nucleation is occurring. On increasing the magnification, it can be seen that the Pb centres have a complex structure and are certainly not hemispherical. This is most clearly seen with SEMS C and D where the surface is at an angle to the beam.

Further more, figure (6) shows four SEM images for lead deposited on stationary gold electrode from 40 mM Pb(II) in 2 M methanesulfonic acid solution at a potential of -0.580 V. Clearly seen from figure (6) that there are different kinds of structures. The magnification has been increased in the order A-D and different sizes are easily determined. At least three different structures can be distinguished; needles, small and big particles. Moreover, the structure of the deposit in figure (5) is not similar or even close to the structures in figure(6). The only difference between these two experiments is the substrate for deposition. Nevertheless, the structure of lead deposit may vary with other factors, such as Pb(II) concentration, electrolyte agitation, additives, temperature and current density [1, 31, 38, 54].

A series of potential step experiments were carried out with a solution of 4 mM Pb(II) in 2 M methanesulfonic acid at rotating vitreous carbon electrode. Figure (7) shows three typical transients. In all cases, the predominant feature is a current which increases with time until a "plateau" is reached. It can be seen that the timescale of the transient changes strongly with overpotential at -0.52 V, the plateau is reached after ~ 200 s while at -0.59 V only ~ 20 s is required. Such transients are expected for a nucleation and growth mechanism. Analysis of the shapes in terms of linear I vs t^n plots was not, however, convincing. It should also be noted that over the potential range shown in the figures, the plateau currents are very similar. This implies that over this potential range the deposition is mass transport controlled in the steady state.

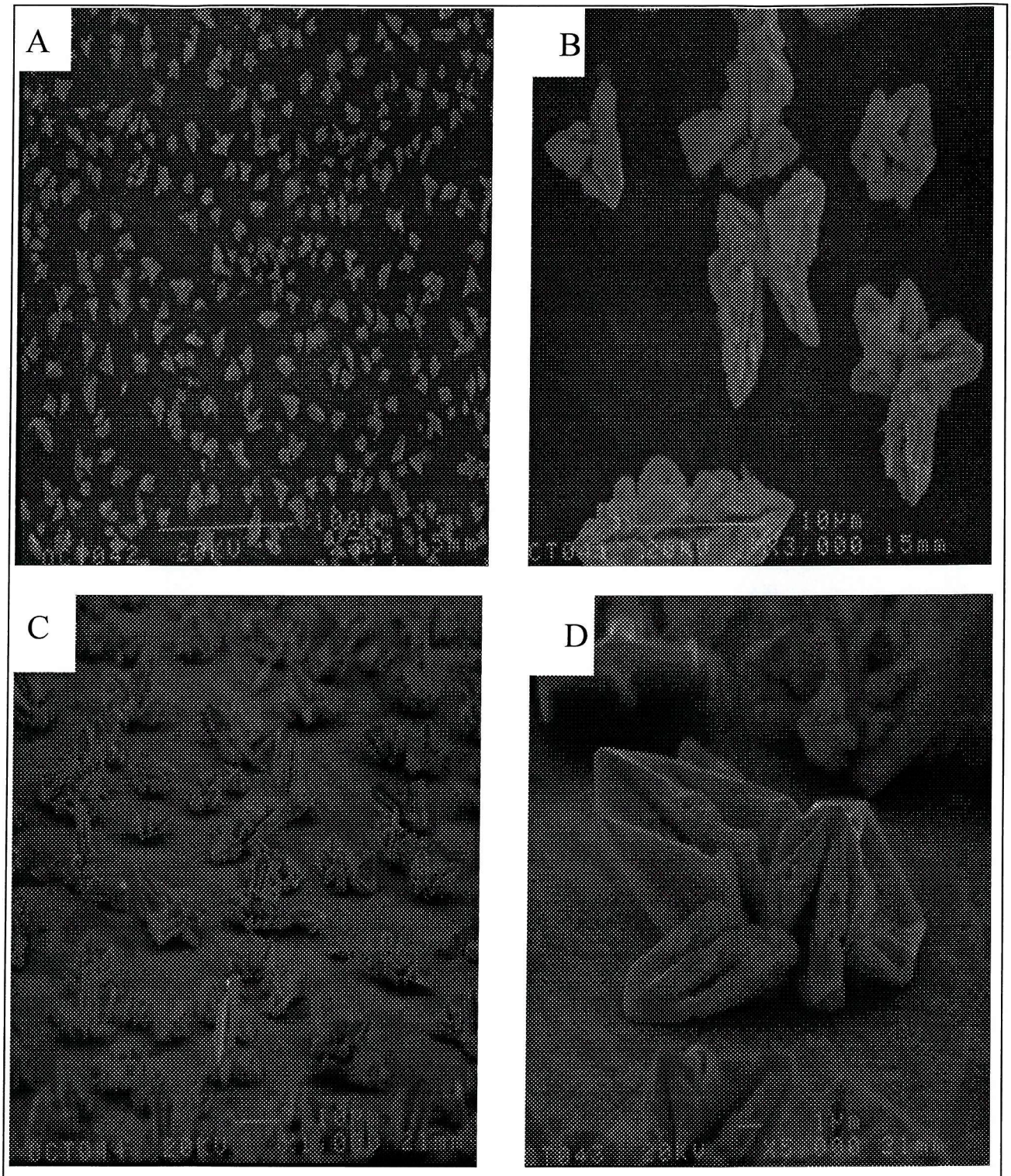

Figure (5) SEM images for lead deposited on vitreous carbon plate from 40mM Pb(II) in 2 M methanesulfonic acid. At deposition potential of -0.6 V (A) ——— 100 μm , (B) ——— 10μm, (C) —— 10 μm, (D) — 1 μm.

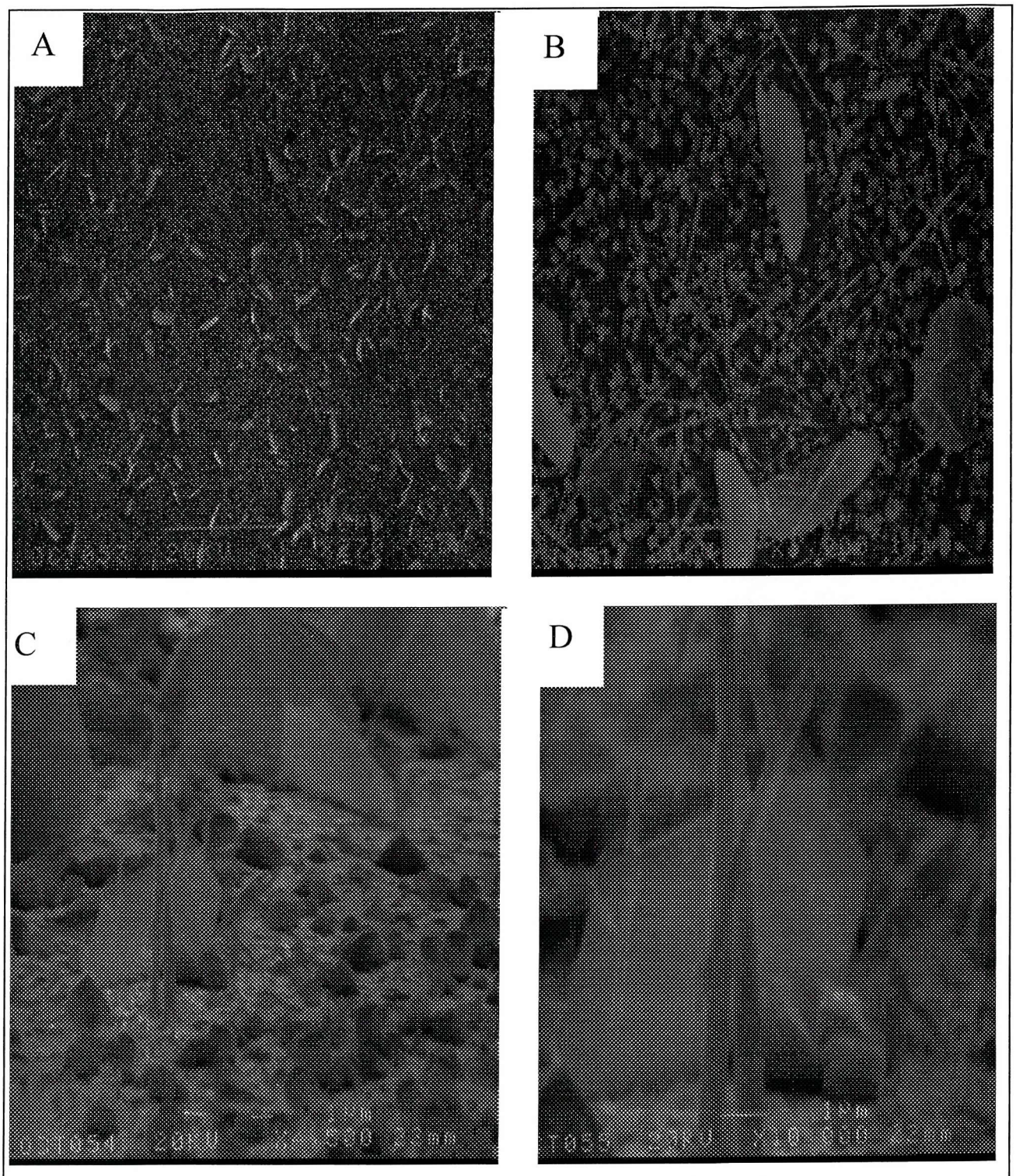

Figure (6) SEM images for lead deposited on gold plate from 40mM Pb(II) in 2 M methanesulfonic acid. At deposition potential of -0.58 V. (A) ——— 100μm, (B) ——— 10μm (C) — 1μm, (D) —— 1μm.

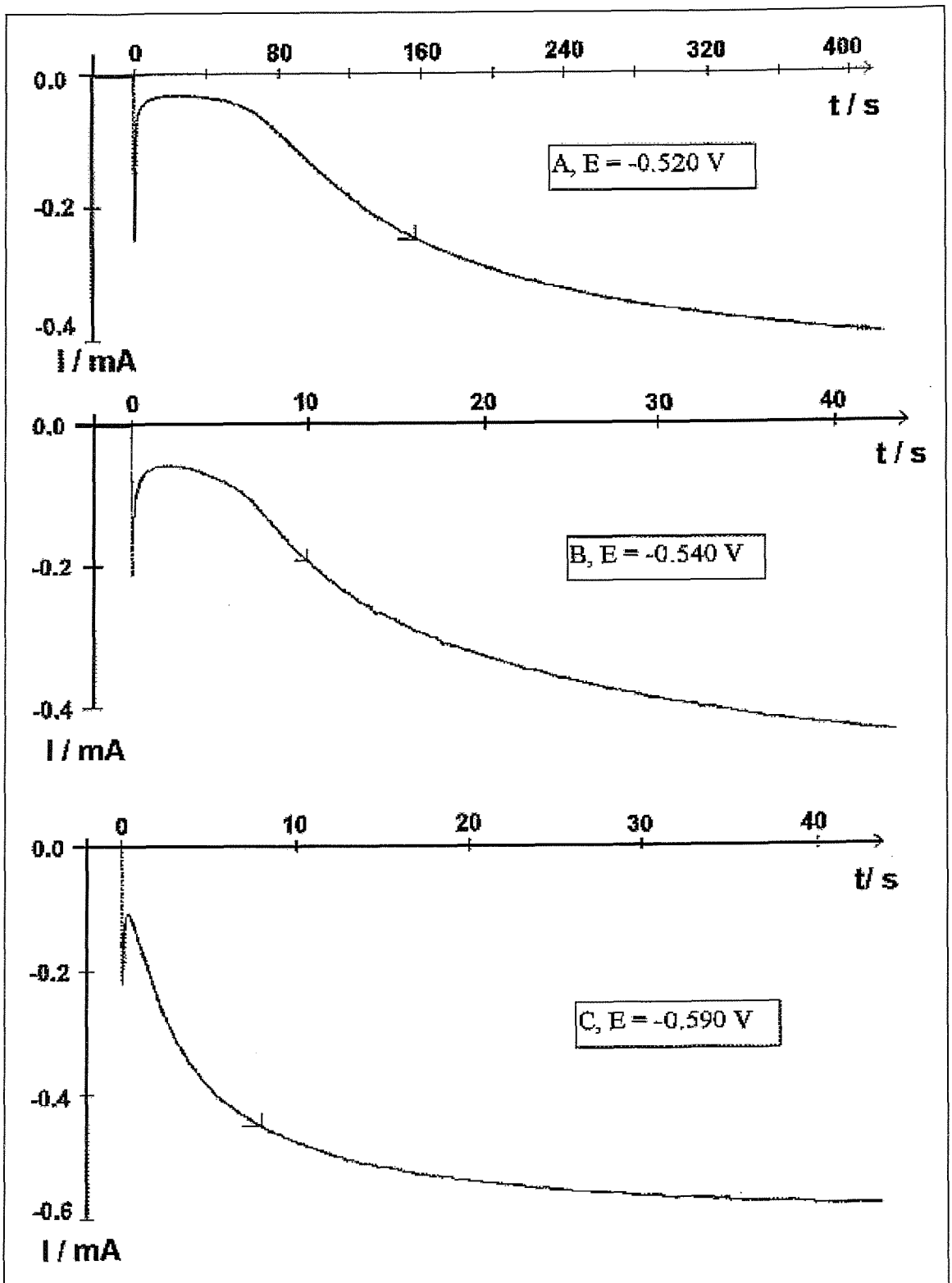

Figure (7) I-t transients recorded on rotating vitreous carbon disc electrode (0.126 cm^2) from 4mM Pb(II) in 2 M methanesulfonic acid solution at a rotation rate of 1600 rpm. The transients have been recorded at room temperature.

In conclusion, according to the above results and discussion the following can be concluded

- E_e^O of the couple Pb^{2+}/Pb in 2M methanesulfonic acid is ~ -0.41 V
- electron transfer is fast
- nucleation requires a small overpotential
- mass transport controlled can be achieved quite easily
- initial nucleation is characterised by three dimensional growth leading to complex structures.

3-2 Parameters affecting the quality of the deposit

Since it is common practice to investigate different parameters that affect the deposition process, lead has been deposited under various conditions. Base metal has been altered in order to find the best adhesion between the deposit and the substrate. Current density, temperature, lead concentration and additive concentrations have also been considered as parameters influencing deposit quality and will be discussed in the following sections.

3-2-1 Lead concentration

A large number of voltammograms have been recorded for solutions of 2-100 mM Pb(II) in 1-2 M methanesulfonic acid at a rotating vitreous carbon disc electrode. As illustrated previously, see figure (1), good quality curves were obtained for concentrations of 40 mM and below; above this concentration the reduction wave becomes distorted by IR drop.

Two voltammograms for 4 and 40 mM Pb(II) in 2 M methanesulfonic acid are reported in figure (8). Well formed and steep reduction waves are observed with good plateaux. The $E_{1/2}$ for the 4 and 40 mM occur at -0.56 and -0.48 V respectively. It is clear that a high Pb(II) concentration decreases the overpotential for deposition of Pb (since the equilibrium potentials for the two solutions differ by only 30 mV), therefore increasing the energy efficiency for the charging process in a battery.

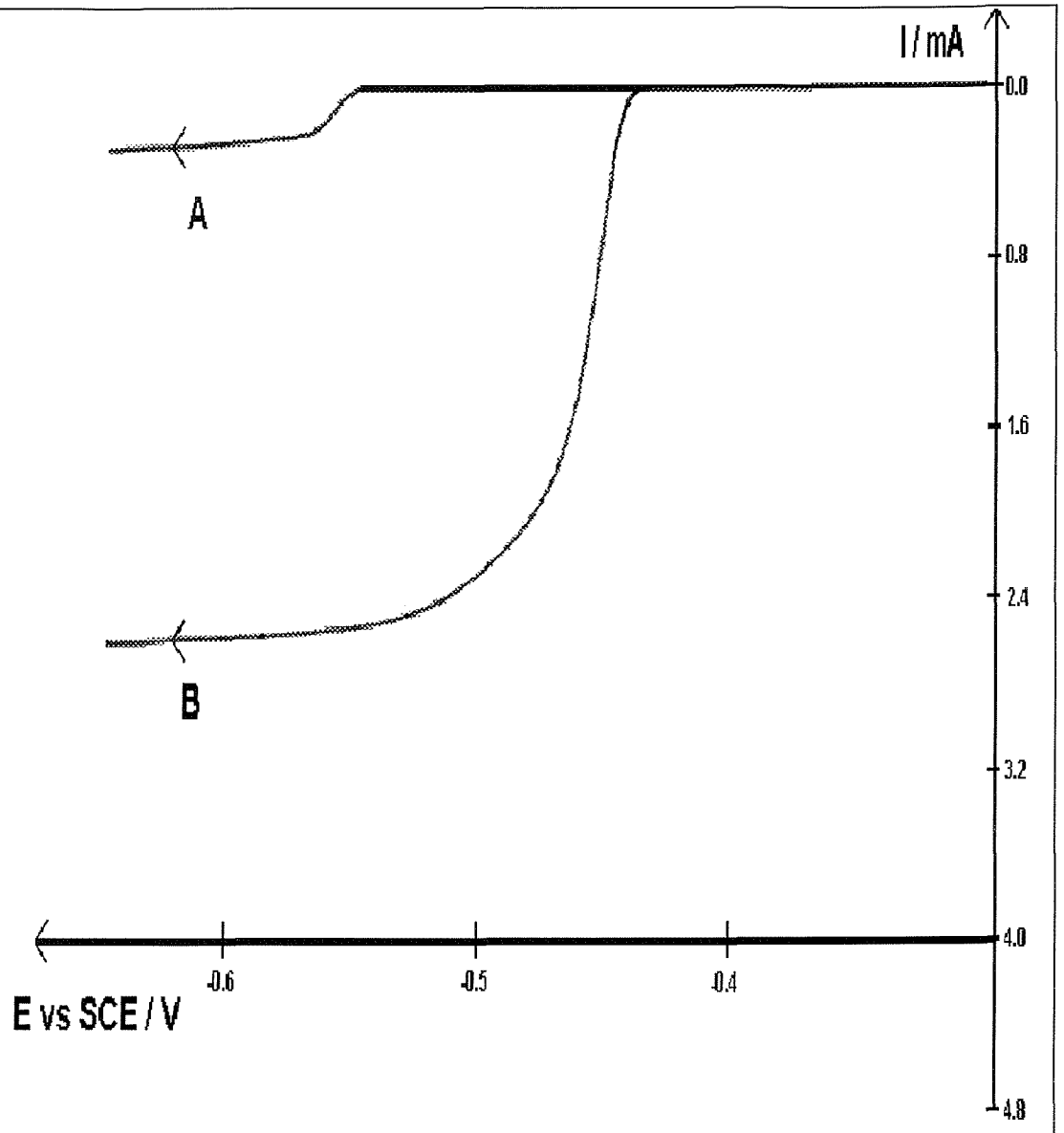

Figure (8) Voltammogram recorded on vitreous carbon rotating disc electrode (0.126 cm^2) from (A) 4 mM Pb(II) and (B) 40 mM Pb(II) in 2 M methanesulfonic acid at a rotation rate of 400 rpm and scan rate of 20 mVs^{-1}. Potential range is -0.3V to -0.75 V.

The rotation rate of the vitreous carbon electrode has been varied to study the effect on the limiting current. Result have been summarised in figures (9) and (10) where the rotation rates of 400, 900, 1600 and 2500 were used in three different concentrations of Pb(II). As can be seen from the figures, plotting the limiting current of the steady state curves against the square root of rotation rate produce straight lines in each case. Moreover, the lines pass through the origin. Clearly with all concentrations of Pb(II) that have been used, I_L is proportional to $\omega^{1/2}$.

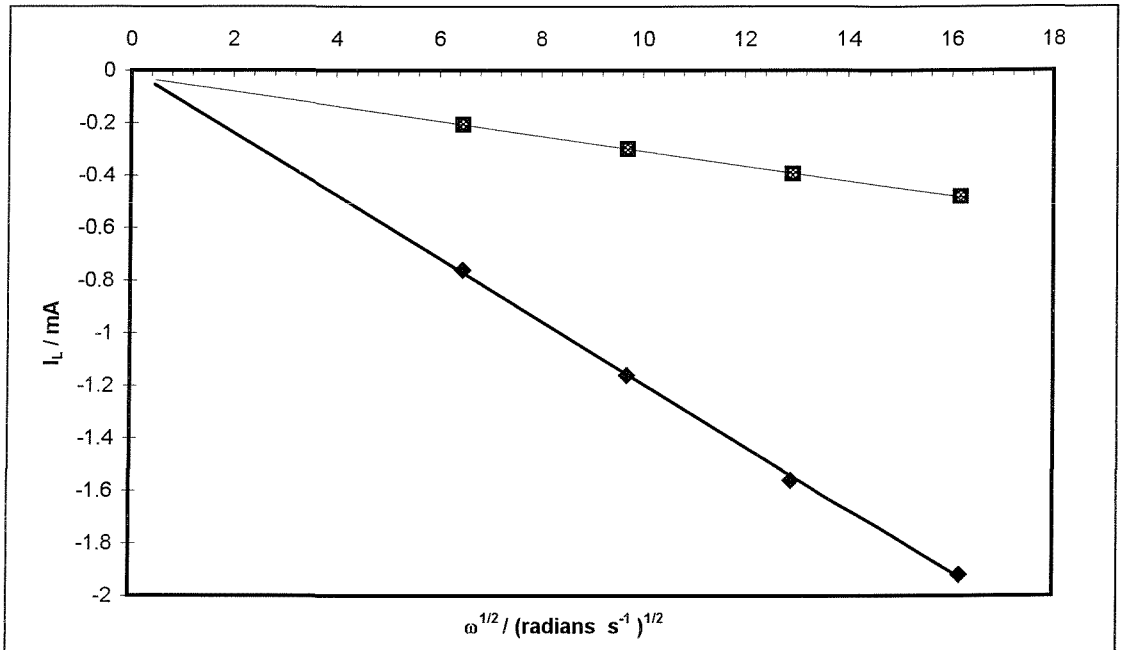

Figure (9) I_L vs $\omega^{1/2}$ for 2 mM and 10 mM Pb(II) in 1 M methanesulfonic acid. (diamonds) 10 mM Pb(II) and (squares) 2 mM Pb(II)

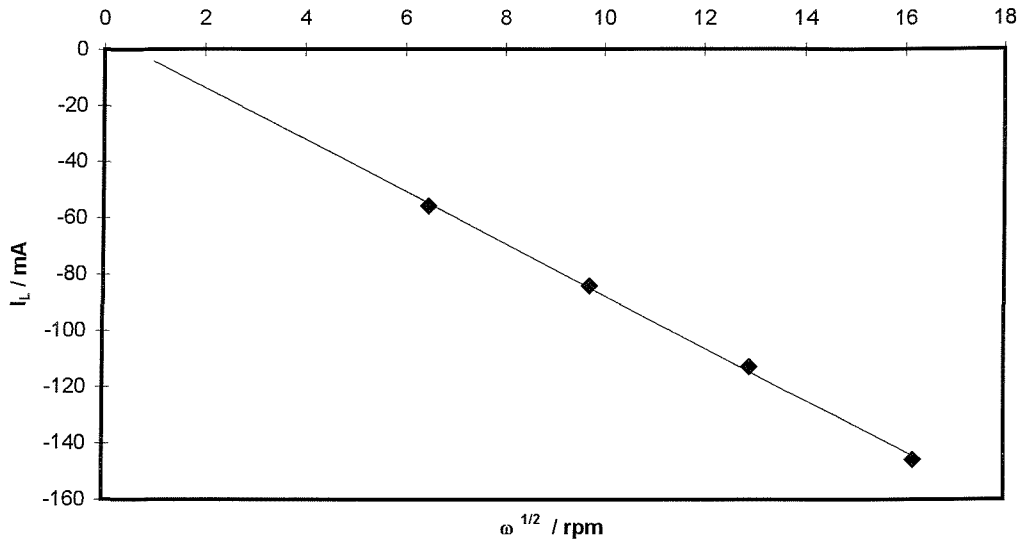

Figure (10) I_L vs $\omega^{1/2}$ for 100 mM Pb(II) in 1 M methanesulfonic acid.

In another series of voltammograms, the Pb(II) concentration has been varied to investigate the effect of Pb(II) on the $E_{1/2}$ and limiting current. From the data represented in table (1), it is clear that the limiting current is proportional to concentration and to the square root of the rotation rate of the RDE.

C / mM	I_L / mA	$10^4 I_L / \omega^{1/2} C$ A cm^{-2} mM^{-1} radian$^{-1/2}$ $s^{1/2}$	10^{10} D / $m^2 s^{-1}$
1.82	-0.12	0.81	5.6
11.0	-0.72	0.80	5.5
40*	-2.6	0.79	5.5
98	-6.8	0.85	6.0

Table (1) Comparison between the voltammograms of various Pb(II) concentrations in 1 M methanesulfonic acid (* in 2 M CH_3SO_3H) recorded on rotating vitreous carbon disc electrode (0.126 cm^2). Rotation rate is 400 rpm.

Further, the reaction is under mass transfer control at the steady state with all concentrations. The diffusion coefficient of Pb^{2+} has been calculated and as expected it was found to be independent on the concentration of Pb(II).

Many plating experiments have been carried out to examine the lead deposit using different concentrations of Pb(II) solutions in methanesulfonic acid. It has been found that good, smooth and compact deposits can be accomplished from solutions of high Pb(II) concentrations together with lignin sulfonate as an additive as will be seen in following section. Moreover, it has been found that the adhesion between vitreous carbon and a lead deposit is not as strong as it should be in order to be applicable in the envisaged battery system. Other alternative substrates will be discussed in the section on base materials.

It has been noticed during preparation of 0.4 M Pb(II) in 2 M methanesulfonic acid solutions that all the lead carbonate initially dissolves in the acid but after 20 minutes, the solution becomes turbid and some white solid precipitates at the bottom of the reaction vessel. The temperature of the solution (50 ml in volume) decreases 3 K during the reaction which indicates an endothermic process. This indicates that a complex is produced when $PbCO_3$ reacts with methanesulfonic acid solution see [69]. Nevertheless, the solubility of this precipitate can be increased by increasing the temperature. For instance, in the above solution it has been noticed that all the precipitate has dissolved when the temperature of the solution increased to 333 K. It was not possible to record high quality voltammograms at a RDE with the 0.4 M Pb(II) solution because of the effects of IR drop.

It can be inferred from discussion above that

- lead deposition potential has been shifted positive with increasing Pb(II) concentration i.e. the nucleation is easier when the concentration is increased.
- I_L is proportional to concentration.
- adhesion between lead deposit and vitreous carbon is not very strong
- deposition at high current density without interference from H_2 evolution will only be possible at high Pb(II) concentrations because of the mass transport limitation.
- diffusion coefficient of Pb(II) in methanesulfonic acid is independent of concentration.
- finally and most importantly, a low overpotential for both lead deposition and dissolution is associated with high Pb(II) concentrations. These characteristics of

Pb^{2+}/Pb in methanesulfonic acid are very good for high energy efficiency in a battery application.

- at this stage, the optimum concentration of Pb(II) at room temperature appears to be 0.4 M.

3-2-2 Acid concentration

The concentration of methanesulfonic acid has been varied in order to study the effect on the voltammetry. Cyclic voltammograms have been recorded on rotating vitreous carbon disc electrode in 40 mm Pb(II) with different methanesulfonic acid concentrations, 0.0, 0.02, 0.2 and 2 M at a rotation rate of 400 rpm. The potential range was -0.15 V to -0.6 V and scan rate is 20 mV s^{-1}. The voltammogram in 2 M acid is shown in figure(1) while for 0.2 M acid is reported in figure(11). In both cases, well formed reduction waves are observed and well defined anodic stripping peaks can be seen. The ratio of Q_A/Q_C is 97.4 % and 92.3% respectively. It can be inferred from these values that the acid has supported both the deposition and dissolution of lead. The response for 0.02 M acid is shown in figure(12). It is immediately clear that the reduction wave is drawn out along the potential axes and no clear limiting current can be identified. Moreover, the anodic stripping peak is very broad. Clearly, the response is distorted by IR drop. Even so Q_A/Q_C = 92.8 %. Without acid, the response is very poor and strongly effected by IR distortion.

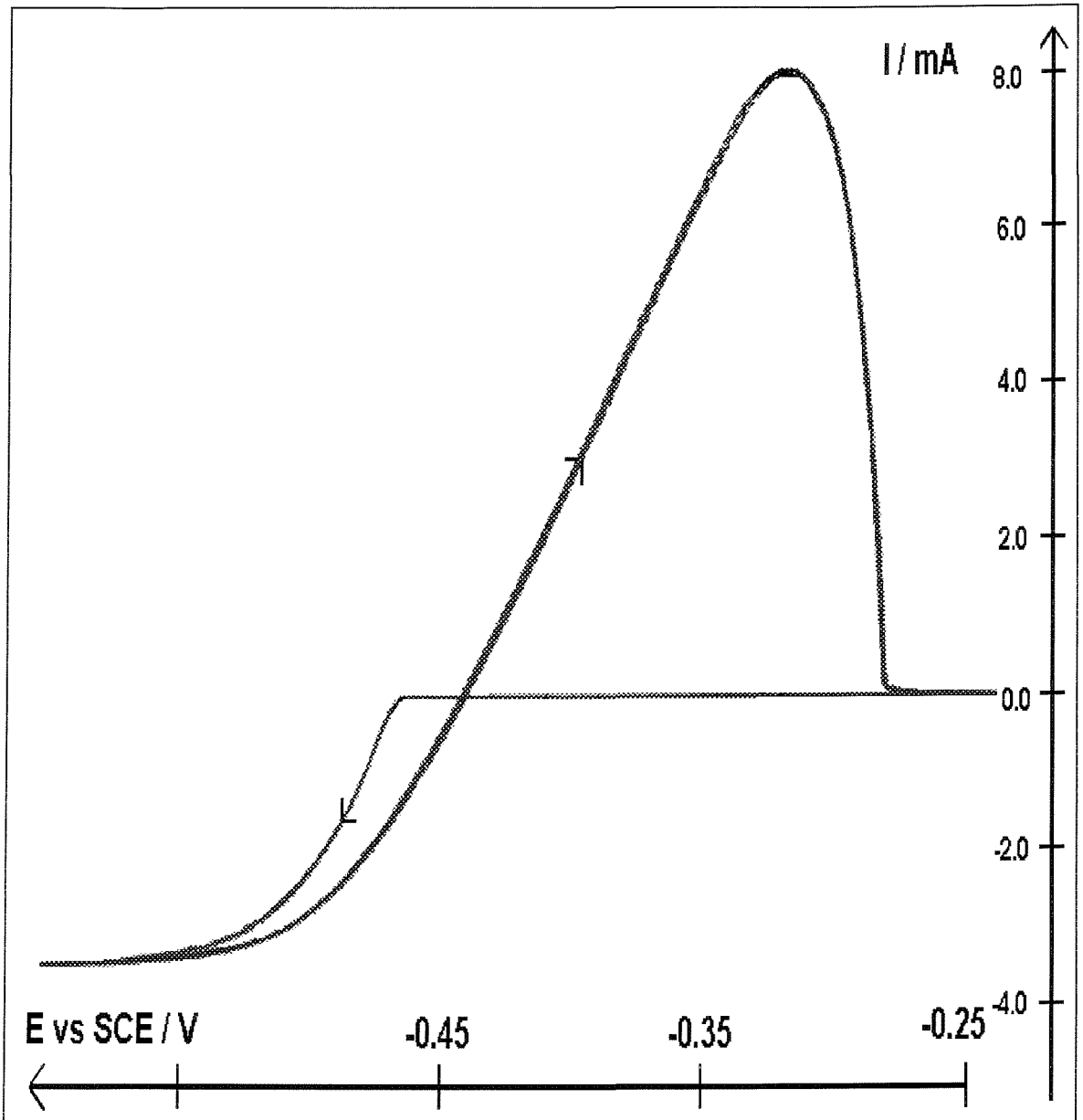

Figure (11) Cyclic voltammogram recorded on rotating vitreous carbon disc electrode (0.126 cm^2) from 40 mm Pb(II) in 0.2 M methanesulfonic acid at 400 rpm at room temperature. the potential range is -0.15 to -0.6 V.

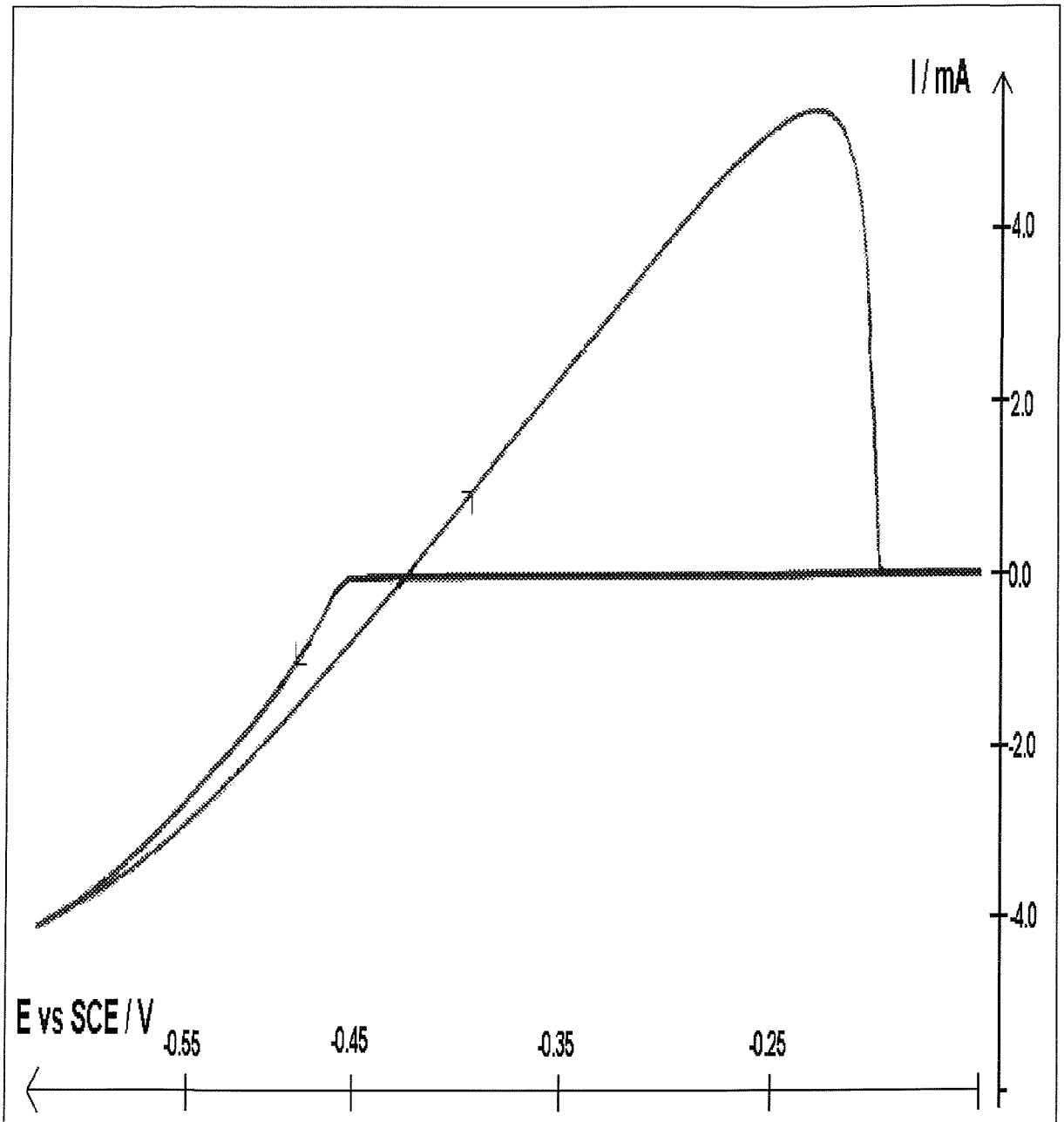

Figure (12) Cyclic voltammogram recorded on rotating vitreous carbon disc electrode (0.126 cm^2) from 40 mm Pb(II) in 0.02 M methanesulfonic acid at 400 rpm at room temperature. the potential range is -0.15 to -0.6 V.

The above experiments clearly show that the acid concentration has a major influence upon the deposition process. The resistance of the solution can be easily decreased by increasing the acid concentration in the plating solution. Free acid then supports the conductivity of the plating bath and reduces the energy required for the charging process and increases the current efficiency. It has been found that the ~ 2 M methanesulfonic acid is satisfactory for good lead plating.

3-2-3 Effect of additives

In the absence of any additives, lead deposits with a very small overpotential, as described in previous sections. The deposit tends to be rough and porous. Dendrites are always associated with lead deposits in the experiments which have been carried out without additive throughout this project. Therefore, addition agents appear essential for lead plating in the methanesulfonic acid solutions. Lignin sulfonate have been used as an additive in various concentrations to investigate its effects on the voltammogram of lead deposition and on the quality of deposit. Lignin sulfonate has been used as an additive agent in electroplating for a long time [68].

The kinetics of the Pb^{2+}/Pb system has been investigated in the presence of the sodium lignin sulfonate by running voltammograms of a solution containing 40mm Pb(II) in 2M methanesulfonic acid, with and without any additive. The cyclic voltammograms have been recorded at a rotating nickel disc electrode at rotation rate of 400 rpm and potential range of -0.3 to -0.65 V. Figure (13) shows the voltammogram without additive ; there is a single reduction wave at $E_{1/2}$ =-0.48 V for lead electrodeposition. The deposition reaches a steady state current where the deposition is under mass transport control conditions with a limiting current density of 20 mA cm^{-2}. In the reverse scan the deposition continues until a potential of -0.45 V where the current decreases to zero which corresponds to the equilibrium potential for Pb^{2+}/Pb system. Positive to -0.45 V an oxidation current is present with an anodic peak at -0.36 V indicating a dissolution process of the deposited lead. The charge ratio, Q_A/Q_C, under the anodic and the cathodic peaks is 99%. This percentage suggests that there is no other competitive reactions with lead deposition hence, the current efficiency is very high. On the other hand, figure(14) shows a recorded cyclic

voltammogram on rotating nickel disc electrode at the same conditions of the above experiment but 1 g/l sodium lignin sulfonate has been added to the solution as an addition reagent. In figure (14) a reduction wave can be seen for lead deposition at a $E_{1/2}$ = -0.53 V. Clearly the wave is drawn out leading to the conclusion that the additive has reduced the rate of deposition of Pb over some of the potential range. The plateau is not well defined. The deposition continues during the reverse scan until a potential of -0.45 V. A dissolution peak appears at a potential of -0.36 V. The charge ratio in this case is slightly lower compared to the solution without additive; Q_A/Q_C = 97 %. Again, there is no other significant competing reaction with lead deposition within the potential range used in these experiments.

Clearly the lignin sulfonate has reduced significantly the deposition rate in the region of the cathodic wave and also has increased the lead deposition overpotential. This effect might be ascribed to an inhibition effect of the lignin sulfonate on the lead deposition process. Therefore, it could be inferred that lignin sulfonate has changed the thermodynamics and kinetics of the Pb^{2+}/Pb system either by forming a complex with Pb(II) or by an adsorption process on the surface of the substrate[see reference 40].

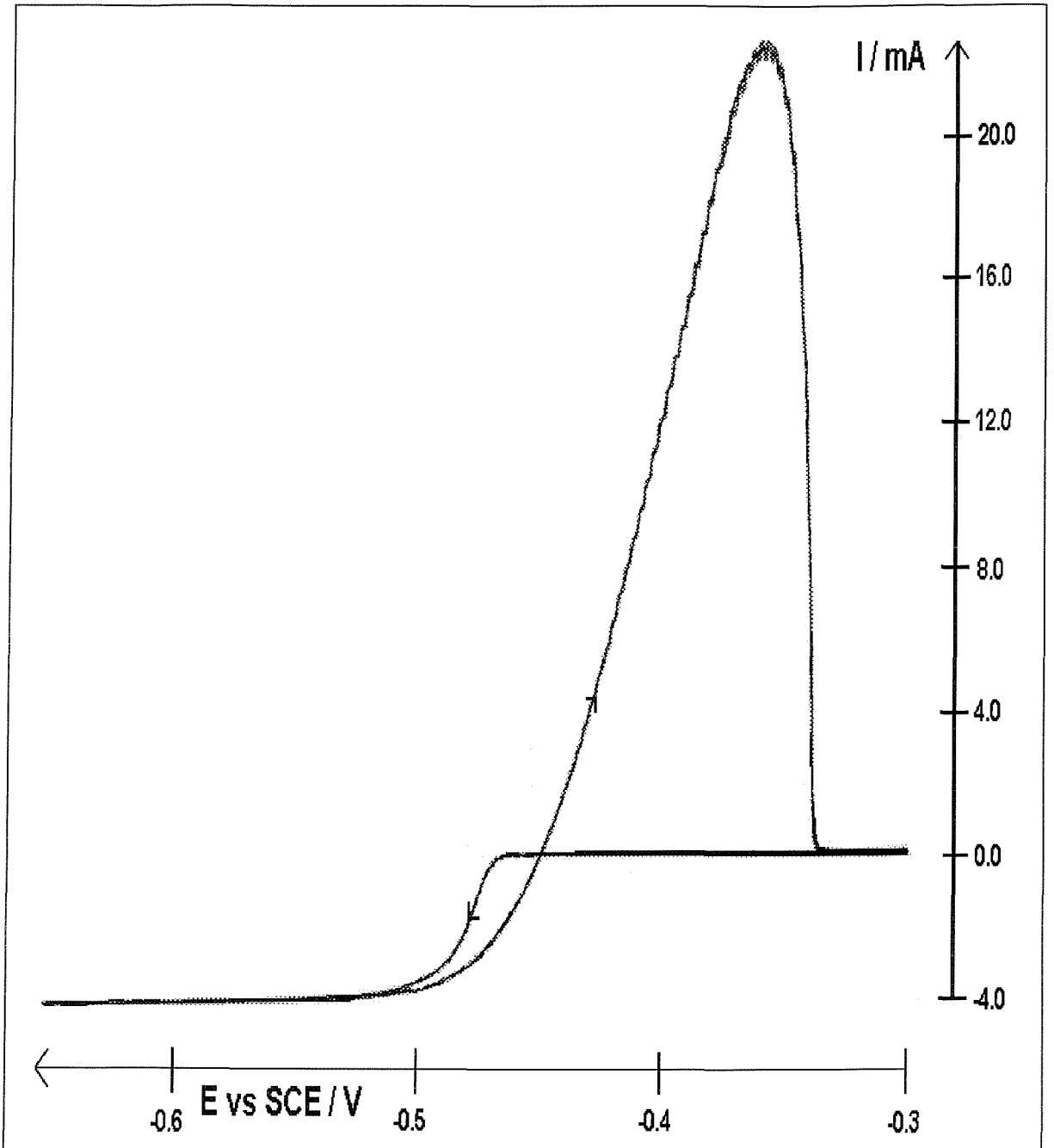

Figure (13) Voltammogram recorded on rotating nickel disc electrode (0.2 cm^2) from 40 mM Pb(II) in 2 M methanesulfonic acid without any additives at a rotation rate of 400 rpm.

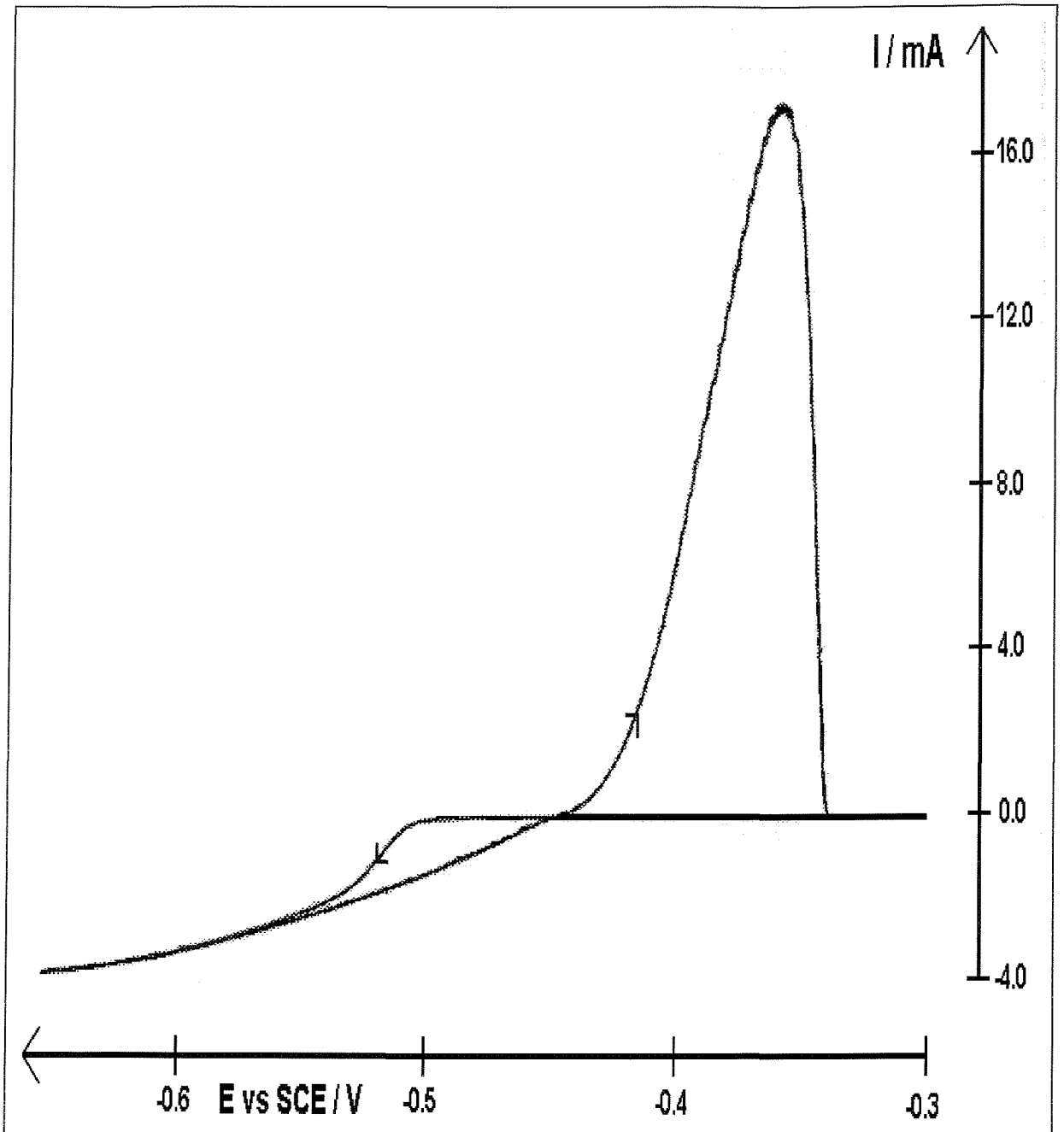

Figure (14) Voltammogram recorded on rotating nickel disc electrode (0.2 cm^2) from 40 mM Pb(II) in 2 M methanesulfonic acid with 1 g/l lignin sulfonate at a rotation rate of 400 rpm.

Figure (15) shows a cyclic voltammogram recorded on rotating nickel disc electrode from 40 mM Pb(II) in 2 M methanesulfonic acid with various additions of lignin sulfonate at a rotation rate of 400 rpm. With 5 g/l lignin sulfonate, the voltammogram clearly shows two reduction waves with $E_{1/2}$ = -0.52 V and -0.60 V and it can be seen that the two waves have almost equal heights. At the lower lignin sulfonate concentrations, the two waves can still be seen but the more negative wave is smaller and less defined. It should be noted that by -0.7 V, there is a limiting current with the same value as in the absence of lignin sulfonate. In other words, all the Pb(II) is then reduced under mass transport control. In addition, it can be seen that the more positive wave is becoming less steep and shifts negative as the lignin sulfonate is increasing.

Different rotation rates were used to examine the effect on the voltammogram which was recorded for a rotating nickel disc electrode from 40 mM Pb(II) in 2M methane sulfonic acid and 1 g/l lignin sulfonate. The result is represented in figure (16). The two reduction waves are now very obvious but reasonable plateaux are seen at the negative at the end of the potential scan. It is clear from the figure that I_L at negative limit is proportional to $\omega^{1/2}$. The average diffusion coefficient was calculated from the current at -0.7 V was $5.4 \pm 0.3 \times 10^{-10}$ $m^2 s^{-1}$.

Lignin sulfonate has a greater effect on lead deposition when vitreous carbon was used as a substrate. Figure (17) shows a cyclic voltammogram recorded on rotating vitreous carbon disc electrode from 40 mM Pb(II) in 2 M methanesulfonic acid and 1.0 g/l lignin sulfonate at a rotation rate of 400 rpm. A reduction wave is seen at a potential of $E_{1/2}$ = -0.63 V indicating lead deposition. Clearly, a significantly higher nucleation overpotential is required when lignin sulfonate is in the solution. A slightly drawn out wave is seen at the end of the negative scan without any clear plateau. If the potential is extended to more negative (> -0.85 V), a second reduction wave and at the same time gas bubbles are easily seen at the surface of the electrode which is an indication of hydrogen evolution. In the reverse scan, the deposition continues with increasing current probably because of an increase in the area of the electrode which, in turn, caused by the development of lead dendrites. The current reaches zero for

Pb^{2+}/Pb system at -0.45 V and holds at zero for a few millivolts before the anodic stripping peak at -0.40 V. The peak is followed by a tail which decreases gradually until it finally reaches zero current. The charge under the anodic peak is not comparable to the charge under the cathodic peak ($Q_A/Q_C \sim 10$ %). Further it has been noticed during the stripping scan that there was some small particles of lead falling down from the electrode. Clearly, this can only lead to the conclusion that the lead does not adhere enough to the surface of the vitreous carbon in the presence of lignin sulfonate (compare with figure 1).

One explanation of two waves would be that the Pb(II) in solution exists in two forms, one which involves lignin sulfonate as a ligand. Some researchers claim that there is an interaction between lead(II) and methanesulfonate (without additives) ions and two stepwise lead complexes are formed in the solution: $[Pb(CH_3SO_3)]^+$, $[Pb(CH_3SO_3)_2]$ and $[Pb(CH_3SO_3)]^{3-}$ [69]. Therefore, the complication may increase in the existence of lignin sulfonate in the solution.

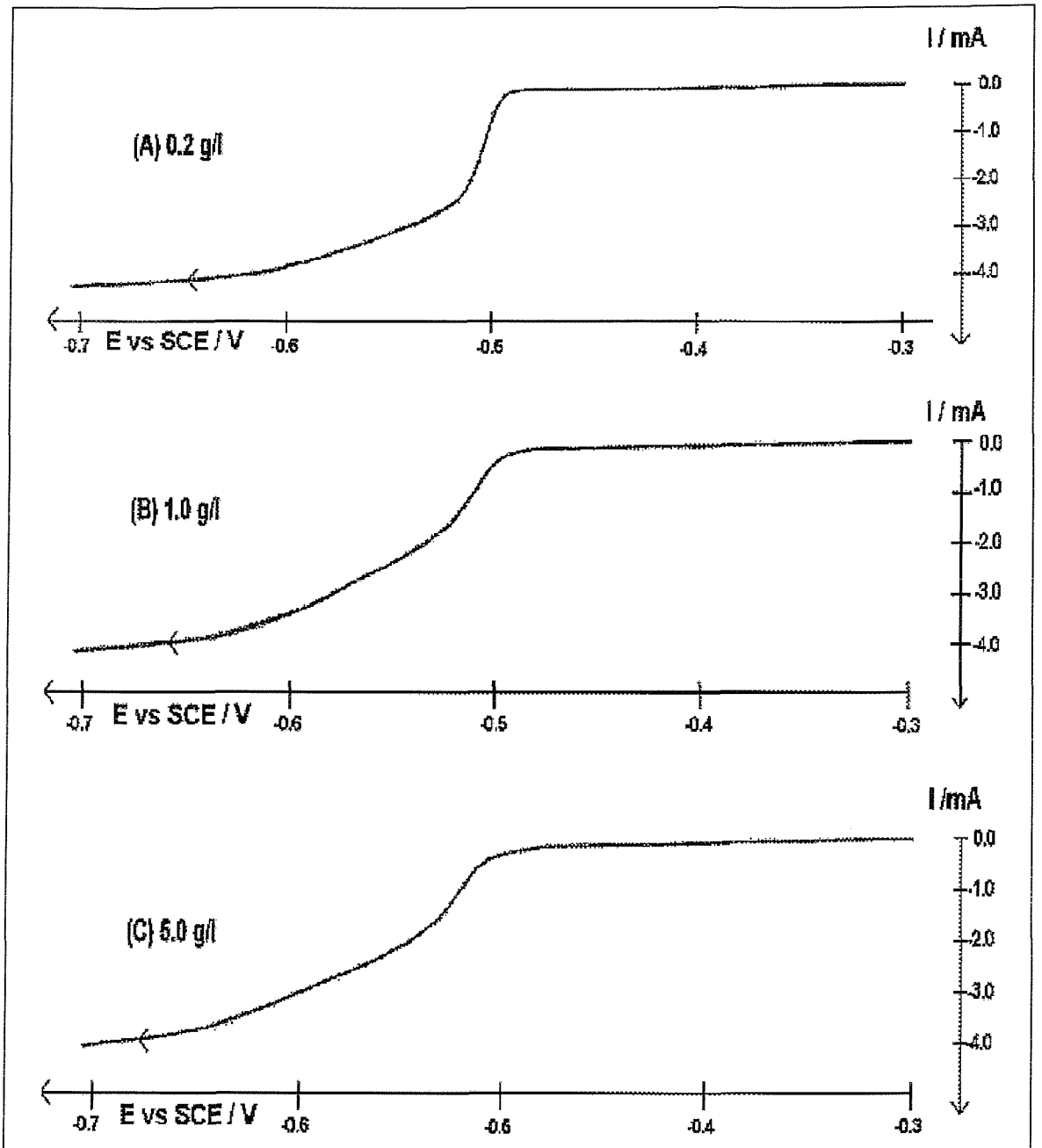

Figure (15) Effect of lignin sulfonate concentration on the voltammogram. Three voltammograms recorded on rotating nickel disc electrode (0.2 cm^2) from 40 mM Pb(II) in 2 M methanesulfonic acid + lignin sulfonate. (A) 0.2 g/l, (B) 1.0 g/l and (C) 5.0 g/l lignin sulfonate.

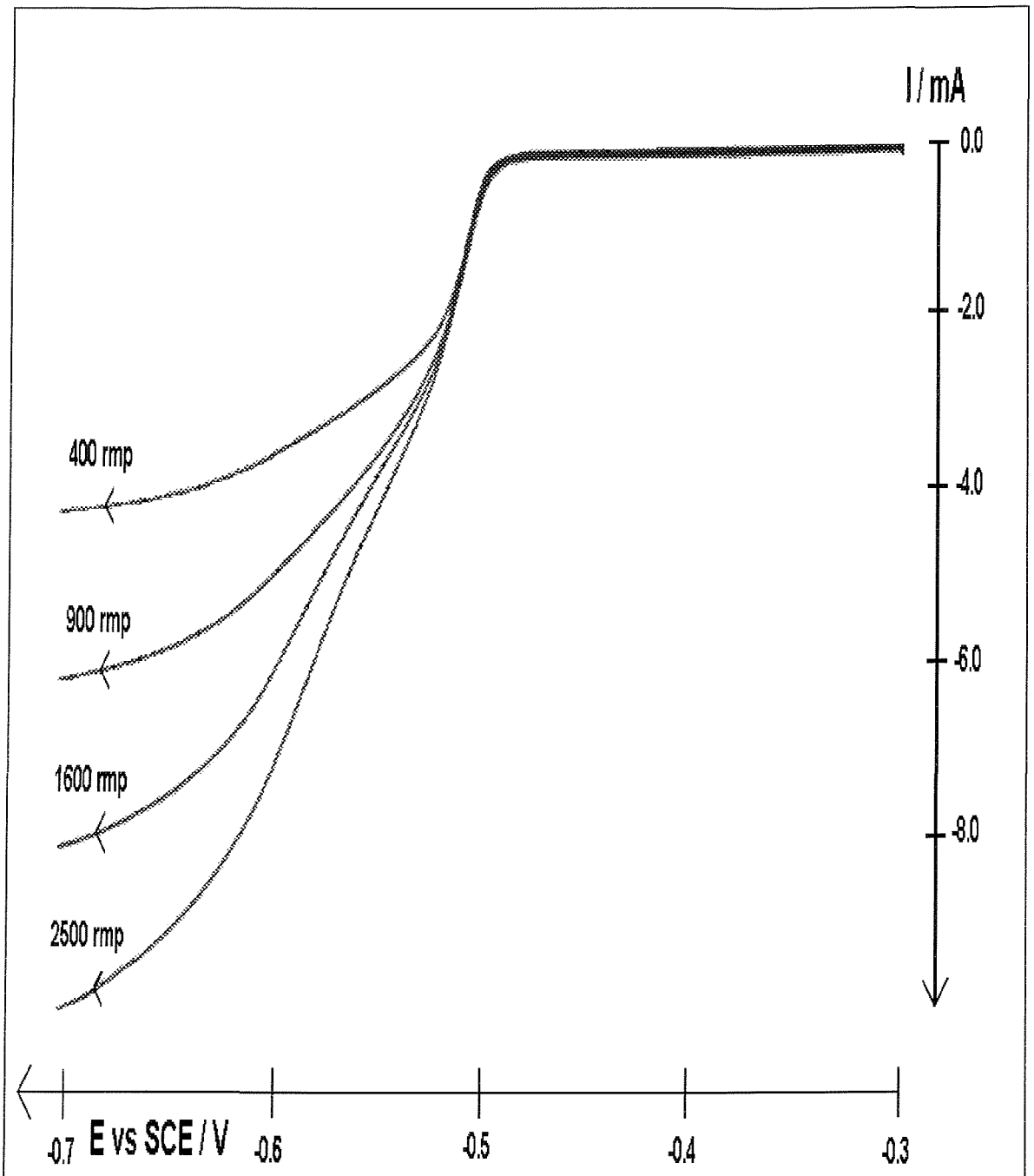

Figure (16) Voltammograms recorded on rotating nickel disc electrode (0.2 cm^2) at various rotation rates from 40 mM Pb(II) in 2 M methanesulfonic acid solution + 1 g/l lignin sulfonate.

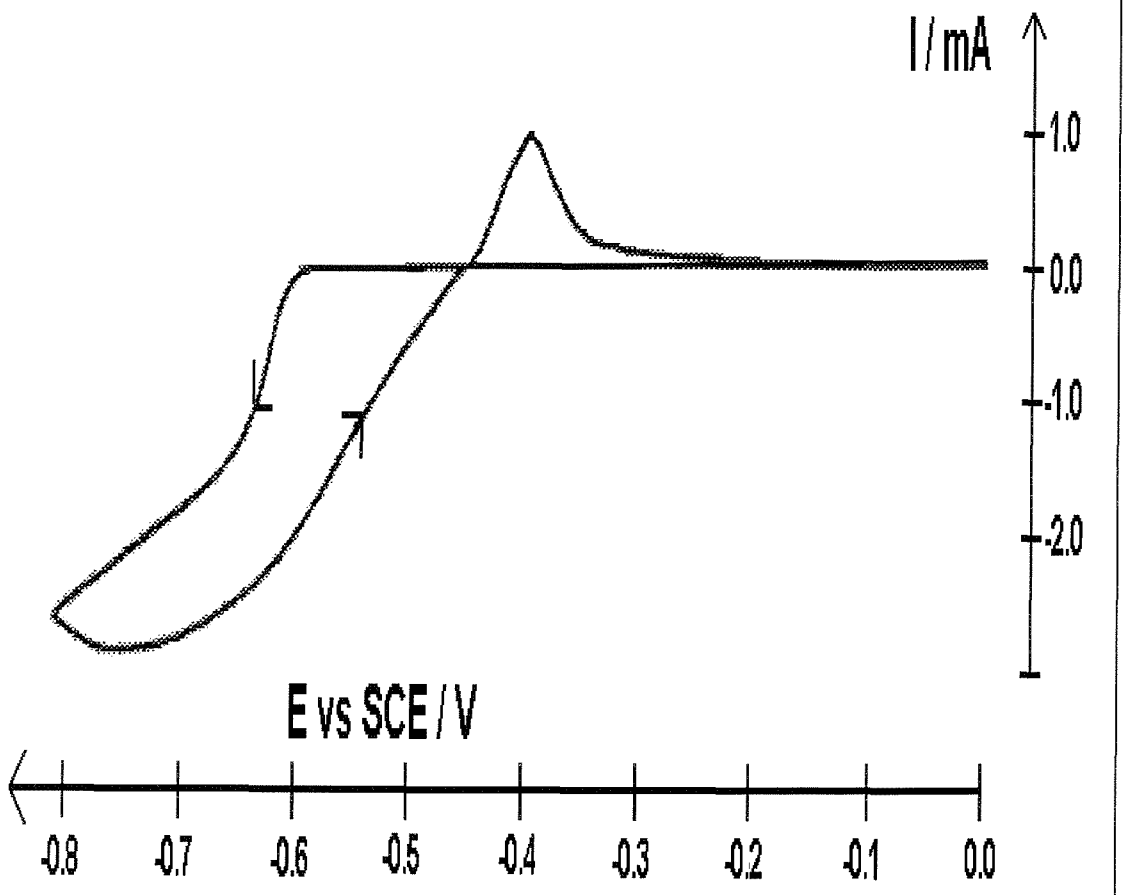

Figure (17) Cyclic voltammogram recorded on rotating vitreous carbon disc electrode (0.126 cm^2) from 40 mM Pb(II) in 2 M methanesulfonic acid solution + 1 g/l lignin sulfonate.

A range of lignin sulfonate concentrations has been used to study the effect on the quality of the deposit. Figures (16-18) compare photographs of lead deposits on a nickel RDE from solutions containing 2 M methanesulfonic acid + 0.4 M Pb(II) with 0.0, 0.1 and 1.0 g/l lignin sulfonate. In all cases the current density is -63 mA cm^{-2} and the charge passed is 85 C cm^{-2} (equivalent of a thickness of 80 μm). Without the additive, the deposit can be seen to be porous and very non-uniform. Even with only 0.1 g/l lignin sulfonate, the deposit is much more uniform except for a slight edge effect. It is also much less porous. When the lignin sulfonate is increased to 1.0 g/l, the

deposit is improved further. Hence it can be seen that low concentrations of lignin sulfonate (0.1- 1.0 g/l) is sufficient to produce smooth, compact and flat lead deposit. The adhesion between the deposited lead and nickel substrate is very strong hence, it can be used as an electrode in a battery. The efficiency of a battery is expected to be reasonable since the deposited lead will not be lost during the discharge process.

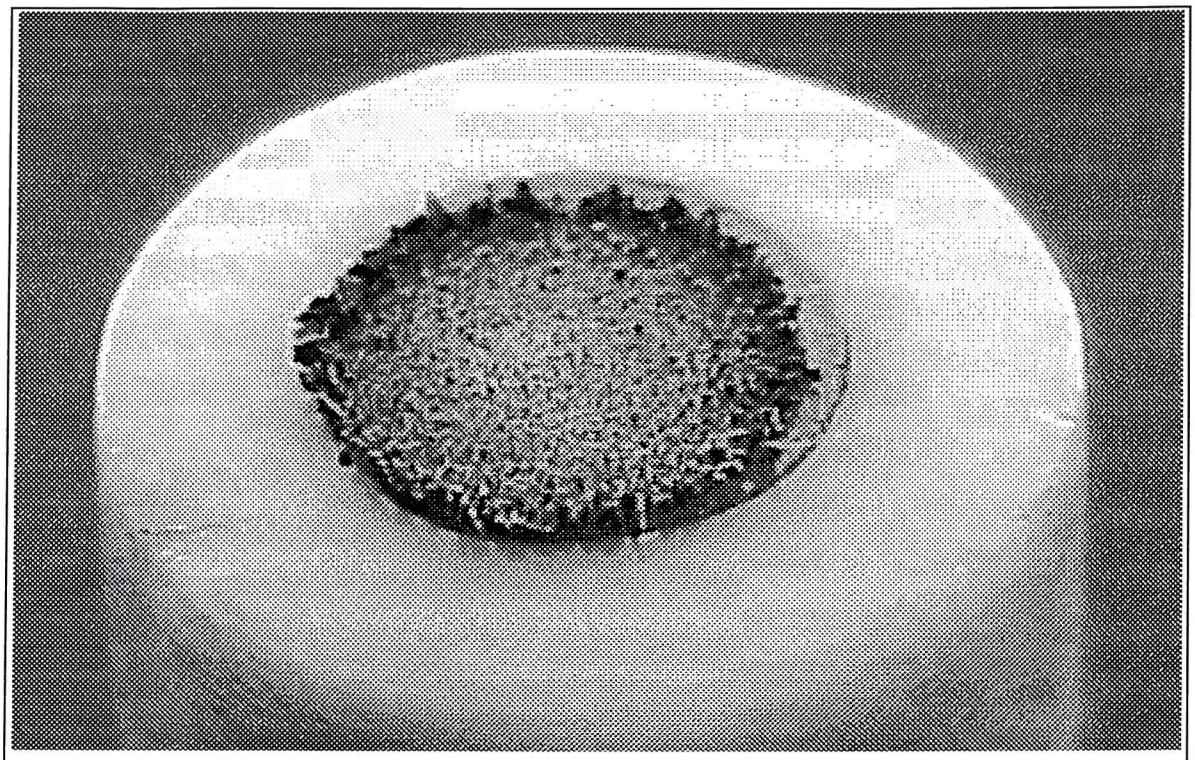

Figure (18) Lead deposited on rotating nickel disc electrode (0.2 cm^2) from 400 mM Pb(II) in 2.0 M methanesulfonic acid and 0.0 g/l lignin sulfonate at current density of -63 mA cm^{-2} at room temp. Rotation rate is 200 rpm. 22.5 min.

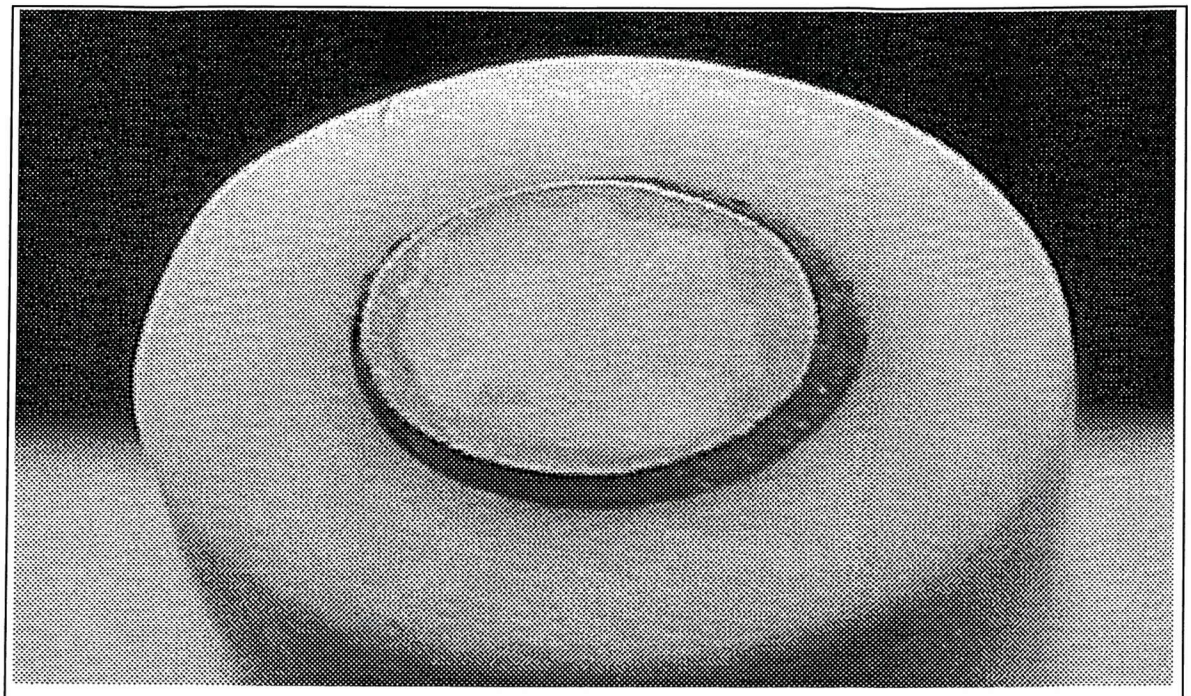

Figure (19) Lead deposited on rotating nickel disc electrode (0.2 cm^2) from 400 mM Pb(II) in 2.0 M methanesulfonic acid and 0.1 g/l lignin sulfonate at current density of -63 mA cm^{-2} at room temp. Rotation rate is 200 rpm. 22.5 min.

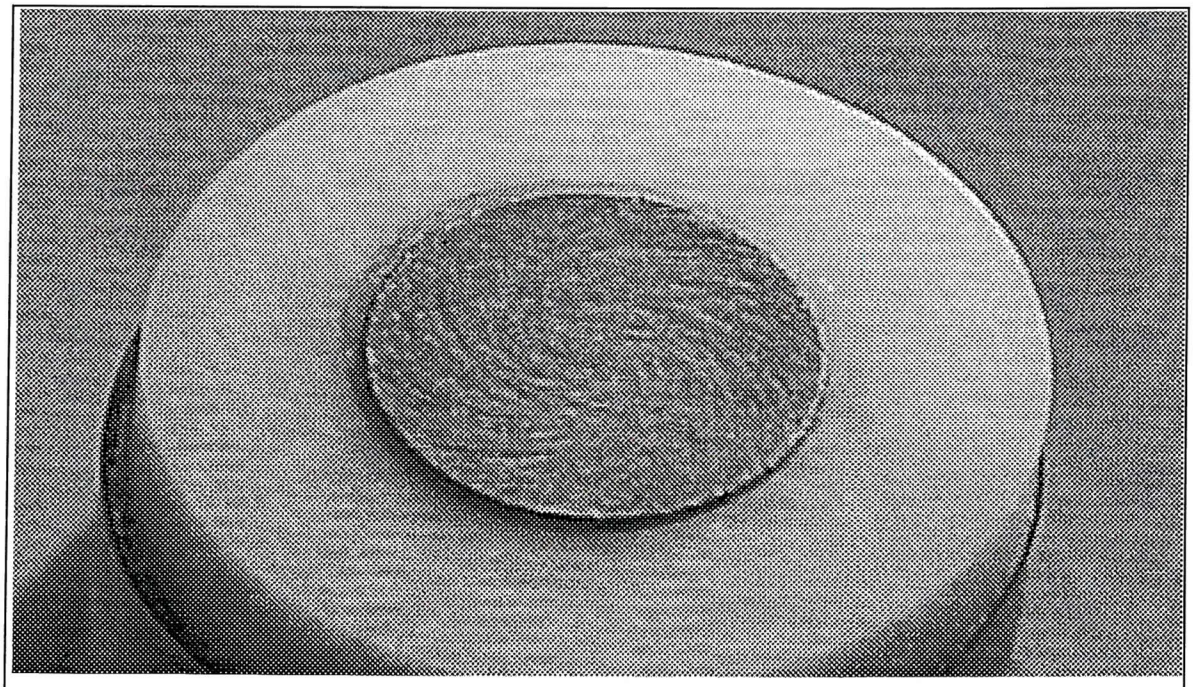

Figure (20) Lead deposited on rotating nickel disc electrode (0.2 cm^2) from 400 mM Pb(II) in 2 M CH_3SO_3H acid and 1.0 g/l lignin sulfonate at current density of -63 mA cm^{-2} at room temperature. Rotation rate is 200 rpm. 22.5 min.

SEM has been used to confirm the smoothing effect of lignin sulfonate on lead deposition. Figures (19-23) show different magnifications of lead deposited on rotating nickel disc electrode at 200 rpm from 0.4 M Pb(II) + 2 M in methanesulfonic acid + 1 g/l lignin sulfonate and using a current density of 8 mA cm^{-2} (deposition charge: -86.4 C cm^{-2}) The deposit is very smooth, compact and free of porous. Even with at very small magnifications the quality still can be seen. Clearly, the effect of lignin sulfonate is very obvious at the conditions used in the previous experiments.

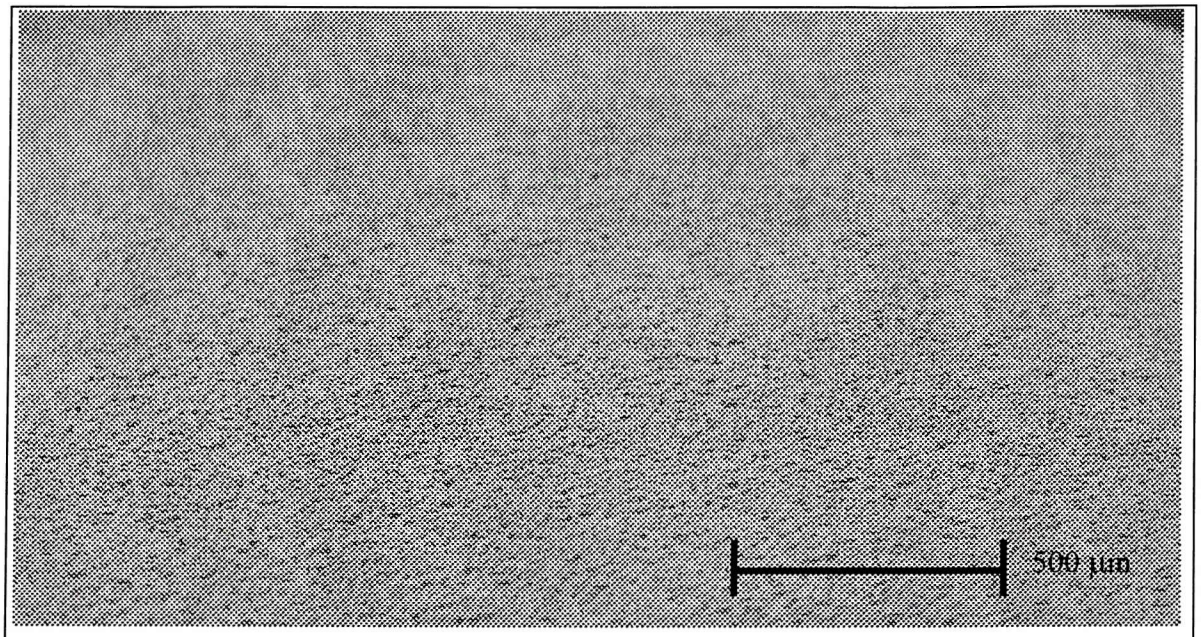

Figure (21) SEM for lead deposited on rotating nickel disc electrode (0.2 cm^2) at 200 rpm and a current density of 8.0 mAcm^{-2} from a solution of 0.4 M Pb(II) in 2 M methanesulfonic acid + 1 g/l lignin sulfonate. Magnification is 50X. Side view with an angle of 70^{O}.

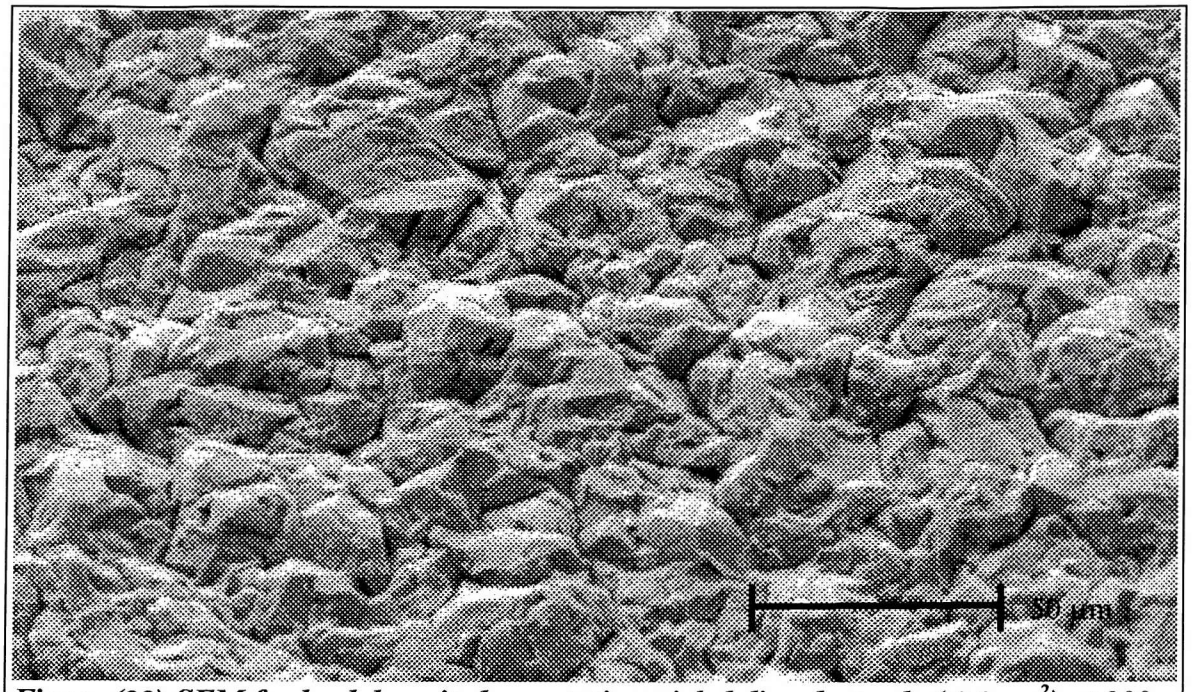

Figure (22) SEM for lead deposited on rotating nickel disc electrode (0.2 cm^2) at 200 rpm and a current density of 8.0 $mAcm^{-2}$ from a solution of 0.4 M Pb(II) in 2 M methanesulfonic acid + 1 g/l lignin sulfonate. Magnification is 500X. Side view with an angle of 70^O.

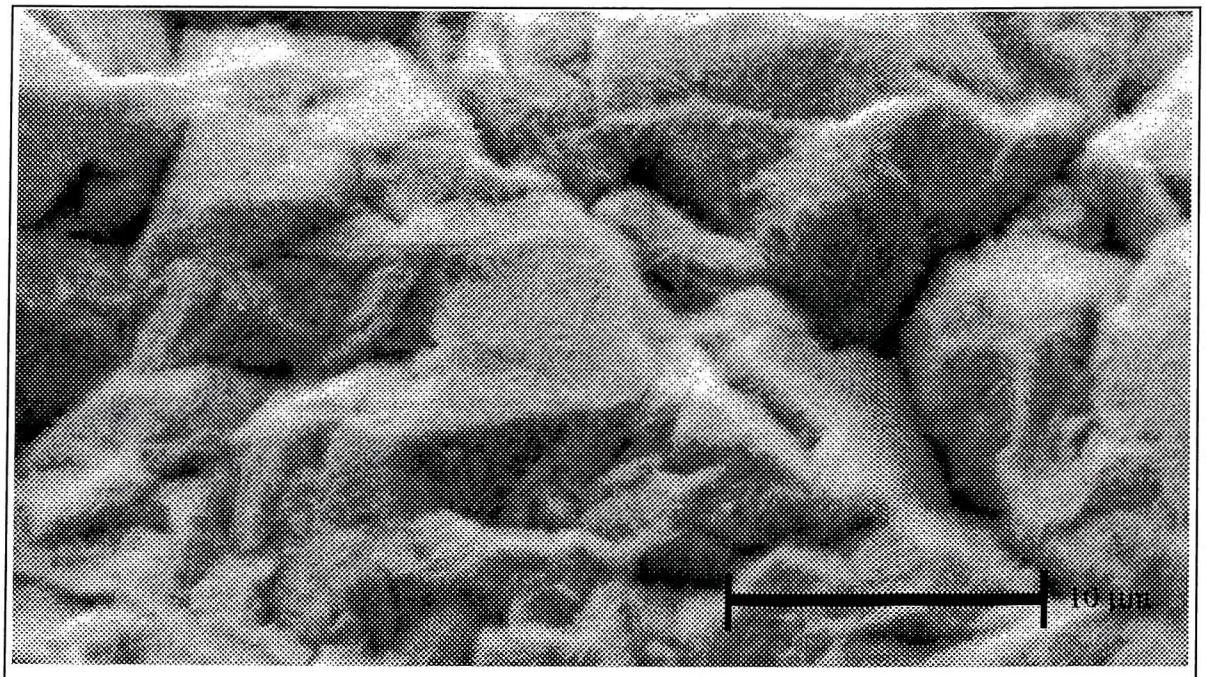

Figure (23) SEM for lead deposited on rotating nickel disc electrode (0.2 cm^2) at 200 rpm and a current density of 8.0 $mAcm^{-2}$ from a solution of 0.4 M Pb(II) in 2 M methanesulfonic acid + 1 g/l lignin sulfonate. Magnification is 2000X. Side view with an angle of 70^O.

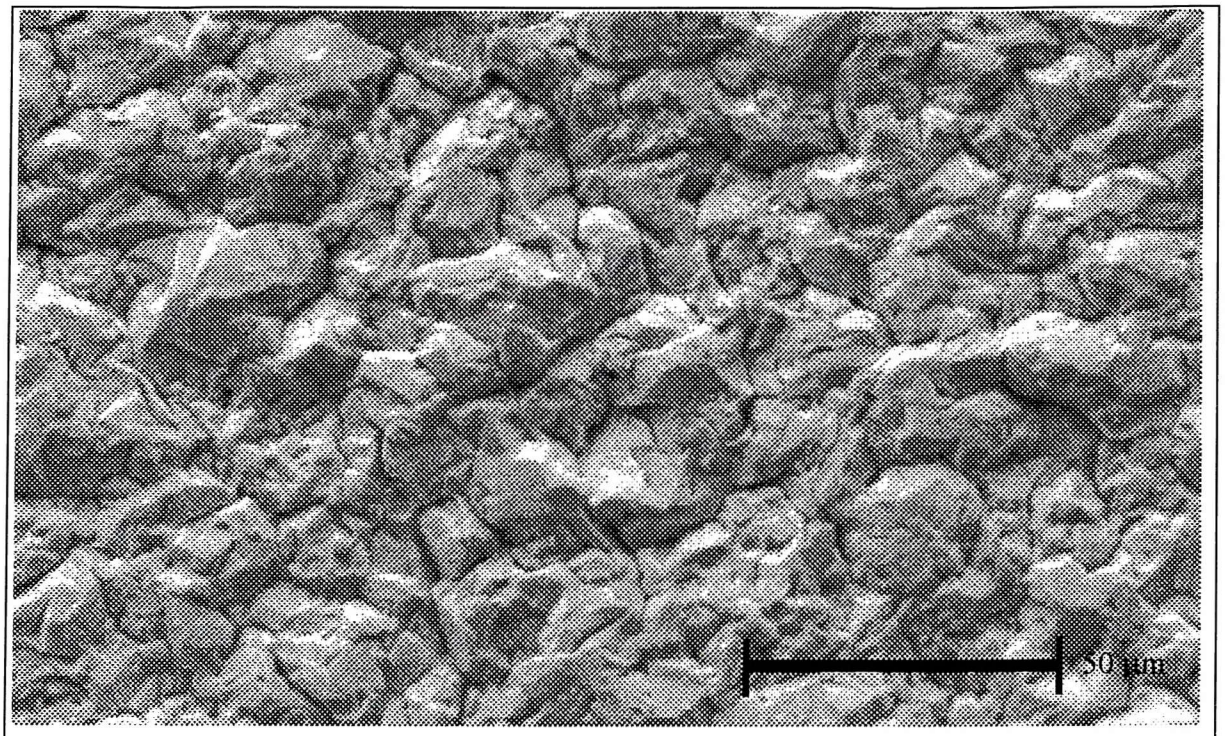

Figure (24) SEM for lead deposited on rotating nickel disc electrode (0.2 cm^2) at 200 rpm and a current density of 8.0 $mAcm^{-2}$ from a solution of 0.4 M Pb(II) in 2 M methanesulfonic acid + 1 g/l lignin sulfonate. Magnification is 500X. Top view.

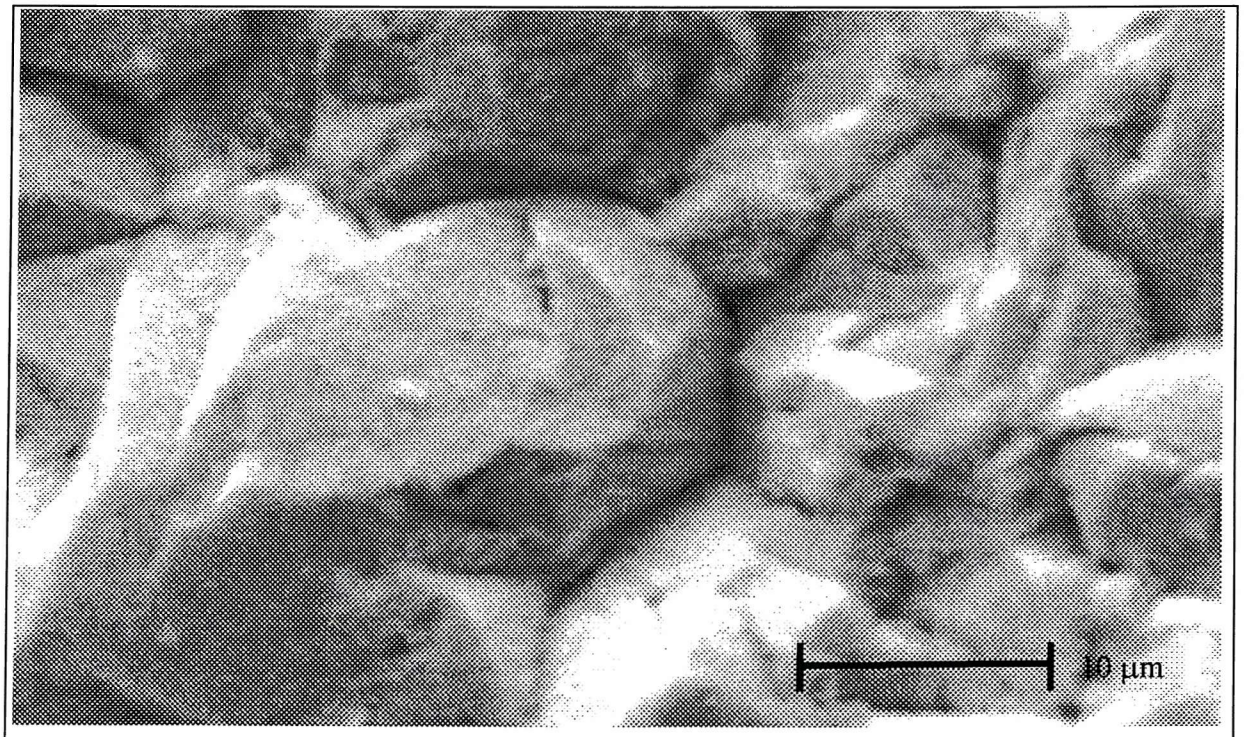

Figure (25) SEM for lead deposited on rotating nickel disc electrode (0.2 cm^2) at 200 rpm and a current density of 8.0 $mAcm^{-2}$ from a solution of 0.4 M Pb(II) in 2 M methanesulfonic acid + 1 g/l lignin sulfonate. Magnification is 2000X. Top view.

It should be noted that the solubility of lignin sulfonate is limited in Pb(II) solutions. For instance, in 0.4 M Pb(II) in 2 M methanesulfonic acid it was noticed that 5 g/l of lignin sulfonate does not completely dissolve in the solution; rather a brown material is precipitated in the bottom of the flask and some is floating on top of the flask. Increasing the temperature does not increase the solubility significantly. On the other hand, 5 g/l lignin sulfonate dissolves in acid only or solutions containing low Pb(II) concentrations. Therefore, it is inferred that lignin sulfonate has a limited solubility in solutions containing high concentration of Pb(II). This may be a viscosity problem or the precipitation of Pb(II) lignin sulfonate. Also it has been noticed that during the preparation of 1g/l of lignin sulfonate in 40 mM Pb(II) in 2 M methanesulfonic acid, that the colour of the solution is yellow-brownish immediately after preparation. Then after using the solution, the colour becomes less sharp and tends to be colourless. It is not clear the change in colour is due to a complexing reaction or consumption of the lignin sulfonate or even hydrolysis of lignin sulfonate in the acid solution .

The following points should be noted :

- sodium lignin sulfonate has improved the quality of the lead deposit and thick deposits may be electroplated.
- SEMs and photos of the lead deposit show that the surface is continuous and compact but made of several μm crystals.
- small amount of the additive is sufficient for a smooth lead deposit.
- the deposition potential of lead has been shifted to negative values in the presence of lignin sulfonate.
- the two waves in the voltammogram in the presence of lignin sulfonate suggests more than one Pb(II) species in the solution.
- diffusion coefficient of the Pb(II) has not been changed significantly in the presence of the additive.
- voltammograms show that the additive has a greater effect on vitreous carbon than on nickel electrodes.

- the adhesion between the lead deposit and vitreous carbon is not very strong and even became very weak in the presence of the lignin sulfonate. On the other hand, adhesion is good on nickel.

3-2-4 Temperature

The effect on the lead deposition voltammogram of temperature has been studied and recorded on two rotating disc electrodes. In one series of experiments, cyclic voltammograms have been recorded on rotating vitreous carbon disc electrode from 40 mM Pb(II) in 2 M methanesulfonic acid solution at a rotation speed of 200 rpm at three temperatures 301, 313 and 333 K. The deposition overpotential has decreased with the increase of temperature. The limiting current has also increased in magnitude as a result of temperature increase. Apart from the deposition potential all other features of the voltammograms are the same at all temperatures. Clearly the thermodynamics of the deposition process has been little affected by the temperature change but nucleation is enhanced at the higher temperature. In addition, the limiting current density increases with temperature.

In another series of experiments, rotating nickel disc electrode has been used in the same solution conditions. Again three temperature have been used. Unlike the vitreous carbon, the deposition potential is the same in all temperatures see figure (26). Nucleation on nickel is always rapid. However the steepness of the reverse scan around -0.45 V increases with temperature. The kinetics of the Pb/Pb(II) couple appears to increase with temperature. Of course, I_L also increases. Therefore, the material of the electrode has a major effect on the Pb/Pb(II) system. It is clear also from the result above that the elevated temperature has facilitated the mass transport of lead ions to the surface and therefore increased the quantity of lead deposit. Elevated temperature also has an effect on the conductivity of the solution since it enhances the movement of the ions in the solution.

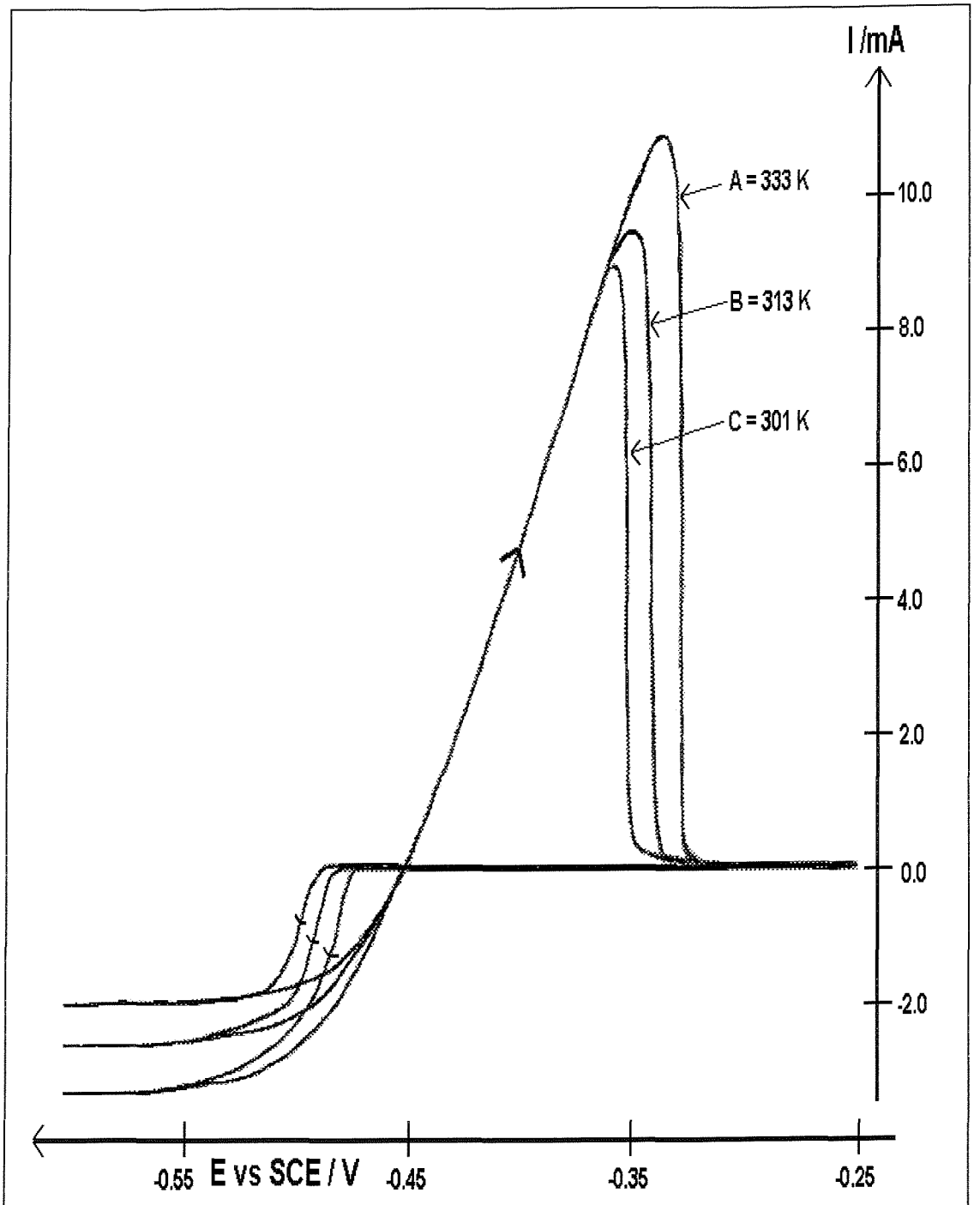

Figure (26) Cyclic voltammogram on rotating nickel disc electrode (0.2 cm^2) from 40 mM Pb(II) in 2 M methanesulfonic acid at various temperature.

Photographs of lead deposited at 298, 313 and 333 K from solution of 2 M methanesulfonic acid + 0.4 M Pb(II) and 1.0 g/l lignin sulfonate (deposition charge: -86.4 C cm^{-2}) are shown in figures (27-29). At the high current density (-128 mA cm^{-2}), the quality of the deposit improves greatly with temperature.

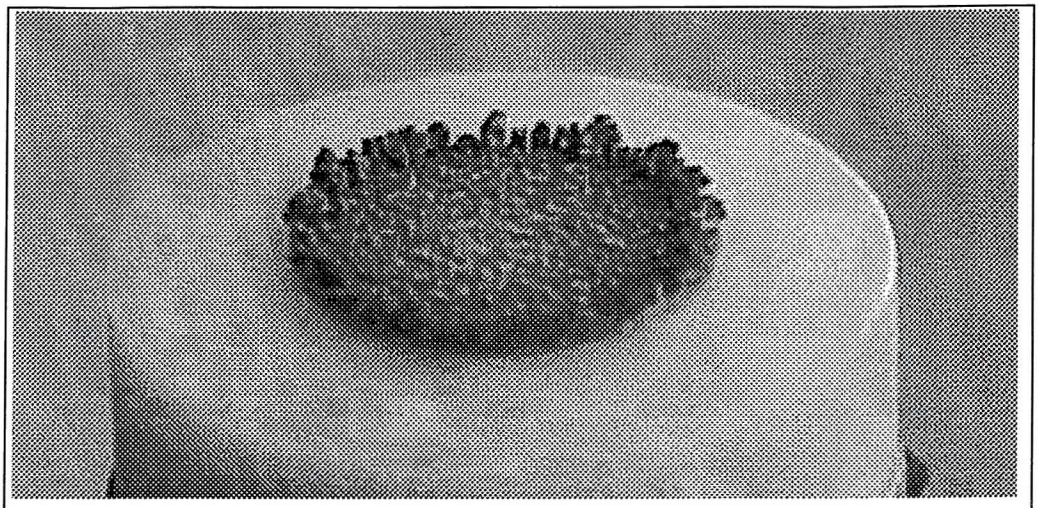

Figure (27) Lead deposited on rotating nickel disc electrode (0.2 cm^2) from 400 mM Pb(II) in 2.0 M methanesulfonic acid and 1.0 g/l lignin sulfonate at current density of -128 $mAcm^{-2}$ at room temperature. Rotation rate is 200rpm. 11.25 min.

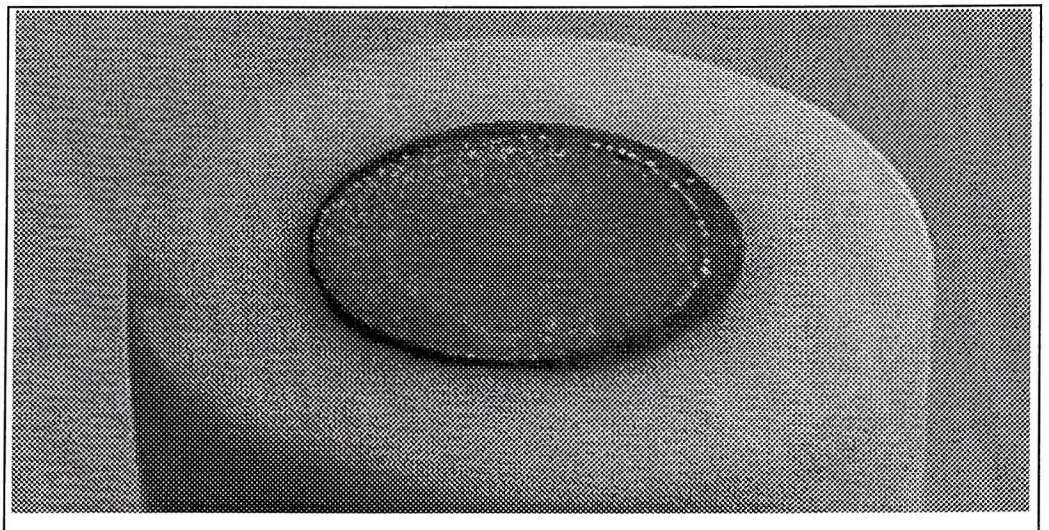

Figure (28) Lead deposited on rotating nickel disc electrode (0.2 cm^2) from 400 mM Pb(II) in 2.0 M methanesulfonic acid and 1.0 g/l lignin sulfonate at current density of -128 mA cm^{-2} at 313 K. Rotation rate is 200 rpm. 11.25 min.

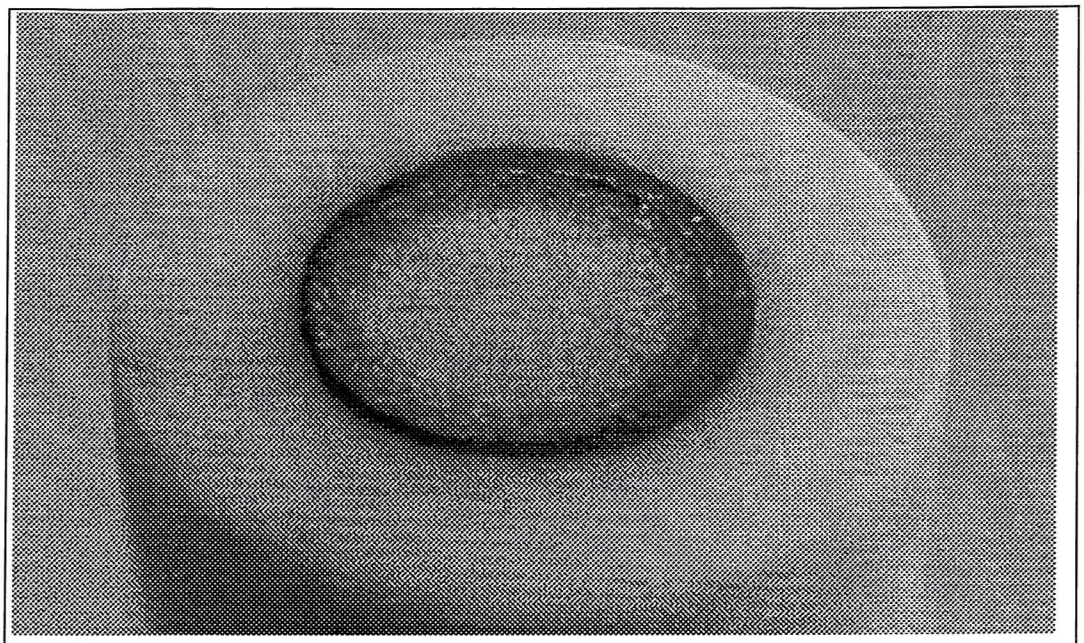

Figure (29) Lead deposited on rotating nickel disc electrode (0.2 cm^2) from 400 mM Pb(II) in 2.0 M methanesulfonic acid and 1.0 g/l lignin sulfonate at current density of -128 mA cm^{-2} at 333 K. Rotation rate is 200 rpm. 11.25 min.

As a result, increasing the temperature of the solution leads to

- an increase in the rate of mass transport.
- an increase in the solubility of Pb(II) and probably lignin sulfonate.
- an increase in the conductivity of the solution.
- improves the quality of the lead deposit.

3-2-5 Base materials

Different materials have been used as substrates to deposit lead from Pb(II) solutions in methanesulfonic acid. Vitreous carbon, gold, nickel, titanium, graphite, mild steel and stainless steel have been used. Deposit quality and adhesion between the deposited lead and the substrate material was the main aim of this study. Many cyclic voltammograms have been carried out on the materials previously mentioned together with a great number of plating experiments. Stability of the substrate in acidic mediums

have been taken into account though no attempt has been made to study the corrosion behaviour of such substrate in the solutions under study.

Gold and nickel were found to give well defined voltammetric waves with flat plateaux. With titanium, vitreous carbon and graphite the voltammograms were not as good. Cyclic voltammograms on vitreous carbon are very distorted in the presence of lignin sulfonate (see above). Less distortion has been seen in the case of graphite. This suggests that the roughness of the surface together with the additive, might affect the cyclic voltammogram features.

In the case of vitreous carbon the effect is very clear and the inhibition effect of lignin sulfonate can be seen in figure (17). The adhesion between the deposited lead and the vitreous carbon is very weak in the presence of lignin sulfonate probably because of the adsorption of the lignin sulfonate on the smooth surface of the electrode hence, this might support the adsorption theory of the additive on the electrode surface[40].

The following tables summarise the effect of base materials on lead deposition with respect to adhesion, smoothness and morphology.

Electrode	**Solution**	**j** **mA/ cm^2**	**Deposit**
Vitreous carbon	Commercial fluoroborate	-8 45 min.	Very little deposit around the edges of the electrode.
Vitreous carbon	Commercial fluoroborate	-16 45 min.	Bad, coarse, porous, spherical lumps, partially covers and not adhered to the surface. There are spherical lumps on the electrode surface with needles at the base of the spherical lumps.
Vitreous carbon	0.1 Pb^{2+} in 2M CH_3SO_3H	-8 45 min.	Silver in colour. Coarse, porous, spherical lumps, partially covered and weak adhered to the surface. There are two kinds of structures; needles and spheres.
Vitreous carbon	0.4 M Pb^{2+} in 2M CH_3SO_3H	-128 35 min.	Silvery lead deposit. The deposit is cylindrical in shape at the edges. The effect of rotation is seen on the curved

			lines on the face of the surface. Two sizes of particles are existed in the deposit. Both of them are without a distinct crystalline shape. It is easy to tear the deposit out of the surface as a whole disc.
Vitreous carbon	0.4 M Pb^{2+} + 0.127M Fe^{3+} in 2M CH_3SO_3H	-127 25 min.	Silver-coloured and rough deposit. At the edges dendrites grow perpendicular to the surface. The shape is best described as a sunflower. The adhesion is weak especially at the edges.
Vitreous carbon	0.4 M Pb^{2+} + 0.127M Fe^{3+} in 2M CH_3SO_3H	-127 30 min.	Lead deposited on the surface with two kinds of structures; sharp and cylindrical. Easy to fall off the surface. The adhesion is slightly improved by surface treatment but not significantly (The electrode was roughened by sand paper 320)
Vitreous carbon	0.4M Pb^{2+} in 2M CH_3SO_3H + 1.0g/l lignin sulfonate	-32 60 min.	The deposit is not very flat. Smooth and no dendrites are at the edges. There are some abrasions on the surface. Adhesion is very weak.
Graphite	0.4 M Pb^{2+} in 2M CH_3SO_3H	-14 45 min.	Uniform lead deposit but does not totally cover the surface. The deposit is coarse, lump-like particles and dark. There are some gaps distributed on the surface. At the edge deposit is thicker than the middle of the electrode. The adhesion between deposited lead and graphite is weak but stronger than the adhesion between deposited lead and VC.
Graphite	0.4 M Pb^{2+} in 2M CH_3SO_3H	-162 30 min.	Rough deposit with cylindrical dendrites at the edges. The adhesion is weak.
Graphite	0.4M Pb^{2+} in 2M CH_3SO_3H + 1.0g/l lignin sulfonate	-32 30 min.	Flat smooth and uniform deposit. Adhesion is better than vitreous carbon.

Table (2) lead deposited on rotating vitreous carbon disc electrode (0.126 cm^2) as well as on rotating graphite disc electrode (0.07 cm^2) from different solutions at a rotation rate of 1600 rpm.

Table (2) summarises the results with carbon electrodes. Two depositions were carried out from a commercial plating bath (see table (3) for constituents of the bath) onto vitreous carbon. The deposits were not good. A number of plating experiments were carried out from methanesulfonic acid solutions but in none of the conditions tried were the deposits satisfactory. Adhesion was very poor and uniform layers were not achieved. Lignin sulfonate improved the situation but the deposits remained of too poor a quality to be useful. The replacement of vitreous carbon by graphite also improved the deposit but not sufficiently for the purpose of the project.

Bath contents and condition	Value
Lead g/l	200
Free fluoroboric acid, g/l	20
Excess boric acid, g/l	
Animal glue, g/l	
Iron, g/l	7
Temperature, °C.	18
Current density, (-j) mA/ cm^2	15
Deposit thickness, μm	50

Table (3) Commercial bath contents and conditions. Supplied by BASF

Table (4) reports similar experiments on other metals. Good adhesion of lead to gold electrodes has been accomplished. Examination of the sample under the microscope has shown that there is an intermetallic interaction between the deposited lead and gold electrode. The interaction is enhanced with time, and stronger adhesion developed. However, this interaction may cause loss of gold by the dissolution in lead. Nickel substrate has even better adhesion with lead but without any intermetallic interactions. Therefore, nickel might be used as an electrode in the methanesulfonic acid battery. Titanium however, is not appropriate since its adhesion with lead is poor and it develops oxides rapidly in the solutions, see [71].

Electrode	Solution	j mA/cm^2	Deposit
Gold stationary electrode.	0.4 M Pb^{2+} in 2M CH_3SO_3H	-10 40 min.	Rough lead deposit on the surface. Under the microscopy, a yellowish structures can be seen. An interaction between the deposited lead and the gold can also be seen. The adhesion between lead and gold is strong and improved with time. The sample has been examined under the microscope two weeks later and found that the interaction has been enhanced further. Moreover, the adhesion has become stronger.
Gold stationary electrode	0.4 M Pb^{2+} in 2M CH_3SO_3H	-20 40 min.	Rough deposit with big particles. The surface is partially covered and the colour of geld is seen. There was not any dendrites around the desk. The adhesion is good.
Gold stationary electrode	0.4 M Pb^{2+} in 2M CH_3SO_3H	-128 25 min.	The deposit is sharp scales and is not only at the edges but distributed randomly on the surface. The edges adhere less to the surface than the middle probably because of there length.
Gold RDE 600rpm	0.4 M Pb^{2+} + 0.127M Fe^{3+} in 2M CH_3SO_3H	-10 45 min.	Coarse lead deposit with no distinct structure shape. The surface is not totally covered with lead.
Titanium 200rpm (etched)	0.4M Pb^{2+} in 2M CH_3SO_3H + 1.0g/l lignin sulfonate	-20 30 min.	Flat, smooth deposit. There are some coloured spots around the edges of the electrode. The adhesion is not strong. The electrode was etched for 10 min in etching solution (25 ml water + 1.3 ml H2SO4 conc. + 2.1 g Ammonium florid)
Titanium 200rpm (not etched)	0.4M Pb^{2+} in 2M CH_3SO_3H + 1.0g/l lignin sulfonate	-20 45 min.	Flat, smooth deposit. The adhesion is better than the etched sample. The electrode was polished by 3M polishing paper.
Nickel stationary electrode.	0.4M Pb^{2+} in 2M CH_3SO_3H + 1.0g/l lignin sulfonate	-32 30 min.	Flat, smooth deposit. There are some small spheres of lead deposited at the edges. The adhesion is very good.
Nickel 1600 rpm	0.4M Pb^{2+} in 2M CH_3SO_3H + 1.0g/l lignin sulfonate	-32 45 min	Flat, smooth deposit. The deposit is slightly thick at the edges and some of the deposit has grown outside the electrode disc. The adhesion is very good.

Table (4) lead deposited on different rotating metals disc electrodes.

Data for steel is reported in table (5) and (6). Deposition of lead from the commercial solution has good quality over a range of current densities from -16 mA cm^{-2} to -256 mA cm^{-2} . Higher current densities produce dendrites and coarse deposits. This solution is designed for lead deposition on steel substrates. The supplier stated that the only additive is Fe(III) but the solution is dark brown and has a strong odour. Some unknown organic additives were suspected.

Electrode	Solution	j mA/cm^2	Deposit
Steel	Commercial fluoroborate	-4 45 min.	No deposition. The steel has corroded and a black layer is produced on the surface probably caused by corrosion.
Steel	Commercial fluoroborate	-8 45 min.	As above.
Steel	Commercial fluoroborate	-16 45 min.	Silver in colour. Good, compact, smooth, uniform, totally covered and adhered to the surface. There are some curved lines on the surface. Brown colour is seen on the platinum mesh secondary electrode may be due to lead dioxide. This material dissolve after couple of hours when no current is passing through the cell.
Steel	Commercial fluoroborate	-32 45 min.	As above and no curved lines is seen on the surface. Lead layer is very uniform.
Steel	Commercial fluoroborate	-64 45 min.	As above. Slightly more deposit is at the edges.
Steel	Commercial fluoroborate	-128 45 min.	As above. The edges are thickening. Some of the deposit is expanded out of the electrode area.
Steel	Commercial fluoroborate	-256 45 min.	As above. More deposit is on the edges and out of the electrode area with a shape of like bars on the plastic sheet.
Steel	Commercial fluoroborate	-512 45 min.	The deposit is grey to dark grey. There are some dendrites at edges. The dendrites are not perpendicular to the surface rather flat and curved because of the rotation. The deposit is rough and not fully uniform. Some of the dendrites dropped during washing of the deposit. The adhesion is not very strong. The dark colour of the solution in the secondary electrode compartment has faded and became lighter.

Table (5) Lead deposition on rotating steel disc electrode from a commercial bath at 1600 rpm.

Table (6) reports deposition experiments on steel from methanesulfonic acid solutions.

Electrode	Solution	j mA/cm^2	Deposit
Steel	0.4 M Pb^{2+} in 2M CH_3SO_3H	-4 45 min.	No deposition. The steel electrode has corroded and black colour has developed on the surface.
Steel	0.4 M Pb^{2+} in 2M CH_3SO_3H	-8 60 min.	As above.
Steel	0.4 M Pb^{2+} in 2M CH_3SO_3H	-16 45 min.	Thin small particles of lead have deposited. There are curved lines on the surface. The deposit is rough, not uniform and not dull. Under the microscope crystals can be seen within the deposit. The deposit is adhered to the surface but less than the adherence of the deposit to the steel in the commercial fluoroborate solution.
Steel	0.4 M Pb^{2+} in 2M CH_3SO_3H	-32 45 min.	As above. The thickness of the deposit at the edges is more than the middle.
Steel	0.4 M Pb^{2+} in 2M CH_3SO_3H	-63 45 min.	As above. The thickness of the deposit at the edges is more than the middle. The deposit is rough .
Steel	0.4 M Pb^{2+} in 2M CH_3SO_3H	-127 45 min.	As above. Dendrites have been grown perpendicularly to the surface and they are very easy to fall from the edges. The adhesion is decreasing with the increase of the current density.
Steel stationary	0.4 M Pb^{2+} in 2M CH_3SO_3H	-127 45 min.	As above except the dendrites on the edges are more complicated and have sharp plates.
Steel	0.4 M Pb^{2+} in 2M CH_3SO_3H	-127, 333K, 20 min.	The roughness has increased with increasing the temperature. The adhesion has decreased.
Steel	0.4 M Pb^{2+} + 0.127M Fe^{3+} in 2M CH_3SO_3H	-64 30 min.	Identical to the deposited lead from solution without iron added.
Steel	0.4 M Pb^{2+} + 0.127M Fe^{3+} in 2M CH_3SO_3H	-128 30 min.	Same as above and the deposit adheres less to the surface.
Stainless	0.4 M Pb^{2+} +	-32	The deposit does not cover all the surface, instead there

steel	in 1.6M CH_3SO_3H	25 min.	are some spherical accumulations randomly distributed. Many sharp dendrites on the edges. The adhesion is very weak. Similar to the deposit on VC.
Stainless steel	0.4 M Pb^{2+} + in 1.6M CH_3SO_3H	-64 45 min.	As above.
Stainless steel	0.4 M Pb^{2+} + in 1.6M CH_3SO_3H + 0.5g/l lignin sulfonate	-8.5 45 min.	Uniform deposit without any dendrites. The surface is not very smooth. Adhesion is very weak.
Stainless steel	0.4 M Pb^{2+} + in 1.6M CH_3SO_3H + 0.5g/l lignin sulfonate	-32 45 min.	As above.
Mild steel, Stationary	0.4 M Pb^{2+} in 2 M CH_3SO_3H + 0.5g/l lignin sulfonate	-20 25 min.	Shiny, flat, smooth deposit without any dendrites. Very adhered to the surface.
Mild steel	0.4M Pb^{2+} in 2M CH_3SO_3H + 0.5g/l lignin sulfonate	-128 35 min.	As above. There are some spheres of lead deposit around the edges.
Mild steel	0.4M Pb^{2+} in 2M CH_3SO_3H + 1.0g/l lignin sulfonate	-128 35 min.	As above. Better smoothness.

Table (6) lead deposited on various rotating steels disc electrodes at 1600 rpm.

The mild steel gave clearly superior deposits. The quality of lead deposited from solutions of 2 M methanesulfonic acid + 0.4 M Pb(II) and lignin sulfonate is similar to the deposits from fluoroborate commercial solution up to -128 mA cm^{-2}. It might be possible to improve the quality of the deposits and even exceed the commercial baths by changing the compositions and/or the conditions of the

methanesulfonic bath. The adhesion between the mild steel substrate and the lead deposited from methanesulfonate solution is very strong. Likewise, the properties of the deposit, smoothness, compactness and flatness, are improved by using the lignin sulfonate as an additive to the plating solution. It should be noted that on open circuit steel corrodes in the acidic medium and the above result were obtained by commencing deposition immediately the steel contacted the solution. Hence, steel cannot be used as an electrode in the envisaged battery if no protection is provided (e.g. using inhibitors).

From the tables above it can be seen that different substrates have different effects on the deposit characteristics (adhesion, morphology, compactness and smoothness). Gold and nickel are the best materials that can be used to deposit lead in methanesulfonic acid solutions. Carbons are stable and inert materials but the adhesion with deposited lead is poor and will decrease the efficiency.

Although no attempts were made to study the corrosion behaviour of nickel in methanesulfonic acid solutions, studies in the literature show that nickel corrodes in methanesulfonic media [70]. However, nickel should be covered with lead in the battery application and deposited lead will not be totally removed during discharge process. Moreover, cyclic voltammogram has been carried out for nickel in 2 M methanesulfonic acid solution. Potential range was + 0.2 to - 0.7 V at room temperature. It has been seen that hydrogen evolution starts at potential of ~ -0.45 V. An oxidation wave is seen at $E_{1/2}$ = -0.1 V indicating a corrosion process of nickel in methanesulfonic acid. The shine on the nickel surface vanishes after many voltammetric cycles in methanesulfonic acid. It should be noted that the oxidation wave of nickel does not appear in solutions containing Pb(II) in methanesulfonic acid. Probably the Pb(II) has inhibited the corrosion process of nickel.

Cyclic voltammograms have been recorded on two electrodes; rotating vitreous carbon electrode and rotating nickel electrode, to compare the charge ratio. The following table summarises the results.

	Nickel			Vitreous carbon		
Rotation rate rpm	Anodic charge C cm^{-2}	Cathodic charge C cm^{-2}	Q_A/Q_C %	Anodic charge C cm^{-2}	Cathodic charge C cm^{-2}	Q_A/Q_C %
0.0	0.15	0.16	97.4	0.12	0.13	89.5
400	0.64	0.66	97.8	0.54	0.57	94.0
900	1.3	1.3	101	0.85	0.91	94.2
1600	2.3	2.3	99.2	1.2	1.3	94.1
2500	3.4	3.4	98.5	1.5	1.6	92.5
3600	4.7	5.0	93.3	1.7	1.8	89.8

Table (7) Comparison between nickel and vitreous carbon electrode with respect to the charge ratio. Charge ratio has been calculated using the weighing method. Data have been recorded from 50 mM Pb(II) in 2 M methanesulfonic acid at a scan rate of 20 mV s^{-1}. Potential range was 0.0 to -0.7 V for vitreous carbon and -0.2 to -0.7 V for nickel.

It can be seen from the data above that nickel has a better charge ratio at the corresponding rotation rate. The relatively low charge ratio of vitreous carbon might be explained based on the slightly poor adhesion between lead deposit and vitreous carbon. When the rotation rate increases the charge ratio decreases because of the weak adhesion. On the other hand, the adhesion between lead deposit and nickel is very strong therefore, the charge ratio is close to one at most of the rotation rates. Moreover it can be expected that the more lead deposited on the vitreous carbon will cause the charge ratio to decrease hence, the energy efficiency will be decrease as well. It should be noticed also that lead tends to build dendrites with large quantities of deposit, for example with high rotation speed or high current densities. This may explain the low charge ratio with nickel at speed of 3600 rpm.

Indeed, the results for vitreous carbon in that table are better than obtained in many experiments. The situation become worse in the presence of lignin sulfonate in the solution. It was commonly noted that Pb powder could be seen in the electrolyte during dissolution and charge ratios of Q_A/Q_C were often as low as 10 %.

In conclusion it is possible to state that

- Gold and nickel are good substrates as cathodes to deposit lead in the envisaged battery.
- Gold is a stable metal in most acidic mediums whereas nickel might corrode in acids however , it is much cheaper than gold.
- Gold reacts with lead to produce inter-metallic compounds. Although this reaction is in favour of good adhesion between lead and gold , it may cause loss of gold electrode with time.
- The adhesion strength between lead and substrates is in the order (Ni, Au, mild steel) > Ti > graphite > vitreous carbon > stainless steel.
- although mild steel has good adhesion with the deposited lead, it is not stable in acidic solutions.
- vitreous carbon is very stable in acids and would be appropriate as an electrode substrate material however, the adhesion with lead is poor.

3-2-6 Current density

Current density has been varied in order to investigate the morphology and smoothness of the lead deposit in presence of lignin sulfonate. The quality of the deposit has been determined using SEM images and digital photos.

Figures (30-33) show lead deposits on rotating nickel disc electrode from 0.4 M Pb (II) + 1.0 g/l sodium lignin sulfonate in 2 M CH_3SO_3H at different current densities; -8.0, -32.0, -63.0 and -128 mA/ cm^{-2}. Up to 63 mA cm^{-2}, the deposits have many of the characteristics required. By eye, they are uniform and reflecting and they adhere to the nickel surface. Clearly, the deposit become more rough at higher currents densities hence, the current should be controlled in order to maintain a certain thickness of the deposit on the electrodes. The thickness of the lead deposit reaches 80 μm at current density of -63 mA cm^{-2} and easily can be increased to thicker deposits before the development of dendrites at -128 mA cm^{-2} . It is possible therefore to increase the thickness of the deposit by increasing the current density together with increasing the lignin sulfonate and/or increasing the temperature of the solution since both factors are in favour of good lead deposits.

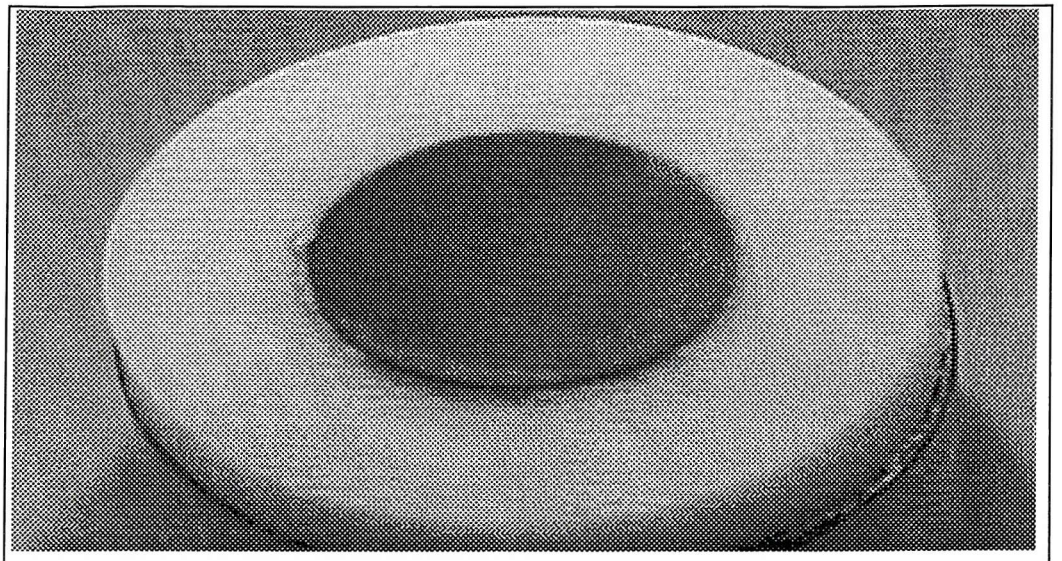

Figure (30) Lead deposited on rotating nickel disc electrode (0.2 cm^2) from 400 mM Pb(II) in 2.0 M methanesulfonic acid and 1.0 g/l lignin sulfonate at current density of -8 $mAcm^{-2}$ at room temperature. Rotation rate is 200rpm. 180 min.

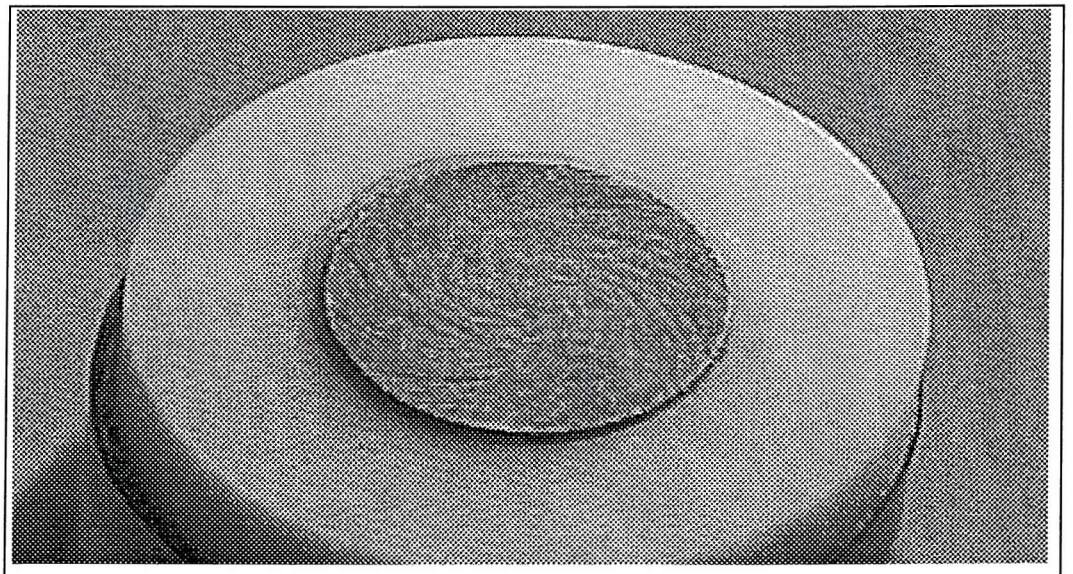

Figure (31) Lead deposited on rotating nickel disc electrode (0.2 cm^2) from 400 mM Pb(II) in 2.0 M methanesulfonic acid and 1.0 g/l lignin sulfonate at current density of -63 $mAcm^{-2}$ at room temperature. Rotation rate is 200rpm. 22.5 min.

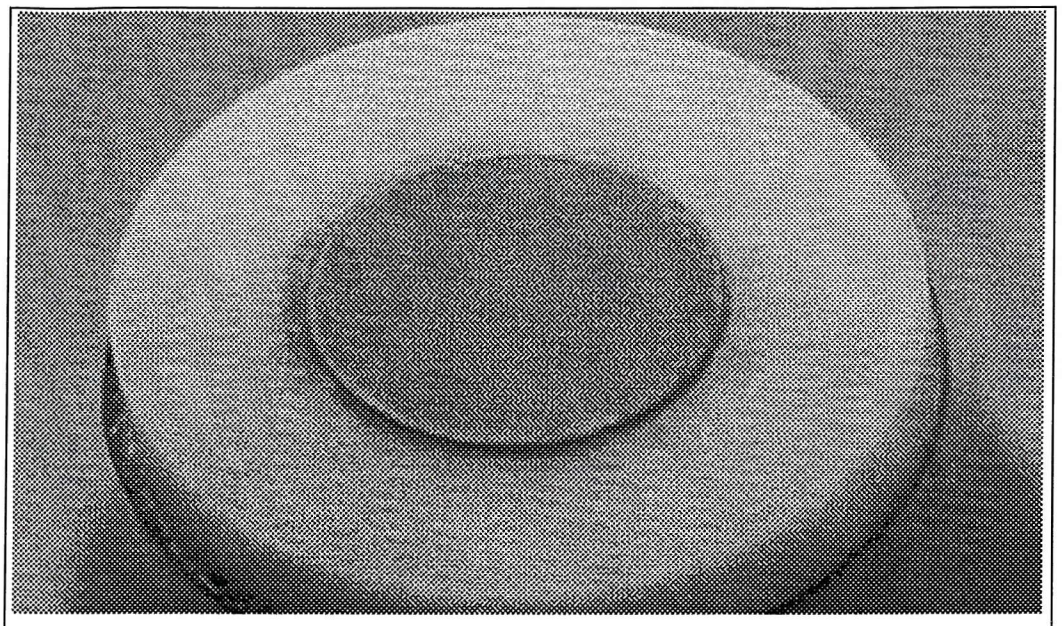

Figure (32) Lead deposited on rotating nickel disc electrode (0.2 cm^2) from 400 mM Pb(II) in 2.0 M methanesulfonic acid and 1.0 g/l lignin sulfonate at current density of -32 $mAcm^{-2}$ at room temperature. Rotation rate is 200rpm. 45 min.

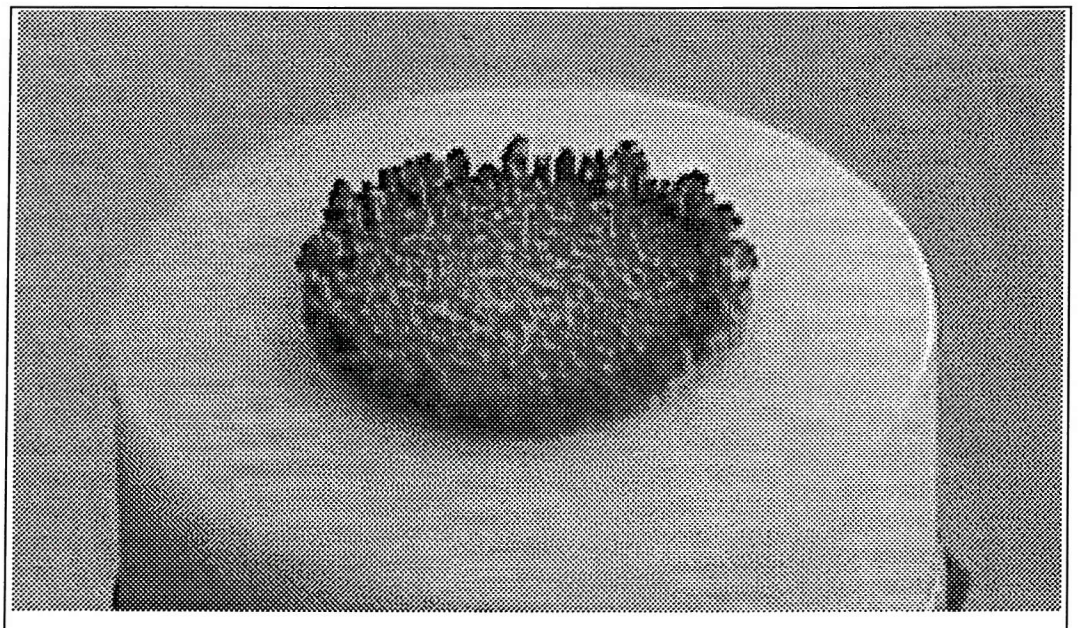

Figure (33) Lead deposited on rotating nickel disc electrode (0.2 cm^2) from 400 mM Pb(II) in 2.0 M methanesulfonic acid and 1.0 g/l lignin sulfonate at current density of -128 $mAcm^{-2}$ at room temperature. Rotation rate is 200rpm. 11.25 min.

In conclusion, current densities up to -63 mA cm^{-2} are applicable to produce satisfactory thick, smooth and compact lead deposits. Other additives are also possible and may enhance good and thick lead deposits at higher values of current densities.

Results and discussion

Chapter (IV)

The anodic deposition of PbO_2

The positive electrode in the methanesulfonic acid battery is lead dioxide. PbO_2 is deposited on an inert anode substrate during charge and dissolved again into the solution during the discharge process. In this chapter, the kinetics of lead dioxide deposition has been studied electrochemically using cyclic voltammetry and potential step techniques. Plating experiments have been carried out to study the morphology smoothness and adhesion of lead dioxide at a number of inert anodes.

4-1 Cyclic voltammetry

Cyclic voltammograms were recorded for the positive electrode on vitreous carbon and gold rotating disc electrodes. Figure (1) shows a typical voltammogram of lead dioxide recorded on vitreous carbon rotating disc electrode from a solution of 0.5 M Pb(II) in 1M methanesulfonic acid solution at a rotation rate of 1600 rpm and a potential scan rate of 20 mV s^{-1}. During the scan to positive potentials, a significant nucleation overpotential can be seen before lead dioxide electrodeposition occurs. The anodic current suddenly increases at potentials higher than 1.7 V and a black precipitate is noticed on the electrode surface during the positive increase of the current. This current is attributed largely to lead dioxide deposition but some oxygen evolution may also be observed. It has been noticed in other experiments that at higher potentials (> 1.9 V) gas bubbles start to accumulate at the edges of the electrode surface. These bubbles are due to oxygen evolution. The reverse scan shows a continuation of the deposition of PbO_2 but with a decrease in the current until the current reaches zero at + 1.37V a potential that provides an approximation of the equilibrium potential for the PbO_2/Pb(II) couple in this acid concentration. The difference in potential between this point and the potential at which the deposition begins on the forward scan corresponds to the nucleation overpotential. A cathodic current then increases as the potential is scanned to less positive potentials and a

symmetrical peak with $E_{1/2}$ = 1.05 V, which corresponds to the reduction of the lead dioxide, is observed. Even negative to the peak some brown deposit remains on the electrode surface. The current gradually decreases in magnitude until it eventually reaches to zero but not immediately after the oxidation peak. Clearly, the reduction of lead dioxide is not straightforward and Pb(II) in solution is not the only product of the reduction process.

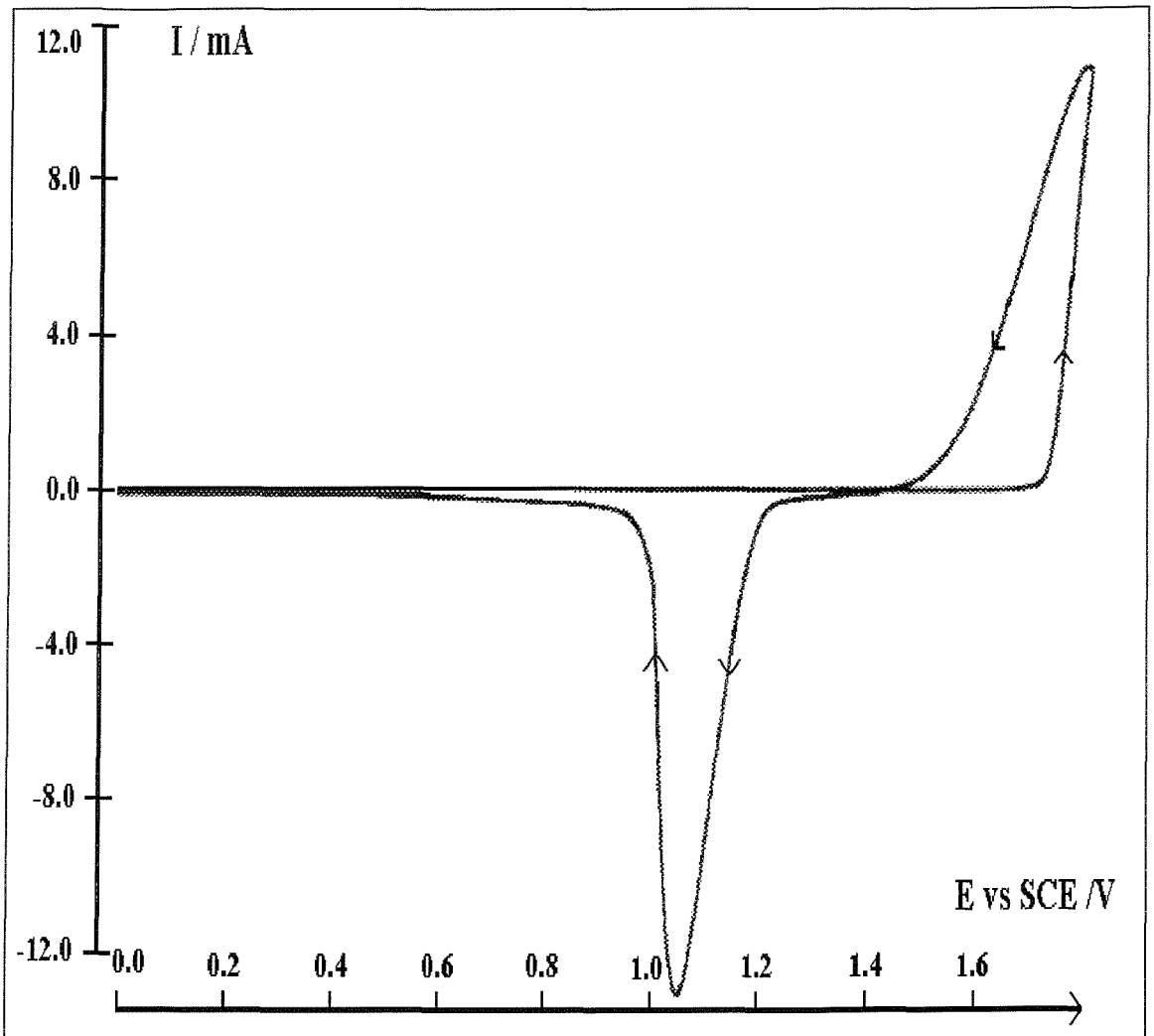

Figure (1) Cyclic voltammogram recorded on vitreous carbon rotating disc electrode (0.126 cm^2) from 0.5 M Pb(II) in 1 M methanesulfonic acid at a rotation rate of 1600 rpm and scan rate of 20 mVs^{-1}.

The charge ratio under the anodic and cathodic areas of this voltammogram (Q_C/Q_A) is 92 %. However, in some experiments the charge ratios were much lower probably due to competitive reactions during the anodic process such as oxygen evolution. More importantly, the poor adhesion between the deposited lead dioxide and the substrate material causes the charge ratio to decrease and some of the PbO_2 will be lost to the solution as a black powder when high quantities are deposited on the electrode surface. This may explain the inconsistency of the charge ratio throughout the voltammograms of lead dioxide on both, vitreous carbon and gold disc electrodes.

All the features of the voltammogram are a function of many parameters (concentrations of Pb(II) and the acid, potential scan rate, positive potential limit etc.) but the response has many good characteristics. The anodic and cathodic charges correspond to the deposition and dissolution of a layers of PbO_2 with a thickness > 1 μm and deposition and dissolution at a rate of 20 mA cm^{-2} occur at an overpotential of approximately 200mV.

The background response for vitreous carbon rotating disc electrode was recorded in 2 M methanesulfonic acid solution and reported in figure (2, A). No significant current was noticed other than the oxygen evolution at high potentials > 2000 mV which means that all the features in the previous voltammogram were due to the presence of Pb(II) in the solution. However, it should be noted that when the sensitivity of the voltammogram is increased, two small waves can be seen between potentials of ca. 1700 and 2000 mV as seen in figure (2, B). The waves might be attributed to adsorption process on the vitreous carbon surface in the absence of Pb(II). These waves should be taken into account when the concentration of the Pb(II), hence the current is low. Also PbO_2 is known to be a better catalyst than vitreous carbon for O_2 evolution and therefore this reaction may be switched on by the deposition of PbO_2 [44].

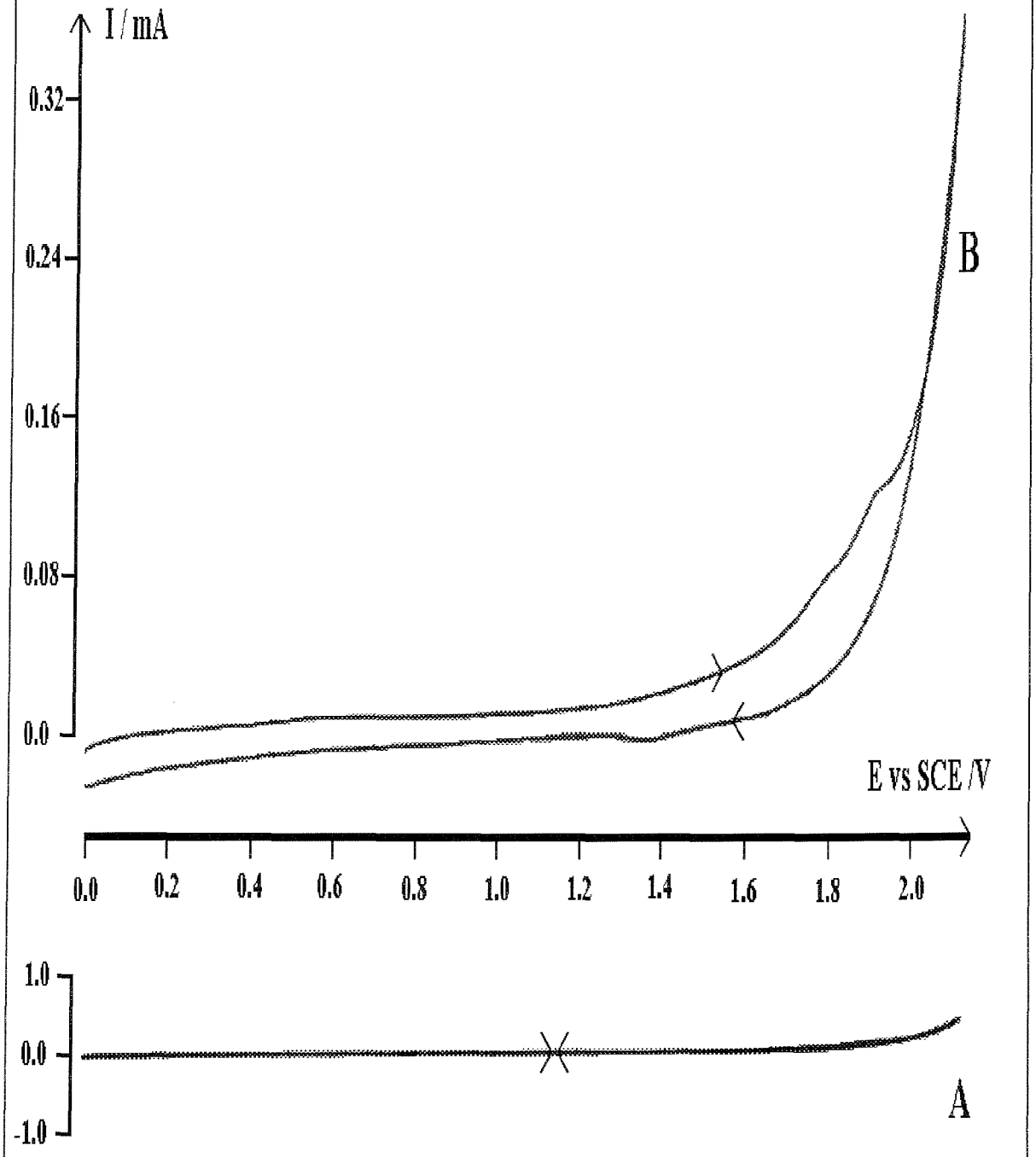

Figure (2) Cyclic voltammogram recorded on vitreous carbon stationary disc electrode (0.126 cm^2) from 2M methanesulfonic acid at scan rate of 20 mVs^{-1}.

The positive potential limit has been varied to study the effect on the lead dioxide deposition. It has been found that the anodic current increased with the increase of the positive potential limit. Unfortunately, the charge ratio decreased with the increase of the positive potential as can be seen in the following table (1).

Positive potential mV	Charge ratio Q_C/Q_A %	Remarks
1750	51	The cathodic peak has a long tail and another broad wave at E_P = ca. 150 mV.
1800	85	
1815	53	
1825	34	Flakes leave the electrode during oxidation
1850	26	As above.

Table (1) Charge ratio of lead dioxide deposition /dissolution processes. The voltammograms were recorded on vitreous carbon rotating disc electrode at 1600 rpm from a solution of 0.5 M Pb(II) in 1 M methanesulfonic acid. Potential scan rate was 20 mV s^{-1}.

From the table above it is seen that as the potential is allowed more positive, the more flakes are detached from the surface and the lower the charge ratio (Q_C/Q_A). Lead dioxide was found to be brittle and it cracks during deposition at high current densities. Clearly, the high rotation speed is not in favour of high charge ratios since the high solution flow would cause the deposit to detached easily from the surface. This type of response was found - with more or less deviations - in all of the experiments that have been carried out with vitreous carbon and gold rotating disc electrodes throughout this project.

Figure (3) shows a voltammogram recorded on vitreous carbon in the same conditions of figure (1) except for the positive potential limit which was increased to 1850 mV. The voltammogram shows good deposition current during the forward scan. A small reduction peak with some noise is seen during the reverse scan. Moreover, a lot of black and brownish flakes are seen dropping from the electrode during this

dissolution peak. It is concluded that the quantity of the lead dioxide deposited on the surface of the vitreous carbon electrode has a key role in determining whether solid PbO_2 detaches from the carbon surface especially during dissolution. It should be mentioned here that the residues on the vitreous carbon disc electrode which were left after the dissolution of lead dioxide, dissolve slowly if the electrode is left at a potential negative to the dissolution peak. Rotating the electrode accelerates the dissolution process. This may indicates that the dissolution of the reduced Pb(II) species have slow kinetics and the dissolution reactions are partially under mass transport.

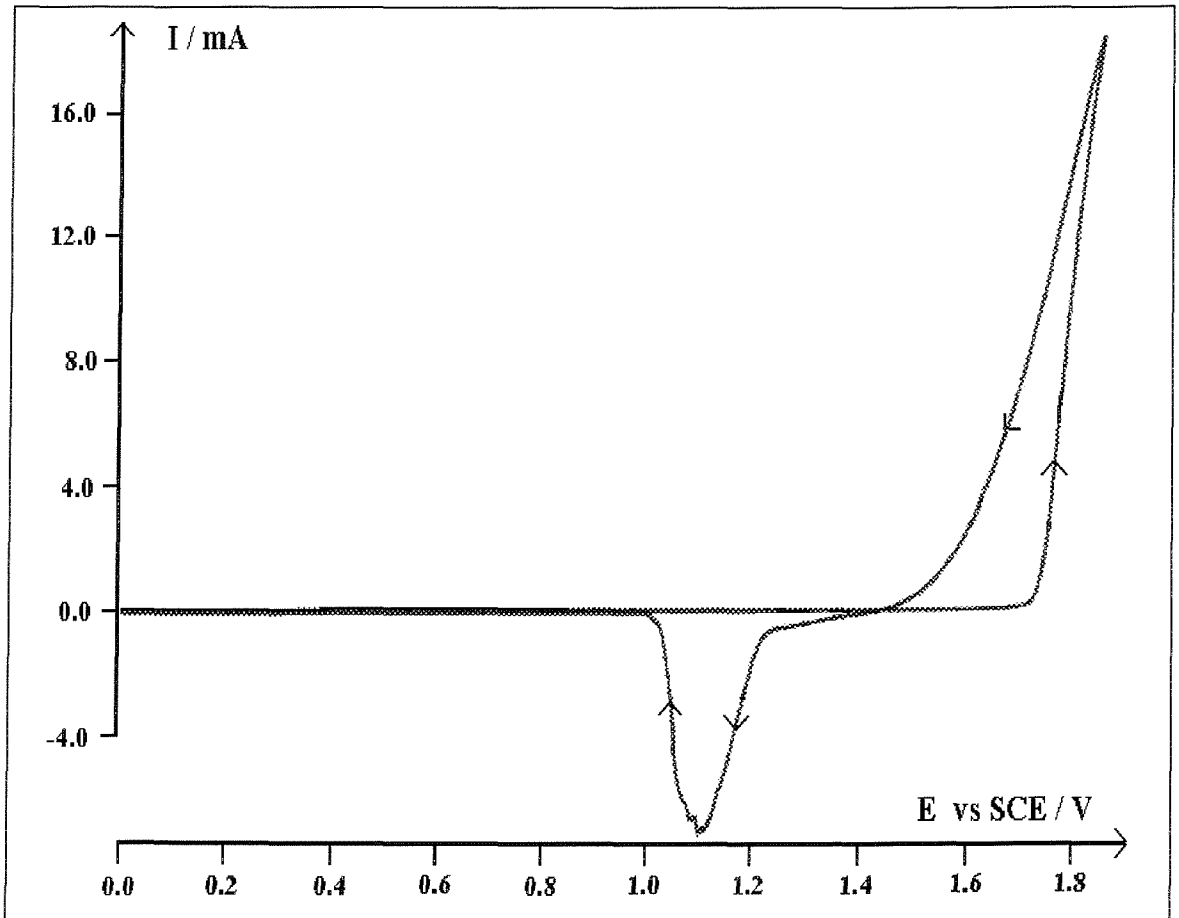

Figure (3) Cyclic voltammogram recorded on vitreous carbon rotating disc electrode (0.126 cm^2) from 0.5 M Pb(II) in 1 M methanesulfonic acid at a rotation rate of 1600 rpm and scan rate of 20 mVs^{-1}. Potential range is 0.0 - 1.85 V.

4-2 *Charge ratio*

The ideal charge ratio between deposition and stripping of the active materials in any battery would be 100%. Unfortunately it is commonly not possible to reach this percentage because of competitive reactions such as hydrogen and oxygen evolution on cathodic and anodic processes respectively and materials detachment if adhesion is poor. However, it may be sufficient to apply the oxidation-reduction system as a storage battery if the charge ratio is at least 75%.

In a series of experiments, the potential was stepped to + 1750 mV where PbO_2 can deposit, held for a period and then scanned back to less positive values to observe the PbO_2 reduction peak. The experiments used a vitreous carbon disc electrode and a solution of 100 mM Pb(II) in 1.4 M methanesulfonic acid. The charge ratio (Q_C/Q_A) was plotted against the charge for oxidation as seen in figure (4). From the figure below it can be seen that the charge ratio reaches a maximum then starts to decrease. It was noted again that during the experiments where thicker lead dioxide is deposited, the greater the loss of solid deposit during the dissolution i.e. the reduction period of the voltammograms. Moreover, in many experiments it has been noticed that the whole disc of lead dioxide falls off during the stripping peak. This behaviour reveals the poor adhesion between the lead dioxide and the vitreous carbon substrate. In these experiments, the thickness of PbO_2 deposited is ~ 1 μm.

It can be seen from figure (4) that the maximum of charge ratio was 50 % which appears very low in these particular conditions. However, higher charge ratios have been observed with different conditions. The charge ratio is subject to different factors such as acid and lead(II) concentrations, substrate material, current density and more importantly the quantity of the deposited lead dioxide as will be seen in the next paragraphs.

The adhesion problem between electrodeposited lead dioxide and vitreous carbon as well as titanium electrodes in solutions other than methanesulfonic acid has been reported by earlier researchers and some solutions have been suggested to

improve the adhesion [36,44,49,50]. Furthermore, all the investigations were concerned with producing a permanent lead dioxide electrode for industrial applications such as waste degradation and the chlor-alkali industries. Whereas in our case the aim is to deposit relatively thick layer of lead dioxide during charge process and dissolve it back during the discharge process in a repetitive manner. This of course, needs a good adhesion between the deposited lead dioxide and the substrate in every charge /discharge cycle.

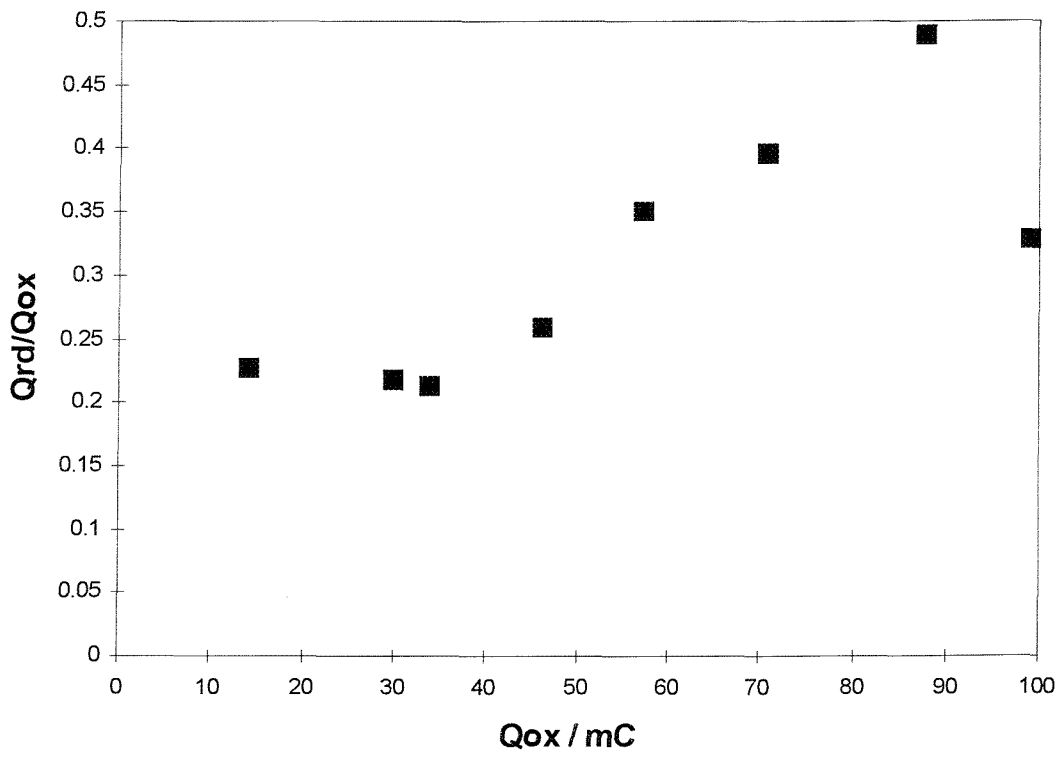

Figure (4) Charge ratio of depositing and stripping lead dioxide for a solution of 100 mM Pb(II) in 1.4 M Methanesulfonic acid on a vitreous carbon rotating disc electrode (0.126 cm^2). The potential was stepped to + 1750 mV, held for a controlled period and then scan back to less positive values at 20 mV s^{-1}. Rotation rate 1600 rpm.

A gold disc electrode was used as the substrate. In figure (5) a cyclic voltammogram recorded on a stationary gold disc electrode from a solution of 40 mM Pb(II) in 2 M methanesulfonic acid is shown. The figure shows a gradual increase in the current at potentials > ca. 1000 mV which is attributed to gold oxidation. The current then increases strongly at E > ca. 1700 mV forming an oxidation peak which corresponds mainly to lead dioxide deposition. The increase of current is steep and the current reaches a maximum of 10 mA cm^{-2} then decreases because of the mass transport effect with the stationary electrode. In other experiments where the potential was over 1900 mV, a steep increase on current is seen due to the contribution from oxygen evolution. Oxygen evolution and lead dioxide deposition are occurring at the same time. During the reverse scan the deposition continues but the current decreases significantly until it reaches the equilibrium potential, 1.45 V where the current is zero. A large, sharp, symmetrical and well defined peak is seen at E_P = 1250 mV corresponding to the dissolution of the lead dioxide. The peak current density is 36 mA cm^{-2} and the charge for the reduction of PbO_2 is 90 mC cm^{-2} (note this is for a more dilute Pb(II) solution than the experimental described earlier) . No flakes in solution were observed during the dissolution period. The current does not return immediately to zero but can be neglected compared to the other more important currents in the voltammogram. The cathodic peak at ca. 900 mV corresponds to the reduction of gold oxide formed for E > ca. 1500 mV. The reduction peak of the lead dioxide is much better than the one produced on vitreous carbon and therefore, this suggests that the adhesion between the deposited lead dioxide and the gold electrode is stronger. The charge ratio (Q_C/Q_A) was estimated for this voltammogram to be 88% and can be increased in different conditions.

It should be noted that, on both vitreous carbon and gold electrodes, the deposit during the scan to positive potentials starts with a brownish colour then turns black. This colour change is probably associated with layer thickness and particle size.

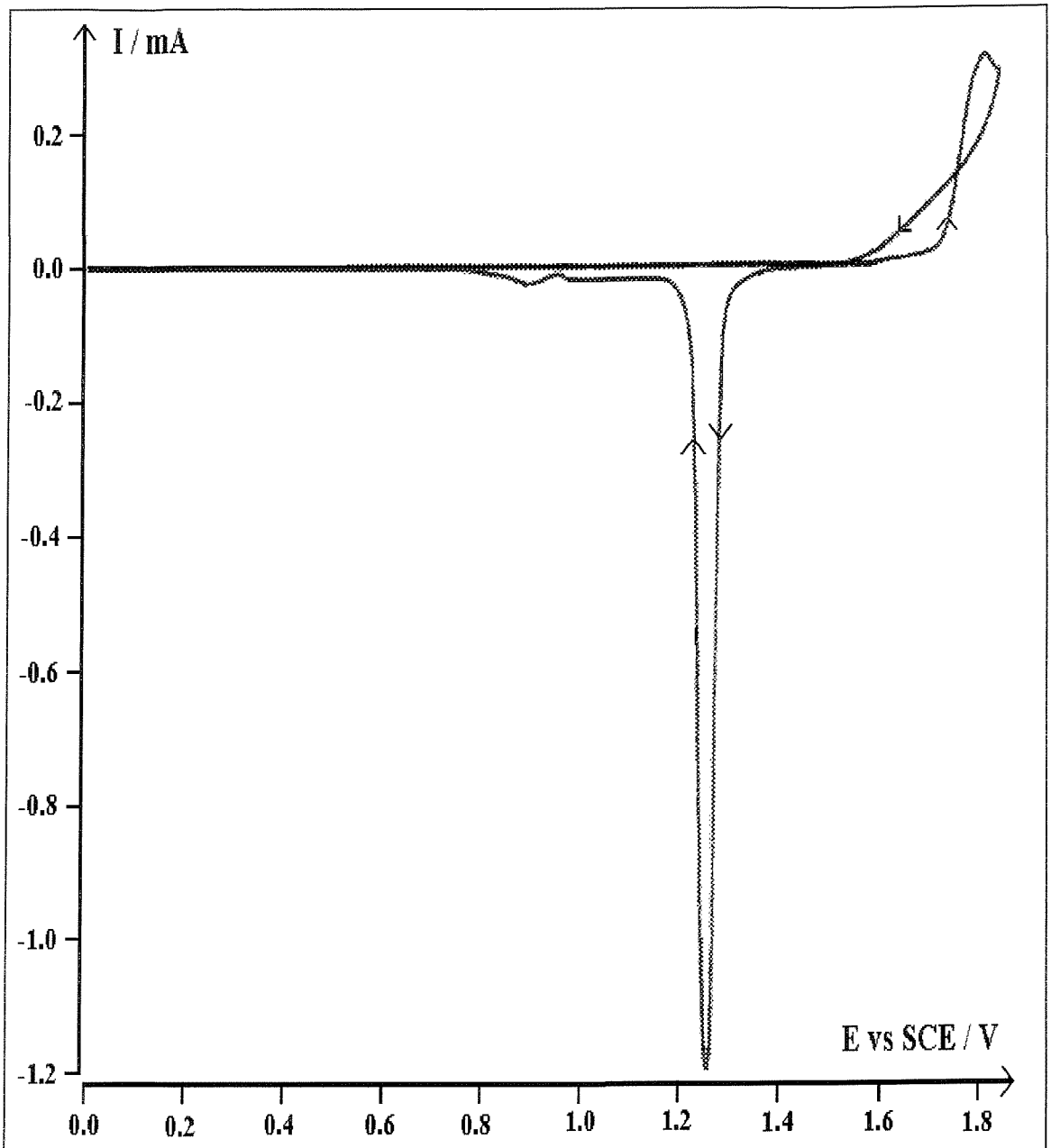

Figure (5) Cyclic voltammogram recorded on gold stationary disc electrode (0.03 cm^2) from 40 mM Pb(II) in 2 M methanesulfonic acid.

Another voltammogram was recorded on gold electrode in 2 M methanesulfonic acid to investigate the behaviour of gold in the absence of Pb(II). The voltammogram is shown in figure (6). The peaks in the voltammogram have relatively small currents. However, a more sensitive voltammogram is shown in figure (7) where oxidation processes are seen on the forward scan at potentials > ca 1000 mV due to gold oxidation. More anodic current is seen at potentials more than ca. 1600 mV which corresponds to the oxygen evolution. The reverse scan shows reduction peaks; the sharp peak at E_P = 950 mV corresponds to the reduction of the gold oxide. The currents associated with gold oxidation/reduction processes should be taken into account when a low concentration of lead is used. It is generally noticed that the dissolution peak of lead dioxide on gold is always thin and narrow therefore the current is very high. Whereas in the case of vitreous carbon, the dissolution peak is broad and usually has a long tail.

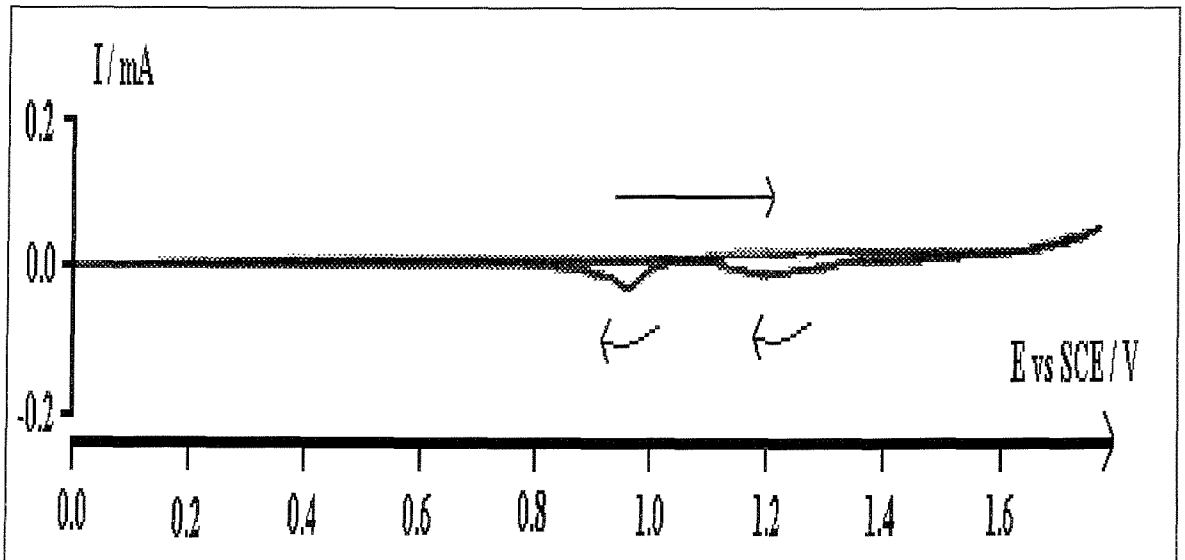

Figure (6) Cyclic voltammogram recorded on gold stationary disc electrode (0.03 cm^2) from 2 M methanesulfonic acid.

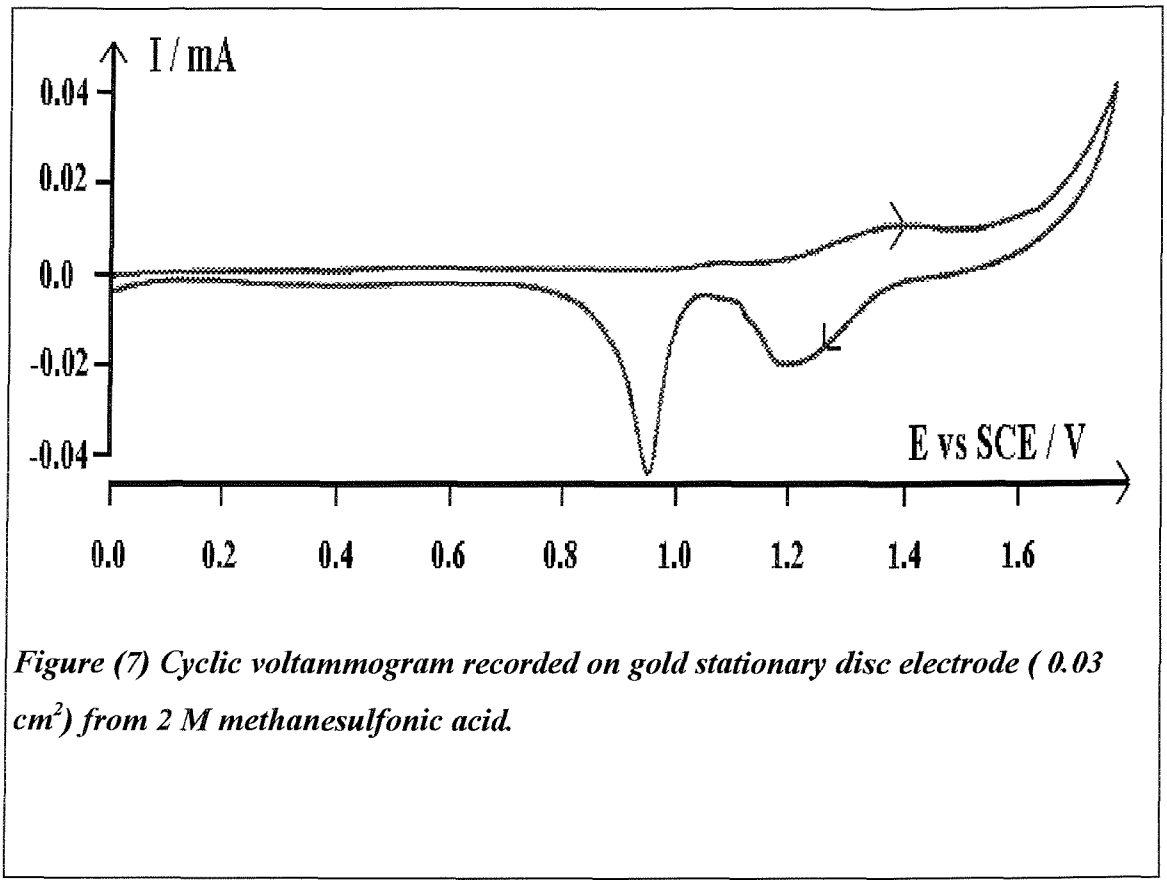

Figure (7) Cyclic voltammogram recorded on gold stationary disc electrode (0.03 cm^2) from 2 M methanesulfonic acid.

4-3 Nucleation overpotential as a function of rotation speed

Varying the rotation speed of the rotating disc electrode has a great effect on the deposition process as can be seen in figures (8) and (9) where the rotation rates were 0 and 400 rpm respectively. The voltammograms were recorded on a gold disc electrode with a positive limit of + 1760 mV. The current has increased rapidly in the case of stationary electrode and hence, more lead dioxide has deposited on the electrode surface. In the case of 400 rpm, the growth has been inhibited by the rotation. Otherwise the two voltammograms have the same features with well defined reduction peaks. The charge ratio (Q_C/Q_A) for 0 and 400 rpm was estimated to be 100% for both of the voltammograms. Clearly, in these conditions the charge ratio is at its maximum values for gold electrode. The rotation has no major detrimental effect on the charge ratio (Q_C/Q_A) for the dissolution /deposition processes. At 0 rpm, the layer of PbO_2 has a thickness of 0.5 μm.

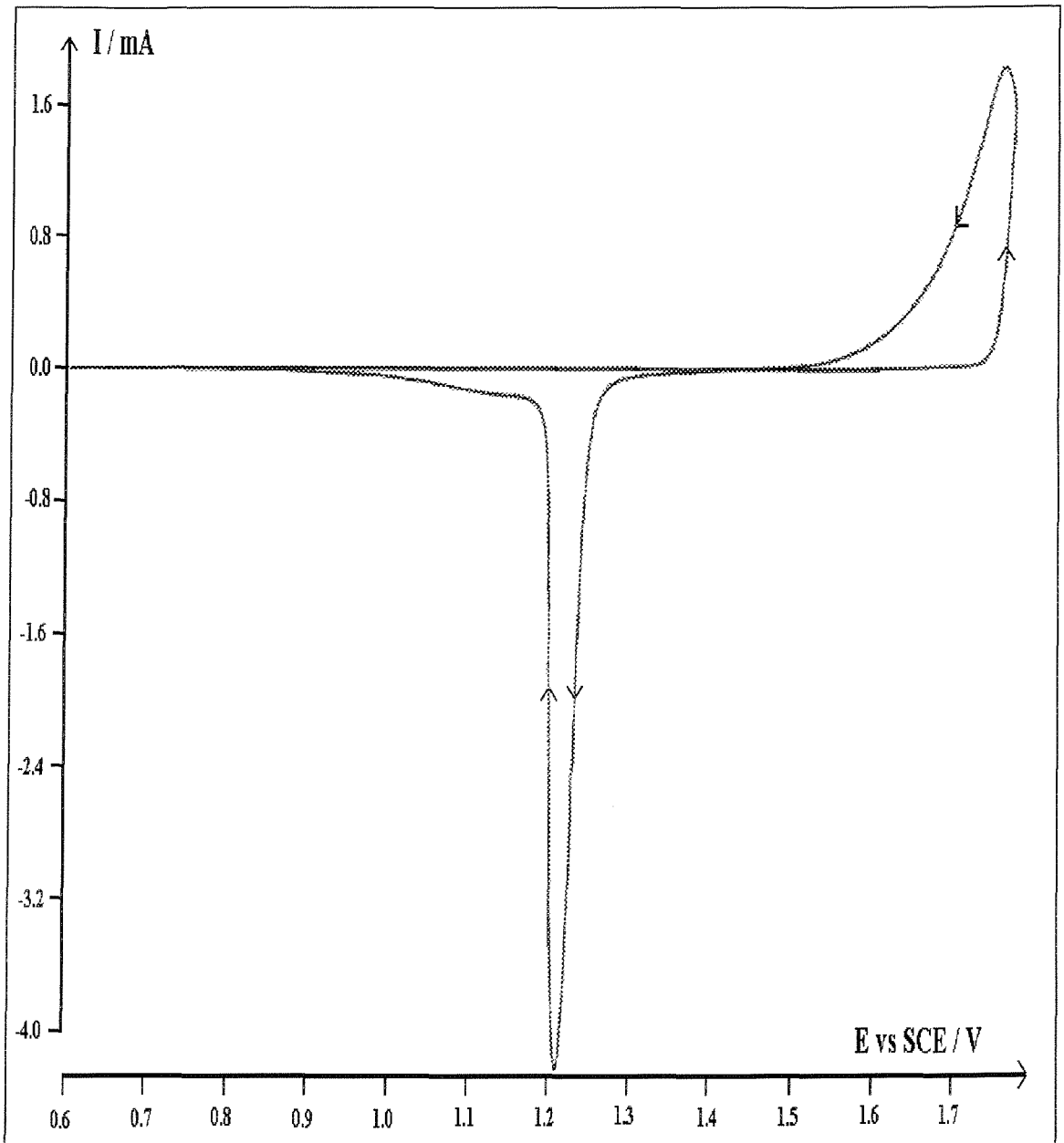

Figure (8) Cyclic voltammogram recorded on gold stationary disc electrode (0.03 cm^2) from 0.4 M Pb(II) in 2 M methanesulfonic acid.

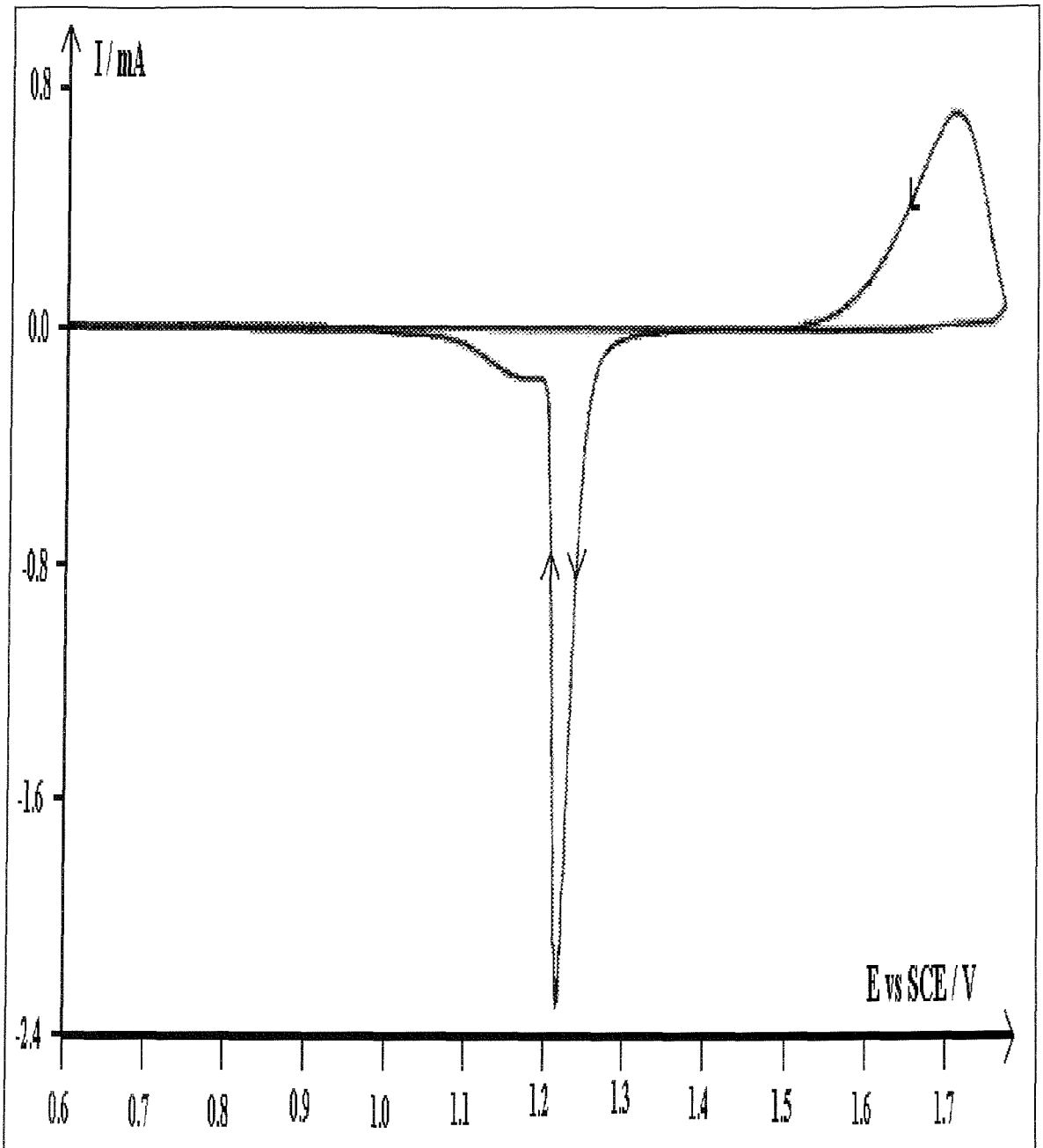

Figure (9) Cyclic voltammogram recorded on gold rotating disc electrode (0.03 cm^2) from 0.4 M Pb(II) in 2 M methanesulfonic acid at a rotation speed of 400 rpm..

It is clear from figures (8) and (9) that the deposition has been affected by the rotation speed. The higher rotation speed has decreased the current for the deposition of lead dioxide. At rotation rates of 1600 and 2500 the current is decreased further. This behaviour indicates that the nucleation and growth of lead dioxide has been suppressed by the movement of the electrolyte. This conclusion has been supported by step potential experiments as can be seen in figure (10) where transients were recorded on gold disc electrode from a solution of 0.4 M Pb(II) and 2 M methanesulfonic acid at 0 and 400 rpm. A potential step to 1620 mV vs. SCE was used. It can be seen from the figure that the induction time - the time needed for the deposition process to start- has increased with the increase of the rotation speed. It can be concluded therefore, that a Pb(IV) species can be lost to the solution if nucleation of PbO_2 is not rapid. The same results have been found using vitreous carbon disc electrode which indicates that the same mechanism applies to both electrodes. These results also have been reported in the literature [30] although for other acids. Special care should be taken while doing transient experiments since any traces of the residues on the electrode could affect the successive experiment. The electrode should be cleaned thoroughly prior to each experiment.

4-4 Potential step technique

In a series of potential step experiments, the influence of the potential has been demonstrated. Figure (11) shows I-t transients recorded on gold rotating disc electrode from solution of 0.4 M Pb(II) in 2 M methanesulfonic acid at potentials of 1600, 1620, 1640, 1660, 1680 and 1700 mV vs. SCE. Clearly seen from the figure below that with increased applied potential, the induction time decreases and the limiting current for PbO_2 deposition increases. Clearly, the increased overpotential has accelerated the nucleation process and facilitated the growth of the deposit. The induction time is an indication of a time dependence of the lead dioxide growth on both vitreous carbon and gold electrodes. The detailed analysis of the shape of the transients was not attempted but it should be noted that at 1.70 V the limiting current is 36 mA cm^{-2}.

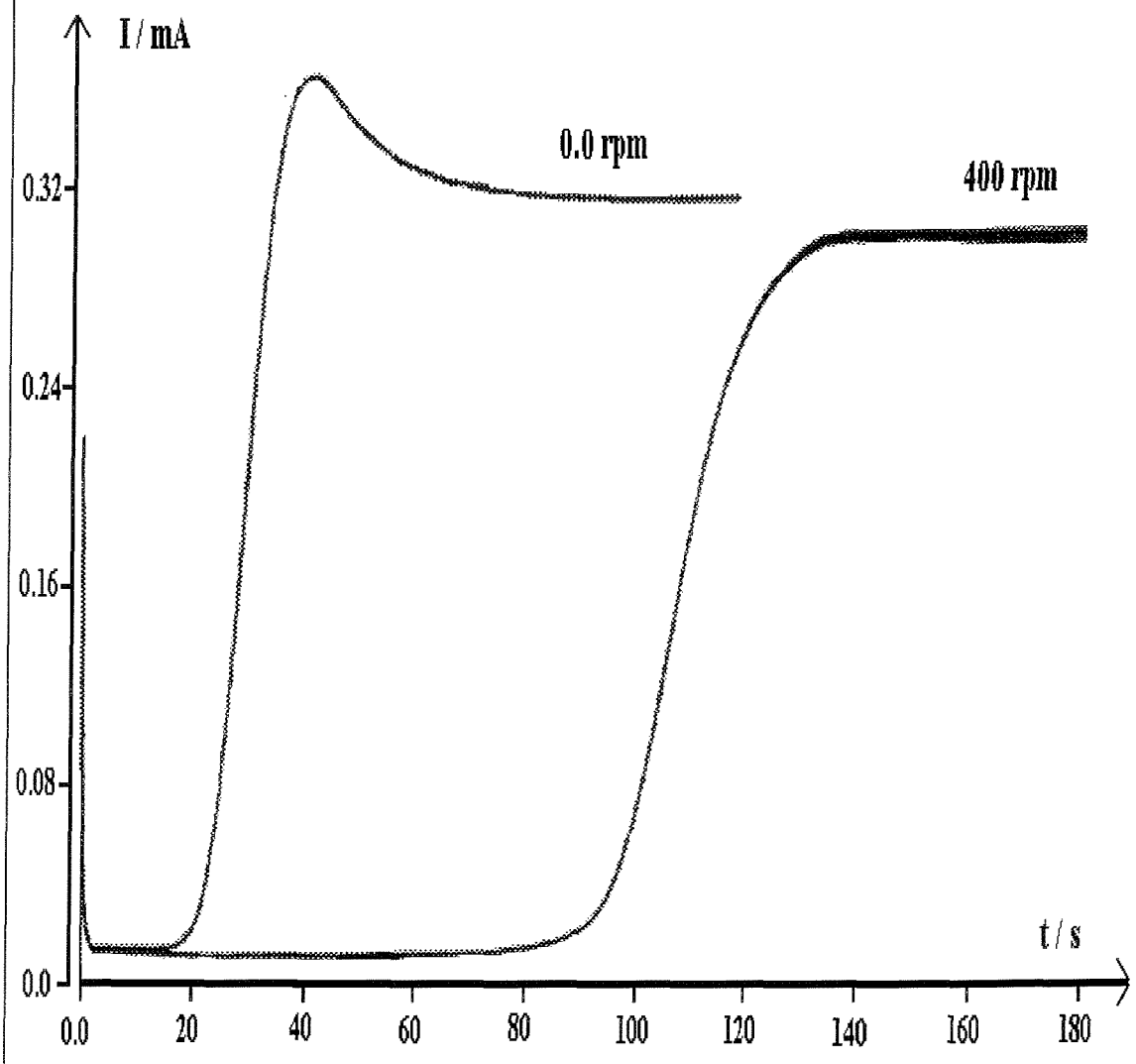

Figure (10) I-t transients recorded on gold disc electrode (0.03 cm^2) from 0.4 M Pb(II) in 2 M methanesulfonic acid.

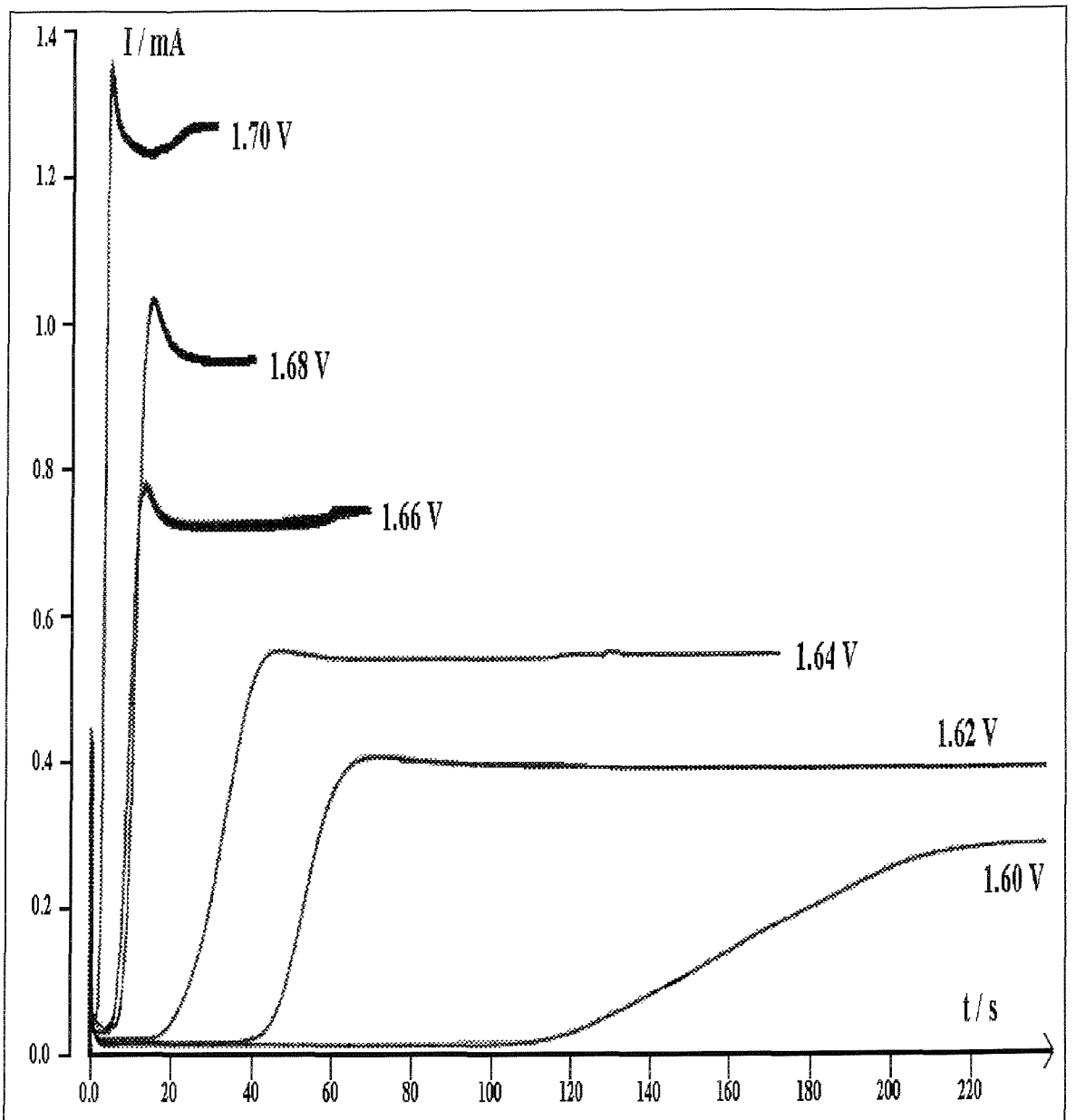

Figure (11) I-t transients recorded on gold rotating disc electrode (0.03 cm^2) from 0.4 M Pb(II) in 2 M methanesulfonic acid at a rotation speed of 200 rpm.

4-5 SEM images

SEMS have been captured for lead dioxide deposited on a vitreous carbon plate from a solution of 40 mM Pb(II) in 1.9 M methanesulfonic acid. A potential step to +1650 mV in figure (12) and +1750 mV in figure (13) was used. From figure (12) it can be seen that when the applied potential is small, the deposit tends to produce smooth and well defined hemispheres. The separation between the neighbour hemispheres is clear. In figure (13) the hemispheres start to coalesce and some parts of the surface are covered by densely overlapping hemispheres. This effect is more visible when the Pb(II) concentration is increased. Figure (14) shows the early stages of growth when lead dioxide was deposited from a solution of 0.4 M Pb(II) in 1.2 M methanesulfonic acid at a potential step of 1630 mV on a carbon plate electrode. It can be seen that hemispheres are rougher but retain the hemispherical shape.

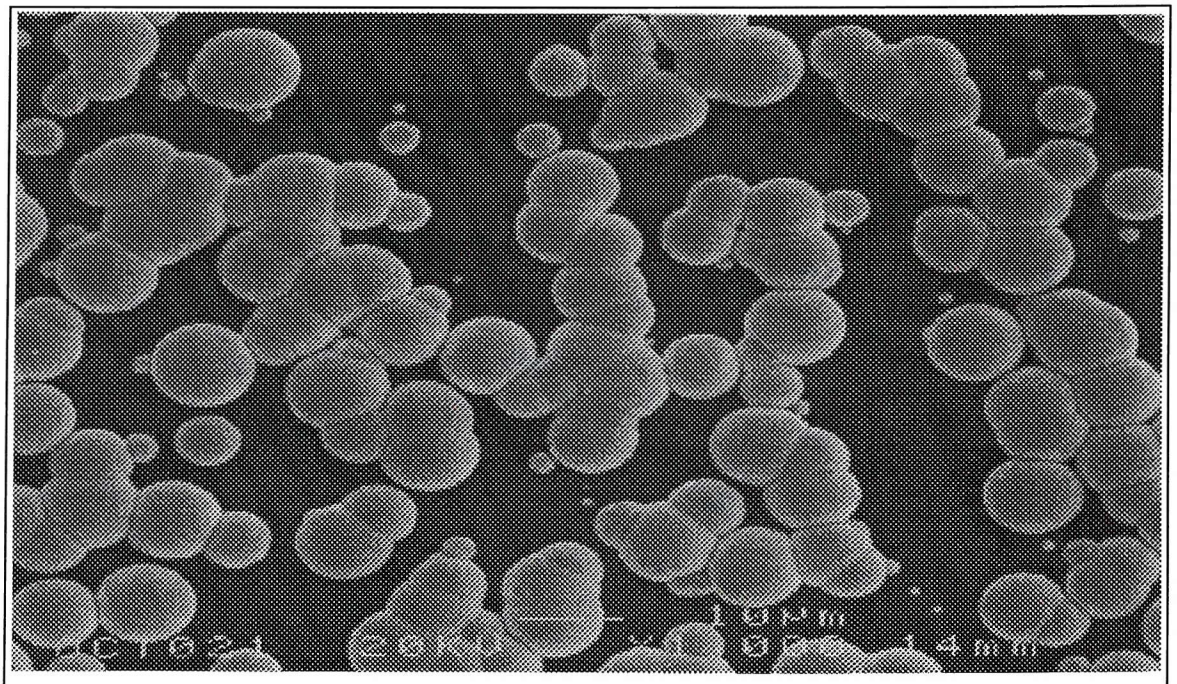

Figure (12) SEM image of lead dioxide deposited on vitreous carbon plate (~ 0.5 cm^2) from 40 mM Pb(II) in 1.9 M methanesulfonic acid. At a potential of 1.65 V for 7.7 minutes.

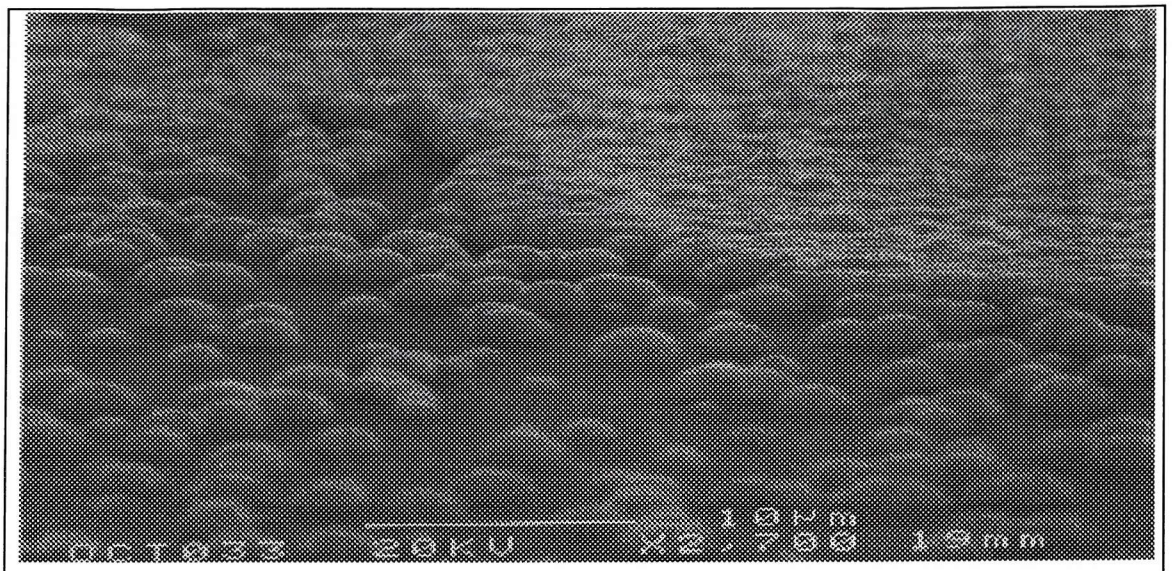

Figure (13) 70^{O} angle SEM image of lead dioxide deposited on vitreous carbon plate (~ 0.5 cm^{2}) from 40 mM Pb(II) in 1.9 M methanesulfonic acid. At a potential of 1.75 V for 35 s.

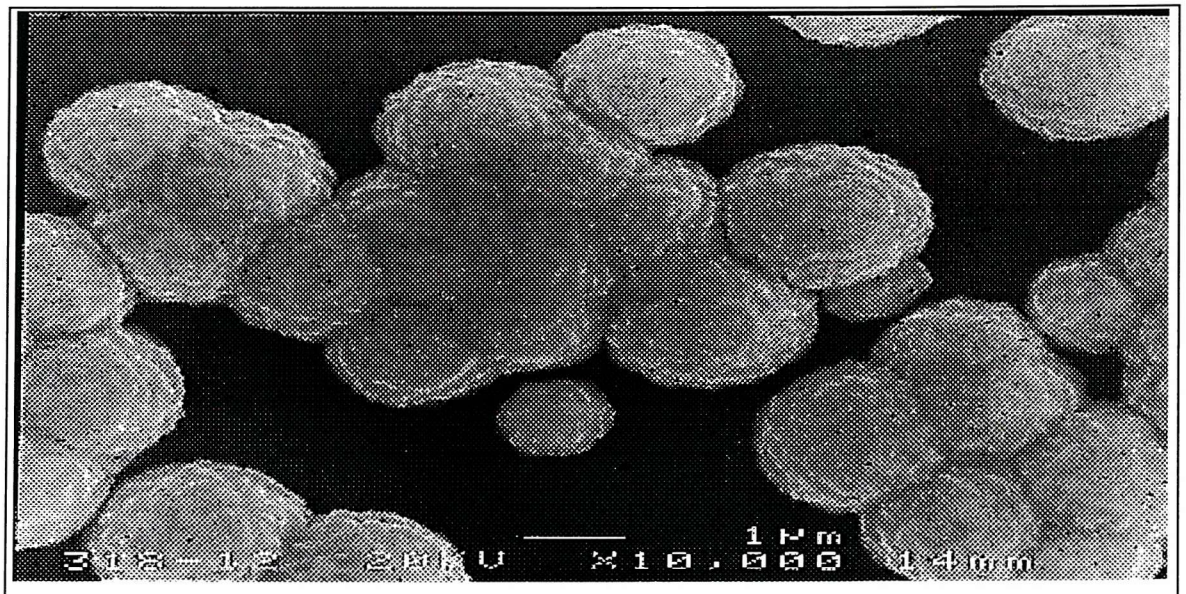

Figure (14) SEM image of lead dioxide deposited on vitreous carbon plate (~ 0.5 cm^{2}) from 0.4 M Pb(II) in 1.2 M methanesulfonic acid. At a potential of 1.63 V.

The SEMS above show nuclei with some variation in size although there are many hemispheres of similar size and it is therefore difficult to ascertain the nucleation mechanism. Growth is certainly 3D. This observation is in agreement with previous work [36]. It can be inferred also that the applied potential and the concentrations of the Pb(II) and methanesulfonic acid have a key role in the size, number of nuclei and morphology of the deposited PbO_2. Moreover, the crystal forms of lead dioxide i.e. α–PbO_2 and β–PbO_2, are also affected by the conditions of the deposition as reported in the literature using X-ray techniques [55]

Some SEMS have been obtained during the dissolution period and represented in figures (15, D) and (16, E). The figures show hemispheres which are less dense and have a "furry" appearance. It is not clear whether this residue represents the remaining lead dioxide or another substance produced during the reduction process such as PbO as suggested by [44]. Nevertheless, SEMS images have not previously been used to observe the residues on the electrode surface after the dissolution of lead dioxide.

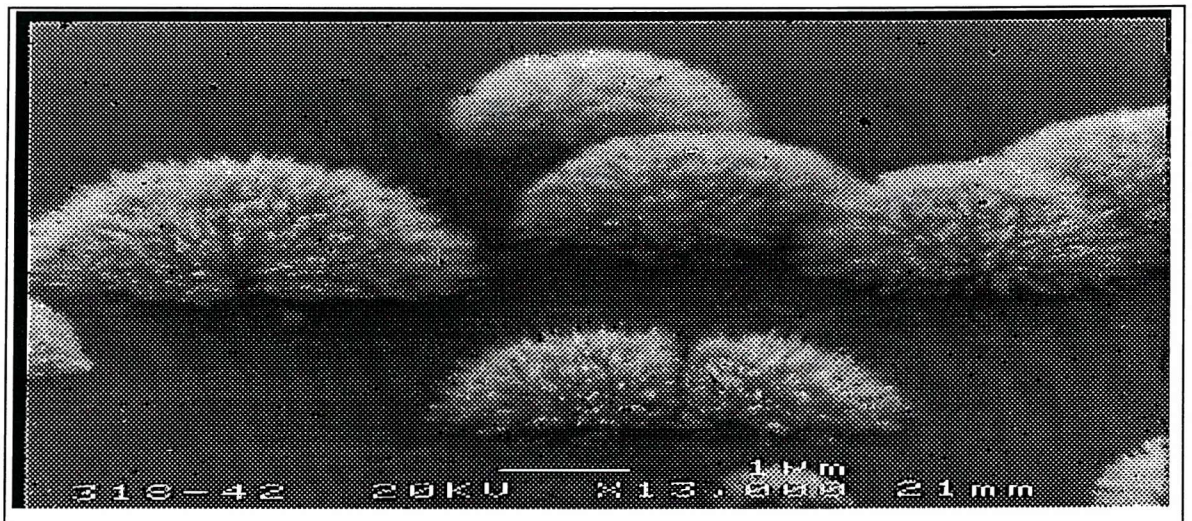

Figure (15) 70^{O} angle SEM image of the residues on the electrode surface after the stripping of lead dioxide. PbO_2 was deposited on vitreous carbon plate (~ 0.5 cm^2) from 0.4 M Pb(II) in 1.2 M methanesulfonic acid. At a potential of 1.65 V

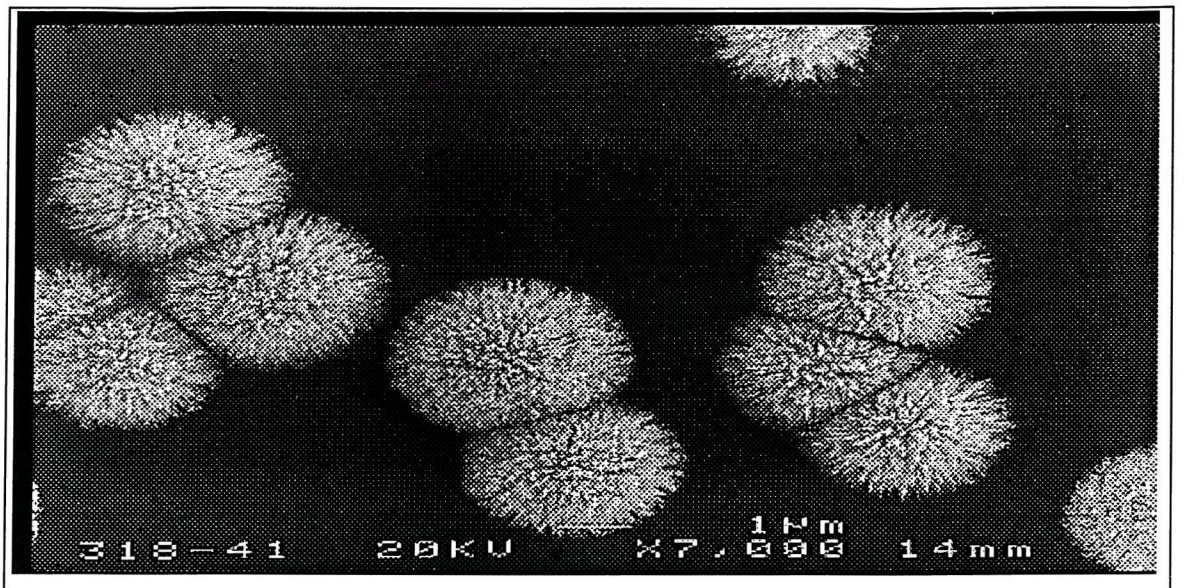

Figure (16) SEM image of the residues on the electrode surface after the stripping of lead dioxide. PbO_2 was deposited on vitreous carbon plate (~ 0.5 cm^2) from 0.4 M Pb(II) in 1.2 M methanesulfonic acid. At a potential of 1.65 V

4-6 Scan rate; effect of the quantity of deposited PbO_2

The effect of scan rate on the voltammogram has been studied. In figure (17), three voltammograms have been recorded on a gold rotating disc electrode from 0.4 M Pb(II) and 2 M methanesulfonic acid solution at a rotation rate of 900 rpm and scan rates of 10, 20 and 40 mV/s. The electrode was cleaned thoroughly prior to each scan. It is seen that decreasing the scan rate causes more lead dioxide to be deposited on the electrode surface. At scan rate of 10 mV/s, it can be seen that the deposition has started at earlier potential since the nucleation process had enough time to create lead dioxide nuclei. At this scan rate, deposition and dissolution of PbO_2 is occurring at current densities > 100 mA cm^{-2}. The reduction peaks are occurring at the same potential and the area under the peaks are proportional to the deposited lead dioxide during the forward scan. Moreover, when the scan rate was increased to 80 mV s^{-1}, no anodic current or cathodic peak the voltammogram was detected with the same current sensitivity. The deposition potential with a scan rate of 5 mV s^{-1} was even earlier and

the quantity of the lead dioxide deposited was very high but the stripping peak was very small. Flakes were seen falling from the electrode indicating that the higher quantities of lead dioxide deposit on the electrode the less charge ratio and probably less adhesion with the surface. The charge ratios (Q_C/Q_A) for 10, 20 and 40 mV s^{-1} were estimated as 70,100 and 100 % respectively indicating that the more deposit on the electrode, more likely it is that solid material is lost to the solution.

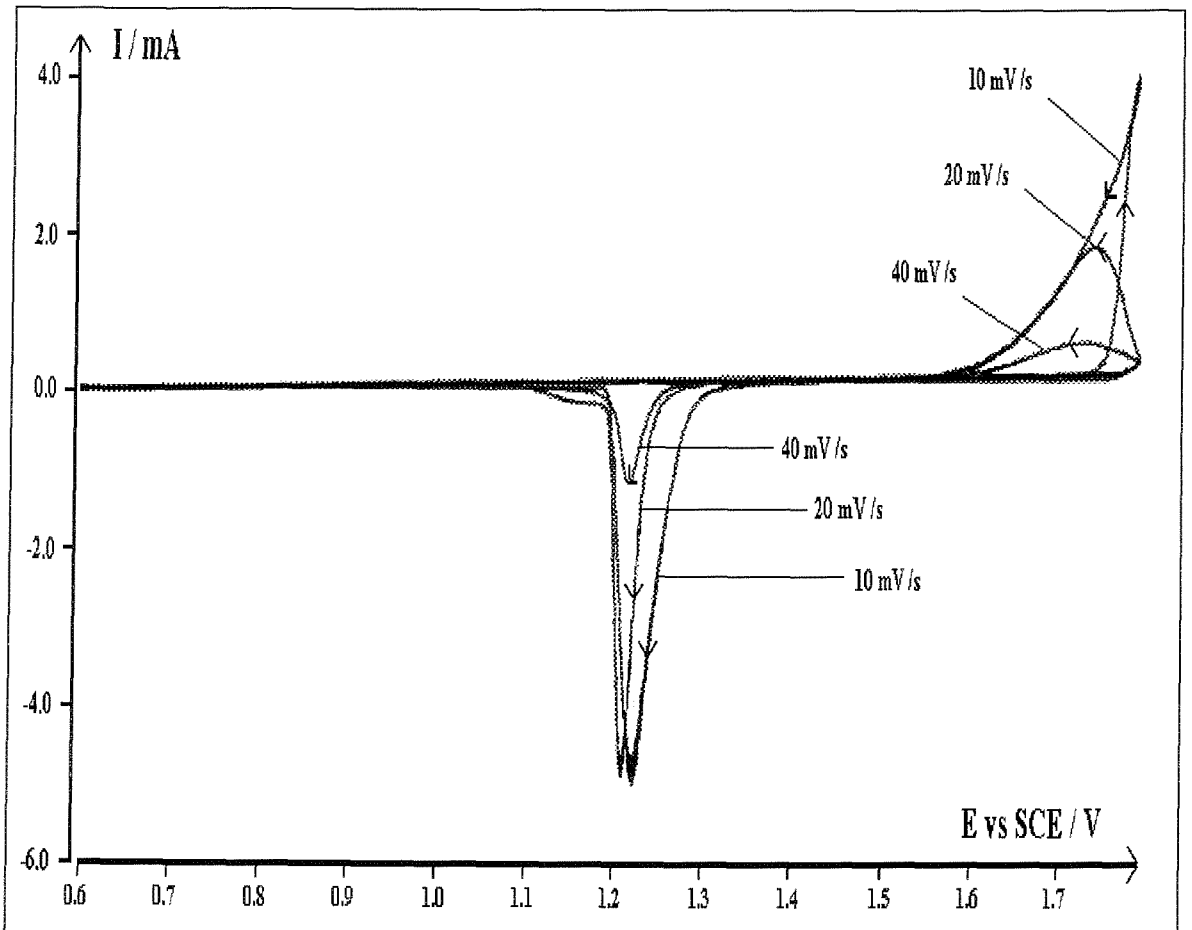

Figure (17) Three cyclic voltammograms recorded on gold rotating disc electrode (0.03 cm^2) from 0.4 M Pb(II) in 2 M methanesulfonic acid at three different scan rates; 10, 20 and 40 mV s^{-1}. Rotation speed was 900 rpm.

4-7 Pb(II) concentration

Cyclic voltammograms have been recorded on vitreous carbon in three solutions containing different Pb(II) concentrations; 400, 40 and 10 mM in 2 M methanesulfonic acid figures (18) (19) and (20) respectively.

Figure (18) shows a voltammogram recorded on vitreous carbon disc electrode from a solution of 400 mM Pb(II) and 2 M methanesulfonic acid. The voltammogram shows a small wave at E > 1700 mV before the rapid increase associated with PbO_2 deposition. These waves have been seen in the voltammogram of vitreous carbon disc electrode in 2 M methanesulfonic acid as in figure (2). Therefore, they might be related to an adsorption process otherwise they might be attributed to loss of Pb(IV) into solution before a solid phase is formed. The current then increases due to lead dioxide deposition. During the reverse scan the deposition continues with decreasing current until the potential reaches the equilibrium at about 1500 mV where the current reaches zero. A symmetrical reduction peak is seen at E_P = 1200 mV representing the dissolution process of lead dioxide. Negative to the dissolution peak is another process around 1000 mV followed by a tail with a reducing current. The charge ratio between the cathodic and anodic scans (Q_C/Q_A) = 95 %.

On the other hand, when 40 mM Pb(II) is used, the nucleation process takes more time to develop solid lead dioxide and therefore the potential is shifted towards more positive values as seen in figure (19). The increase of current during the deposition of lead dioxide is less sharp compared to 400 mM Pb(II) indicating a slower growth of the deposit because of the concentration decrease. The reduction process is not as clear as expected. There is a family of peaks spread over a wide range of potential. From the shape of the cathodic scan, it is concluded that there are more than one step in the dissolution process i.e. PbO_2 goes through more than one species before it finally transformed to Pb(II). Even more, different behaviour is seen with 10 mM Pb(II) where no, or little, lead dioxide is deposited on the electrode and severe corrosion is observed on the vitreous carbon surface. It is not clear why this is happening in the lower concentration of Pb(II). Therefore, it can be concluded that vitreous carbon is limited in use to high concentration of Pb(II).

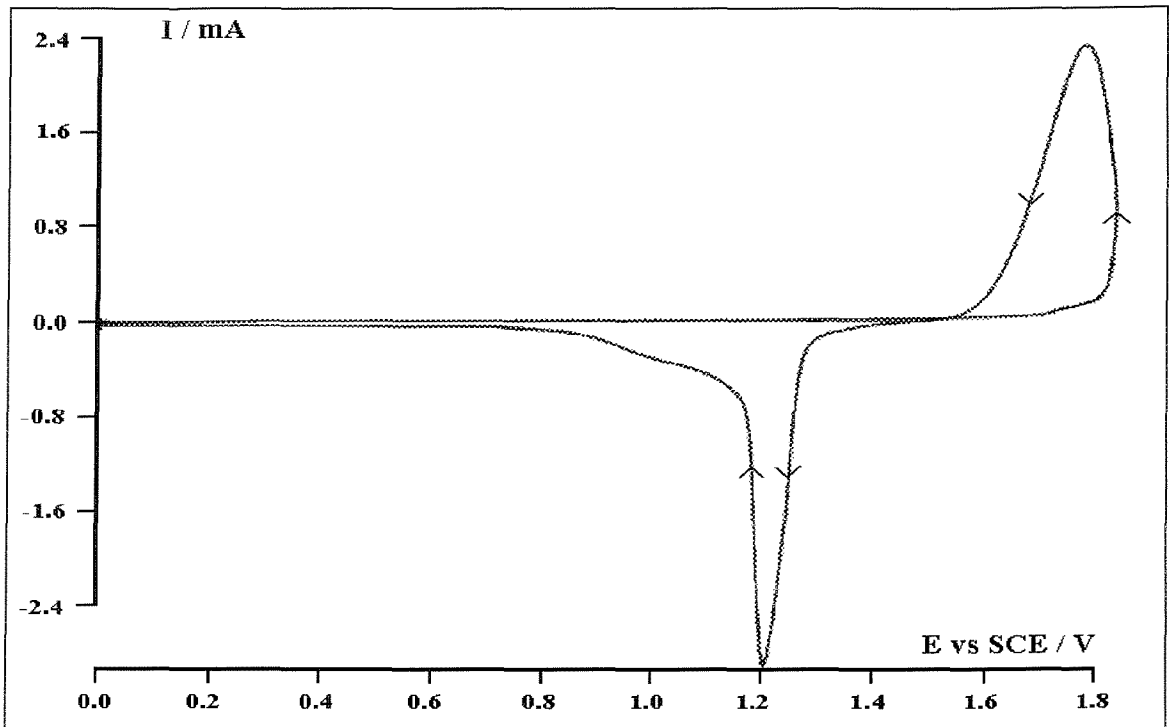

Figure (18) Cyclic voltammogram recorded on vitreous carbon rotating disc electrode (0.126 cm^2) from 0.4 M Pb(II) in 2 M methanesulfonic acid at a rotation speed of 400 rpm.

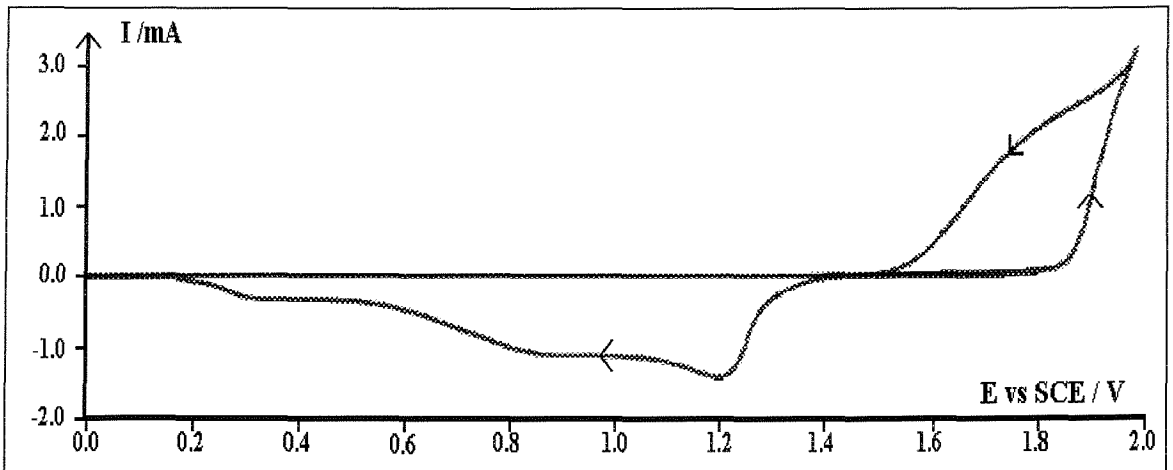

Figure (19) Cyclic voltammogram recorded on vitreous carbon rotating disc electrode (0.126 cm^2) from 40 mM Pb(II) in 2 M methanesulfonic acid at a rotation speed of 400 rpm.

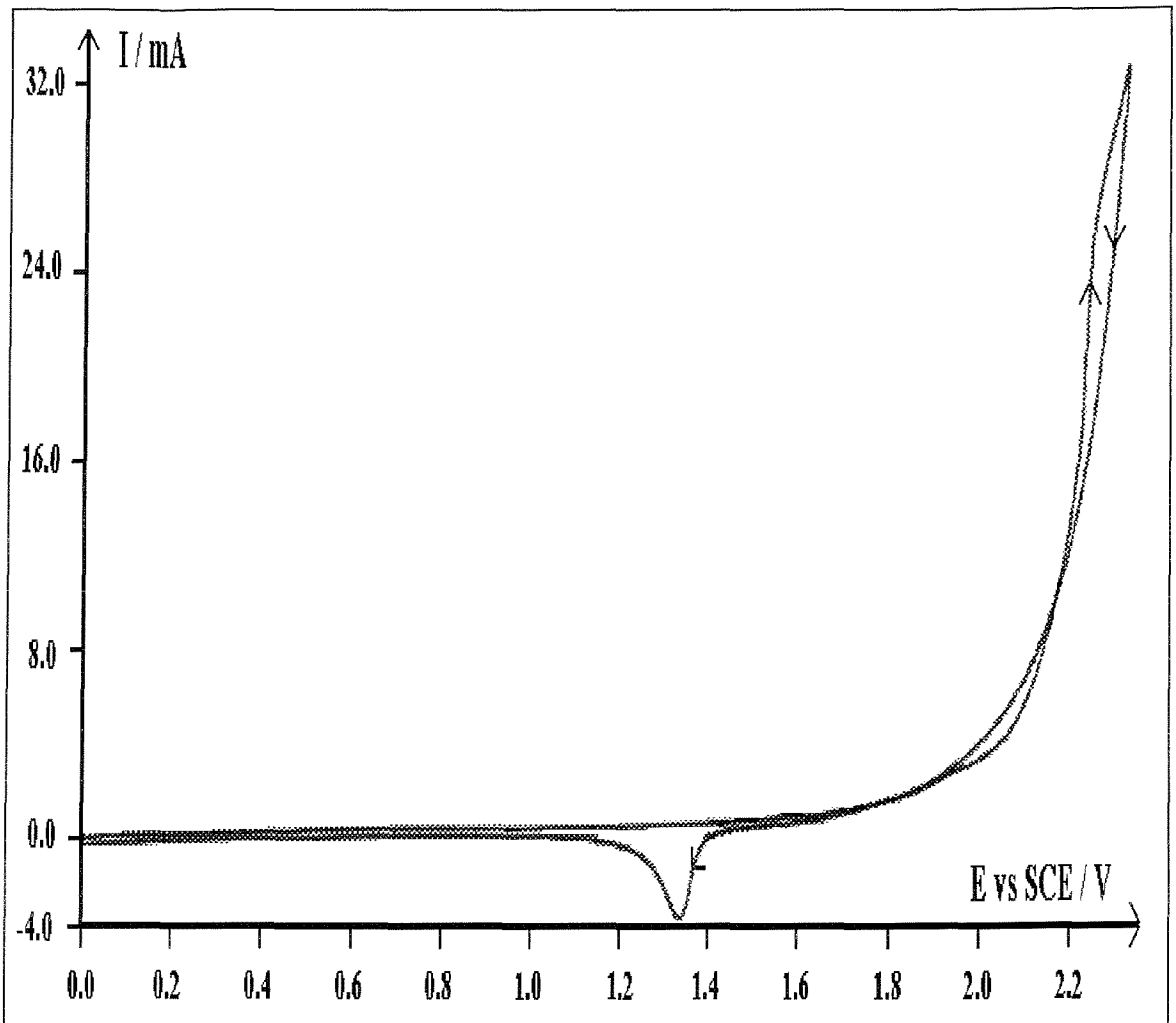

Figure (20) Cyclic voltammogram recorded on vitreous carbon stationary disc electrode (0.126 cm^2) from 10 mM Pb(II) in 2 M methanesulfonic acid.

Gold however, does not corrode in any of the above concentrations. The voltammograms in figures (21) (22) and (23) were recorded on a stationary gold disc electrode from 400, 40 and 10 mM Pb(II) in 2 M methanesulfonic acid solutions respectively. In 400 mM Pb(II), lead dioxide deposits on the electrode and the current increases promptly at E > ca. 1700 mV and continues during the reverse scan due to lead dioxide deposition. A symmetrical, narrow and sharp reduction peak is seen at E_P = ca. 1200 mV due to the dissolution of lead dioxide. Negative to the dissolution peak, a tail with a relatively low current is seen which eventually decreases to zero at the end of the cathodic scan. The cyclic voltammogram has well defined features and no

interference is seen. The dissolution peak is very sharp indicating fast kinetics during the dissolution process compared with vitreous carbon electrode. The charge ratio Q_C/Q_A is 99 % which is higher than the corresponding vitreous carbon electrode hence, it can be inferred that gold is a better substrate than vitreous carbon in this context. The same features of the deposition/dissolution processes when the Pb(II) concentration is reduced to 40 mM with slight differences. The small peak at E_P = ca. 900 mV is due to reduction of the Au oxide. No major changes has been noticed with 10 mM Pb(II) except for the oxidation of the gold electrode at potentials > 1200 mV. The reduction peak of the Au oxide becomes more prominent because of the sensitivity of the voltammogram.

Clearly, gold shows better voltammograms than vitreous carbon in all the concentrations that have been used probably because of a slightly more adherence with the deposited lead dioxide.

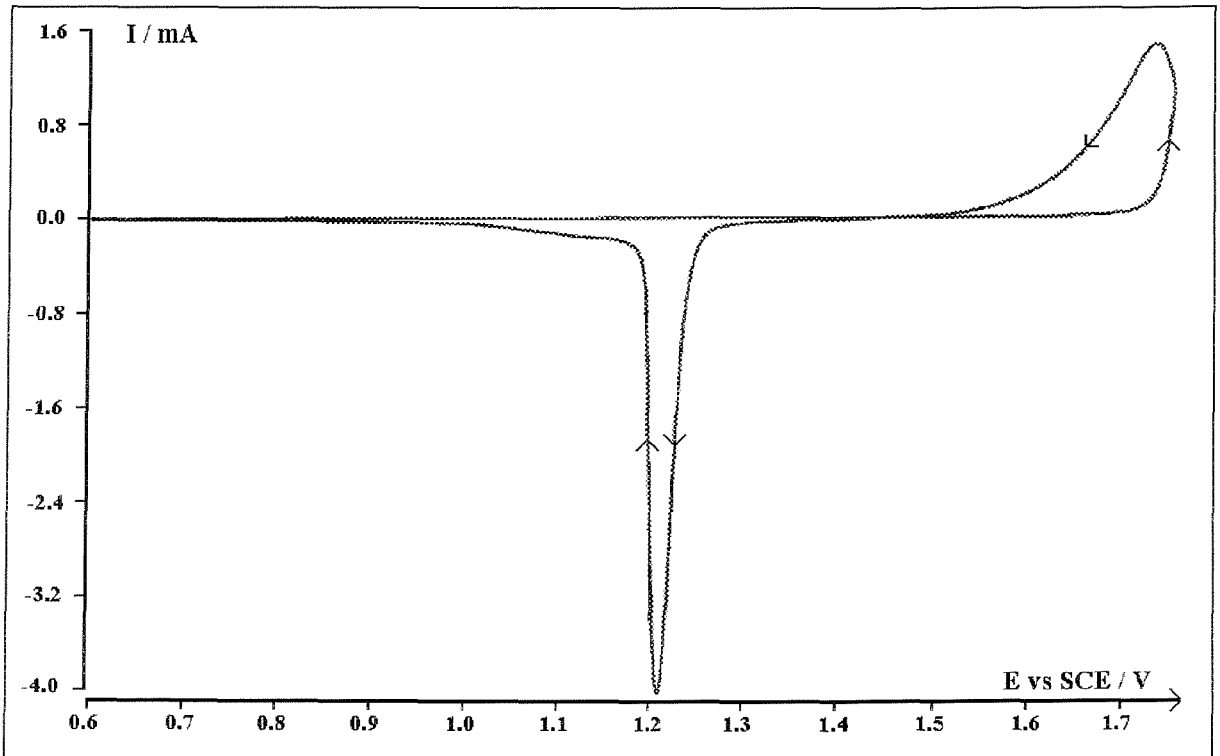

Figure (21) Cyclic voltammogram recorded on gold stationary disc electrode (0.03 cm^2) from 0.4 M Pb(II) in 2 M methanesulfonic acid.

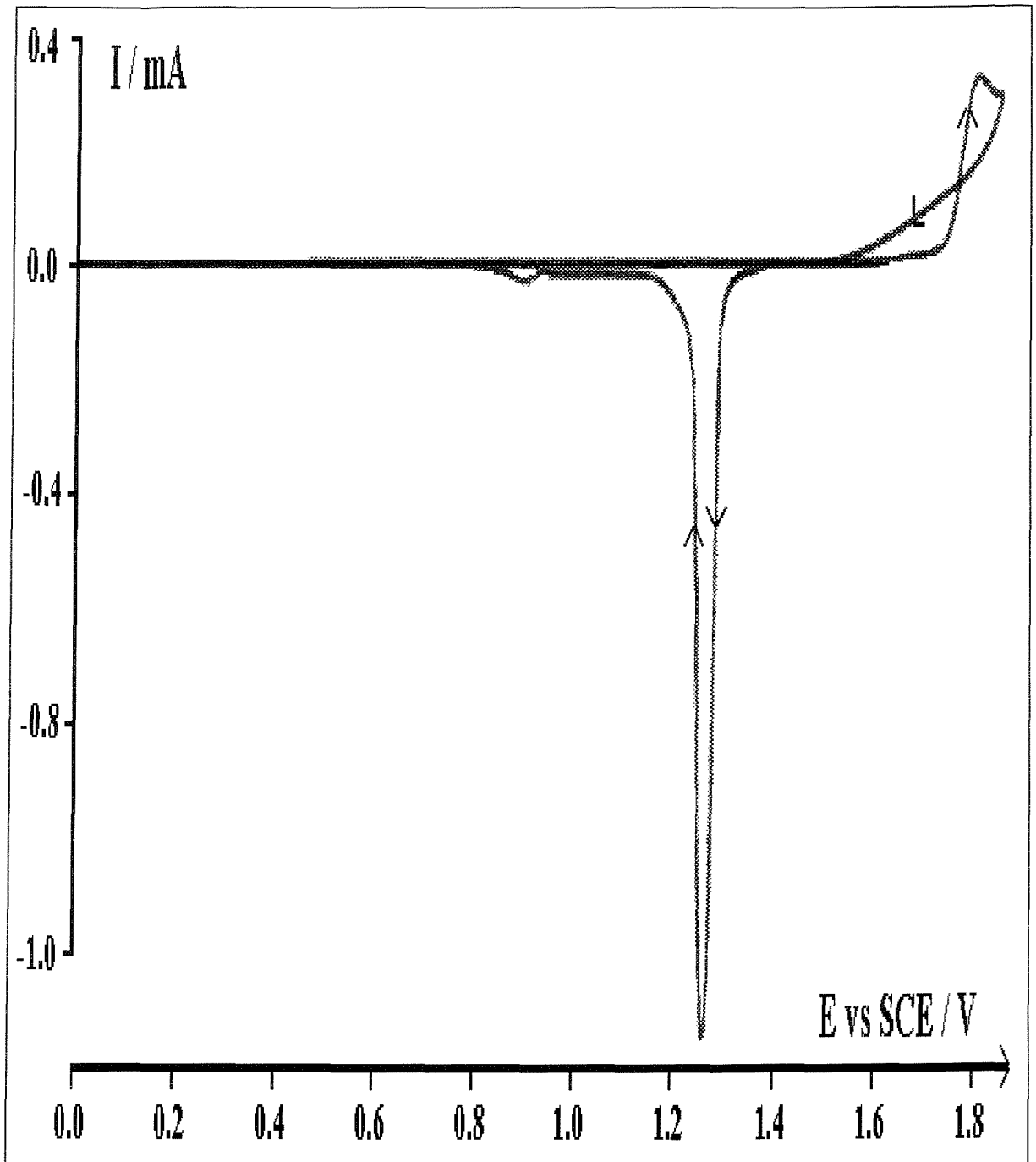

Figure (22) Cyclic voltammogram recorded on gold stationary disc electrode (0.03 cm^2) from 40 mM Pb(II) in 2 M methanesulfonic acid.

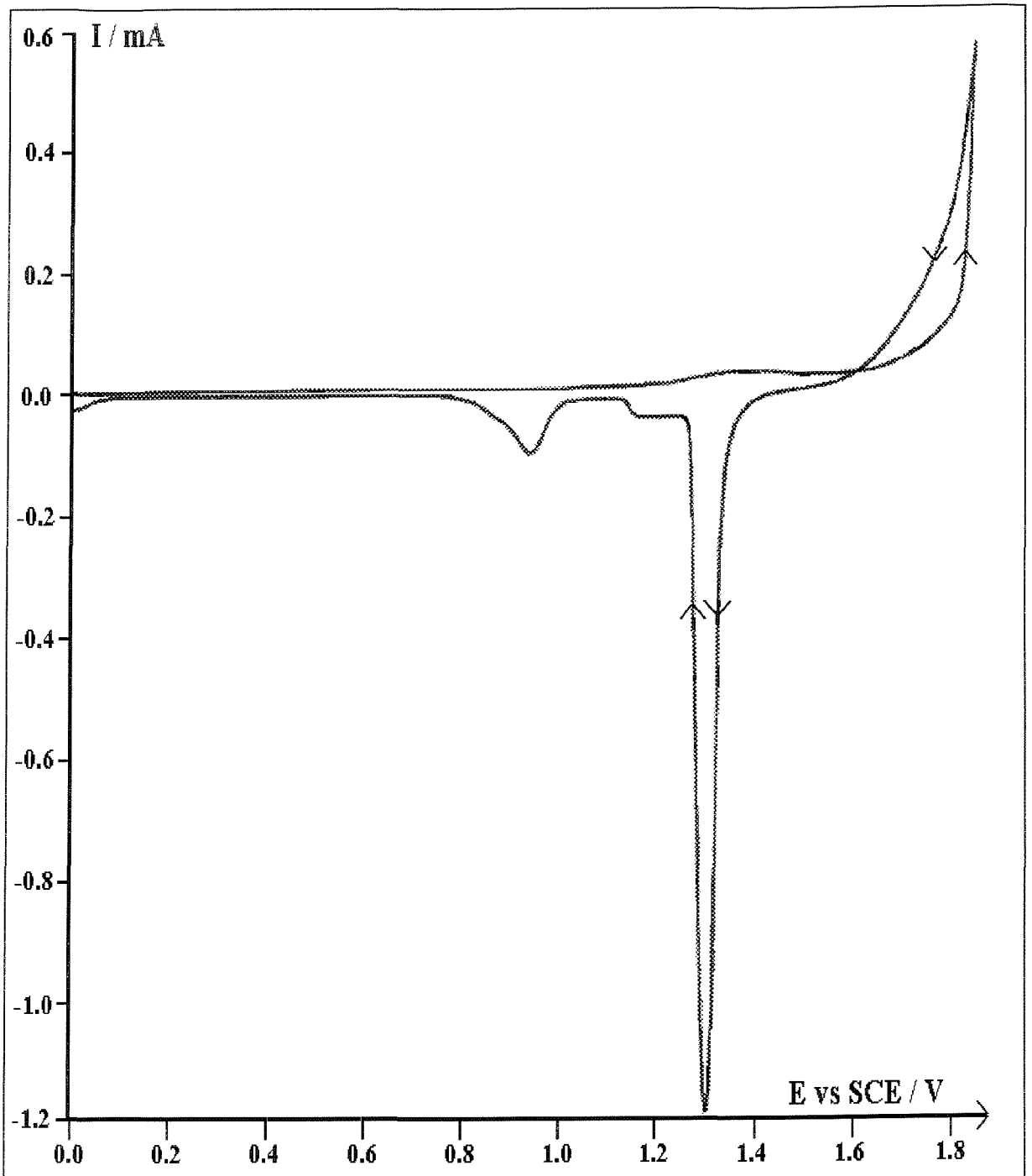

Figure (23) Cyclic voltammogram recorded on gold stationary disc electrode (0.03 cm^2) from 10 mM Pb(II) in 2 M methanesulfonic acid.

4-8 Methanesulfonic acid concentration

The methanesulfonic acid concentration has been varied to investigate the effect on the voltammetric features. Figure (24) shows a voltammogram recorded on vitreous carbon disc electrode from 400 mM Pb(II) in 0.2 M methanesulfonic acid solution. The voltammogram shows well defined deposition currents. The deposition has started at earlier potentials (E < ca 1700 mV) compared with 2 M methanesulfonic acid solution. A broad reduction peak is seen followed by a tail during the reverse scan. Some black flakes have been seen during the dissolution. A coloured residue is left on the electrode at the end of the scan. However, when the electrode is left at 0.0 V for enough time, the residues dissolve into the solution. The shape of the voltammogram in the following scan will be affected by the quantity of the residues on the electrode. More flakes are seen with thick deposits where the positive potential limit is increased. The charge ratio (Q_C/Q_A) was estimated to be 100 %.

Figure (25) shows another voltammogram at gold in the 0.2 M acid. It was not possible to detect any flakes falling from the electrode surface during the cathodic scan, the charge ratio (Q_C/Q_A) was estimated as 100 %. With higher quantities of lead dioxide deposited on the electrode, the dissolution peak expands even more and divides into more than one peak as in figure (26).

The pH of the solution increases during the reduction process due to the consumption of the acid. Hence in the lower acid concentration, there is more danger of forming PbO or $Pb(OH)_2$ by reduction of the PbO_2. Acid deficiency within the layer on the electrode is likely when the bulk acid concentration is low. It is also noted that the colour of the deposit is changing during the reduction process on both vitreous carbon and gold electrodes which leads to the conclusion that the tail at the end of the reduction scans is due to such compounds.

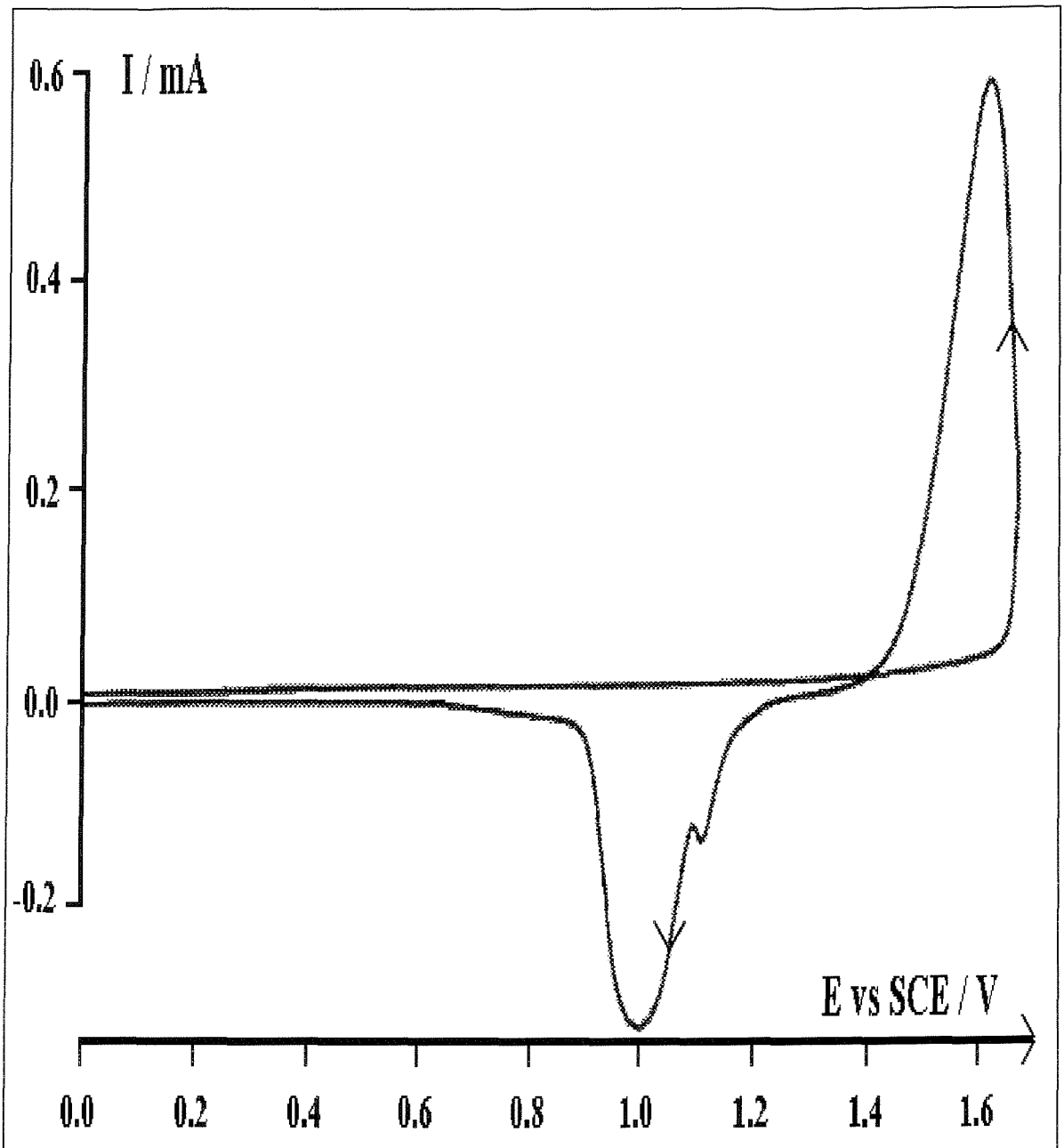

Figure (24) Cyclic voltammogram recorded on vitreous carbon stationary disc electrode (0.126 cm^2) from 0.4 M Pb(II) in 0.2 M methanesulfonic acid.

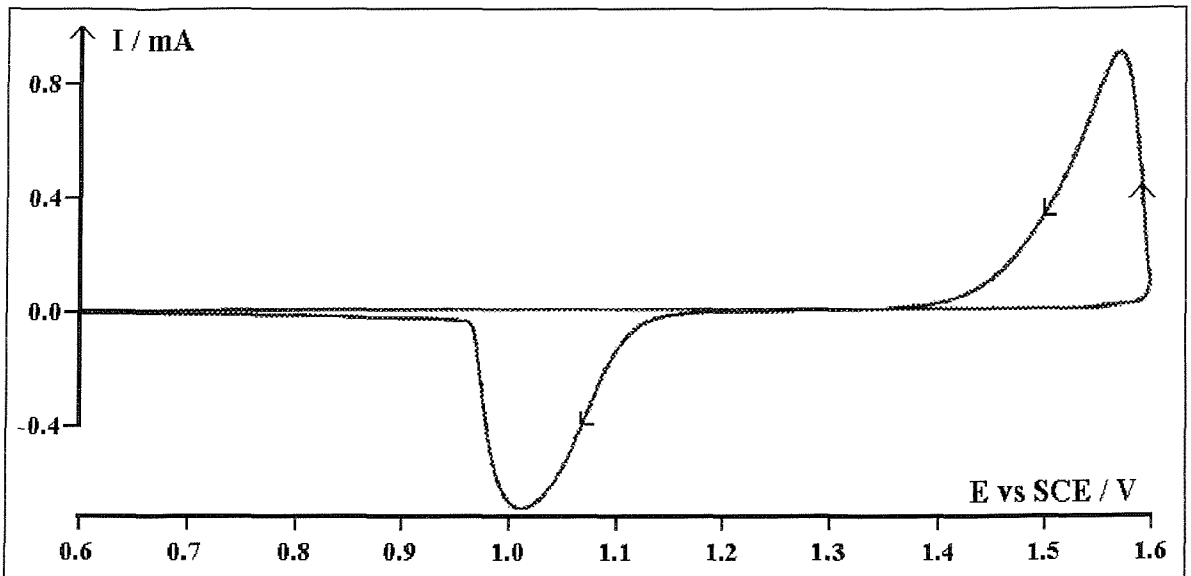

Figure (25) Cyclic voltammogram recorded on gold stationary disc electrode (0.03 cm^2) from 0.4 M Pb(II) in 0.2 M methanesulfonic acid.. Potential limits 0.6 - 1.59 V.

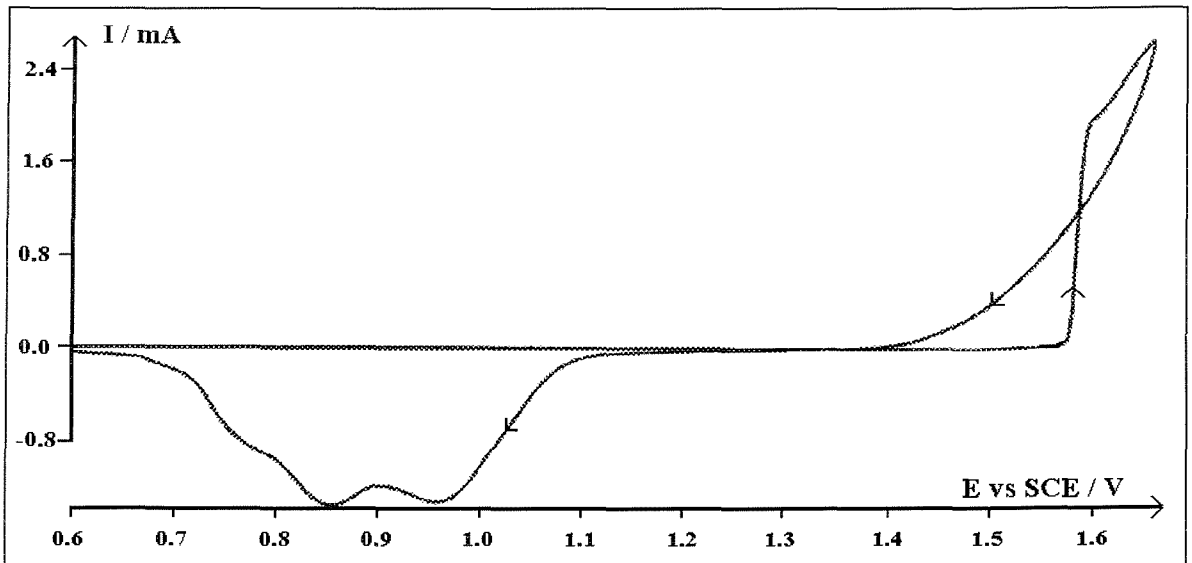

Figure (26) Cyclic voltammogram recorded on gold stationary disc electrode (0.03 cm^2) from 0.4 M Pb(II) in 0.2 M methanesulfonic acid. Potential limits 0.6 - 1.65 V.

It is assumed that the reason of the loss of the deposit during the dissolution process is the poor adhesion between the lead dioxide and the electrode. The dissolution starts at the electrode surface where a gap between the deposit and the electrode is existed causing the deposit to drop from the electrode.

Clearly, the acid concentration has a clear effect on the nucleation process of lead dioxide deposition. Higher concentrations of acid depress the nucleation therefore, higher potentials are needed for nucleation and growth of the deposit. In contrast, the reduction of PbO_2 is easier in the more acidic solution.

4-9 Current density

Oxygen evolution is an inevitable competing process since it proceeds simultaneously with the deposition of lead dioxide. The quantity of oxygen evolved is a function of the applied potential i.e. at high current densities the rate is high (see table 1). This, of course, lowers the charge efficiency of the battery. Another negative effect of the gas bubbles is that these bubbles will cause the PbO_2 deposit to be spongy and expanded as seen in figure (35).

4-10 Effect of lignin sulfonate

Lignin sulfonate was used to enhance lead deposition during the cathodic charging process. The proposed battery system does not contain any separator between the anode and cathode compartments therefore, the anodic behaviour of lignin sulfonate in Pb(II) and methanesulfonic acid solution during the deposition of lead dioxide was studied. Figure (27) shows a voltammogram recorded on vitreous carbon disc electrode for a solution of 400 mM Pb(II) in 2 M methanesulfonic acid + 1 g/l lignin sulfonate. The voltammogram shows an oxidation current for lead dioxide deposition and a sharp reduction peak at E_P = ca. 1200 mV followed by a slow decreasing current which does not decay to zero at the end of the cathodic scan. The overall shape of the response is not greatly changed by the presence of lignin sulfonate but the growth of the lead dioxide has been inhibited by the presence of lignin sulfonate

and the deposition potential has been shifted to higher values. There was no other anodic waves hence, it is inferred that the lignin sulfonate does not degrade on lead dioxide at positive potentials. The charge ratio is much lower in the presence of lignin sulfonate. Q_C/Q_A = 42 % while it is = 99 % in the absence of lignin sulfonate (note that the E_2 is lower in this case). It is also seen that the current of the tail is higher compared to the solution which does not contain the additive.

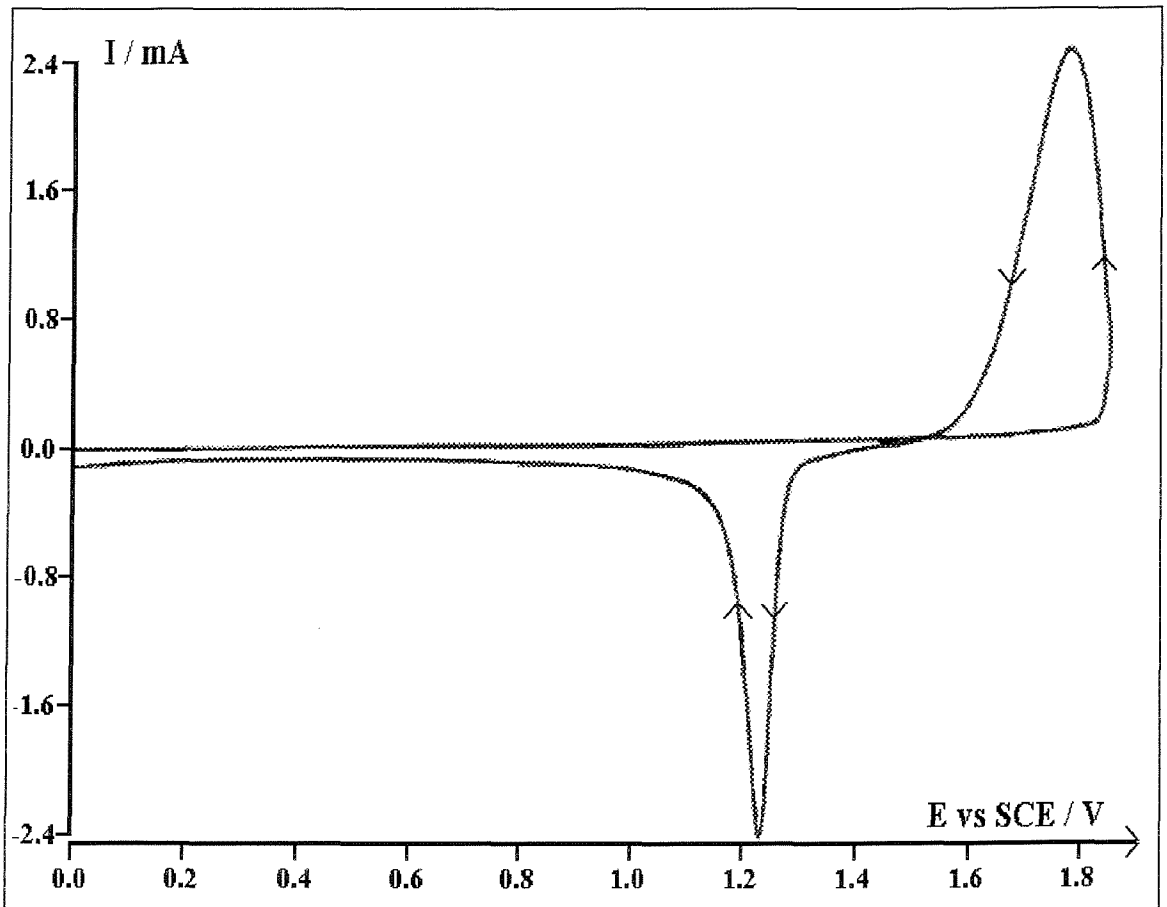

Figure (27) Cyclic voltammogram recorded on vitreous carbon stationary disc electrode (0.126 cm^2) from 0.4 M Pb(II) in 2 M methanesulfonic acid + 1 g/l lignin sulfonate. Potential limits 0.0 - 1.83 V.

Lignin sulfonate has similar effect on the voltammogram which recorded on gold disc electrode as presented in figure (28). Again, the anodic scan has the same features when lignin sulfonate was added to the solution except for a slight positive shift of the deposition process i.e. E > ca. 1750 mV (E = ca.1750 mV in the absence of lignin sulfonate). The reduction peak remains sharp but there is obvious further reduction at less positive potentials. The charge ratio (Q_C/Q_A) = 73 % while (Q_C/Q_A) in the absence of the lignin sulfonate = 100 %. Clearly, the lignin sulfonate has decreased the charge ratio and inhibited the deposition of lead dioxide on both, vitreous carbon and gold electrodes.

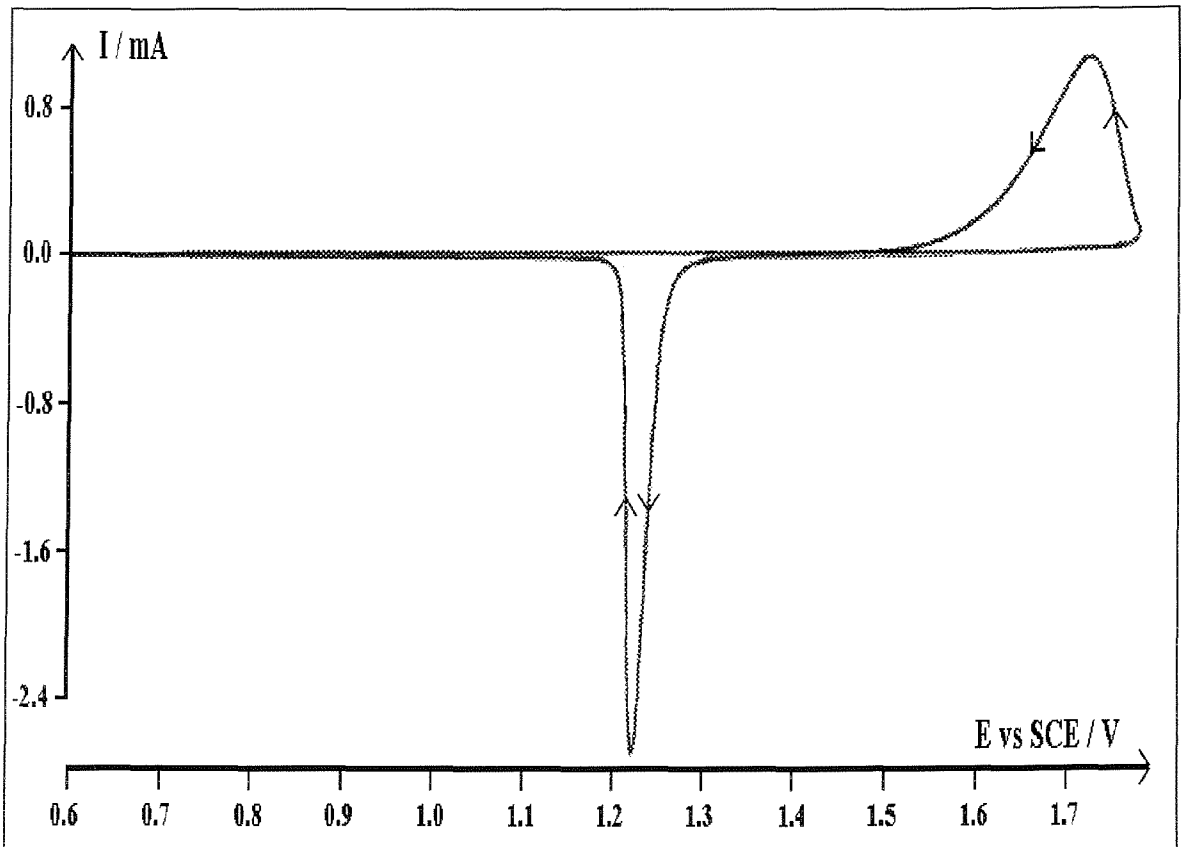

Figure (28) Cyclic voltammogram recorded on gold stationary disc electrode (0.03 cm^2) from 0.4 M Pb(II) in 2 M methanesulfonic acid + 1 g/l lignin sulfonate. Potential limits 0.0 - 1.77 V.

In order to confirm all the features of the previous voltammograms on vitreous carbon and gold disc electrodes, two voltammograms were recorded on vitreous carbon and gold rotating disc electrodes from a solution of 2 M methanesulfonic acid and 1 g/l lignin sulfonate without any Pb(II) as seen in figures (29) and (30) respectively. Clearly there are no significant waves in the voltammograms due to the presence of lignin sulfonate in the solution. This is an indication of its stability to oxidation in these conditions and no interference with the deposition of lead dioxide within the applied potential range. Even on lead dioxide, lignin sulfonate shows no degradation behaviour as mentioned above. However, in a plating experiment of lead dioxide, it has been noticed that the deposit is porous and foam like because oxygen has coupled with the deposit which in turn caused by the lignin sulfonate (see plating section below). The effect is not clear when the electrode is in a vertical position which may facilitate the removal of the gas bubbles away from the surface.

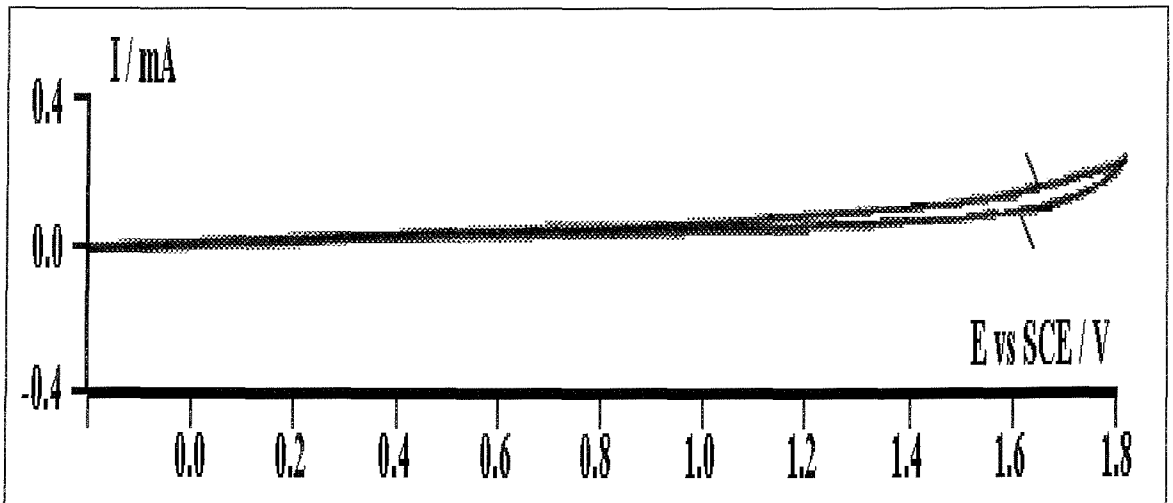

Figure (29) Cyclic voltammogram recorded on vitreous carbon stationary disc electrode (0.126 cm^2) in 2 M methanesulfonic acid + 1 g/l lignin sulfonate. Potential limits 0.0 - 2.0 V.

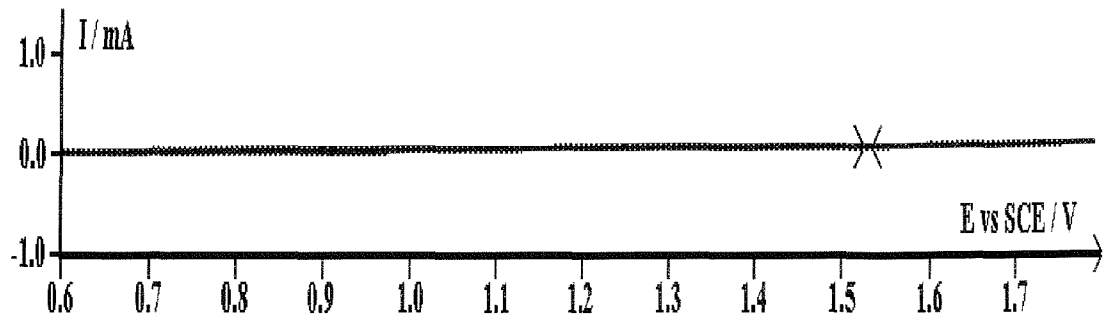

Figure (30) Cyclic voltammogram recorded on gold stationary disc electrode (0.03 cm^2) in 2 M methanesulfonic acid + 1 g/l lignin sulfonate. Potential limits 0.6 - 1.78 V.

Vitreous carbon and gold electrodes have different characteristics in both cases i.e. in the presence and the absence of lignin sulfonate. However it can be concluded that lignin sulfonate does not degrade on lead dioxide electrode. The charge ratio has decreased in the presence of lignin sulfonate but there were no flakes in the solution indicating that the effect was on the kinetics of the dissolution of lead dioxide.

4-11 Multiple scans

Multiple scan cyclic voltammetry has been applied to study the effect of any residues on the electrode surface after the first scan, on the subsequent scans. Figure (31) shows seven successive scans recorded on vitreous carbon rotating disc electrode from solution of 0.4 M Pb(II) and 1.2 M methanesulfonic acid. The first scan shows an increase of current at E = ca. 1800 mV which can be attributed to lead dioxide deposition. The deposition continues during the scan back. A reduction peak is seen at E_P= 1150 mV then the current decreases gradually. The second scan starts immediately after the first scan. A wave is seen at E > ca. 1600 mV before the current increases again which probably indicates the oxygen evolution reaction. As in the first scan, the lead dioxide deposition continues in the scan back then a reduction peak with higher current is seen at E_P = ca 1100 mV. The peak has shifted to a negative potential. In the

subsequent scans, the first oxidation peak is increasing with the number of scan. The current which is attributed to oxygen also increases but not as great as the first peak. All the reduction peaks are symmetrical and well formed. The current increases as a result of the increase in the deposition. At the seventh scan, it seems that the deposition has reached a stable position and a fixed quantity of lead dioxide is deposited during the anodic scan. There was some brown residues on the electrode after the experiment and some small flakes have been noticed in the cell. Some flakes also seen during the deposition of lead dioxide which indicates that the adhesion is very poor between the deposit and the electrode.

Clearly, there were some residues on the electrode which have not dissolved completely during the stripping scan and these have influenced the subsequent cycles. The residues are accumulating on the electrode surface after each scan. The residues are not only lead dioxide, but also some other lead compounds that are difficult to dissolve during the stripping scan. In some other experiments, the brown residues have been found on the Teflon sheath surrounding the electrode disc and covering a circular area which increases with the number of scan.

On the other hand, the voltammograms show no deterioration during 7 cycles. Indeed, the performance from a battery viewpoint is improving. Reasonable charge balance is seen with layers that are thickening with cycling. By the 6^{th} cycle, deposition and reduction are both occurring with a current density > 200 mA cm^{-2}.

Similar results have been found on gold electrode. Further, it has been noticed that the initial potential has an influence on the shape of the voltammogram in the succeeding scans. The more positive potential is the starting potential, the earlier the growth of the deposit and vice versa. This indicates that the residues during the reduction period is influenced by the potential and/or time and still contains traces of PbO_2. Also, it has been noticed that the hold time, i.e. the time between the scans at the negative limit, strongly influences the rate of PbO_2 deposition. In other words, when the electrode is left at the lower potential after the first scan for enough time, the potential at which the growth of the deposit takes place increases. That of course

indicates that the residues of the reduction process are not easily dissolves during the back scan. Some researchers claim that the residue is PbO [48] see above.

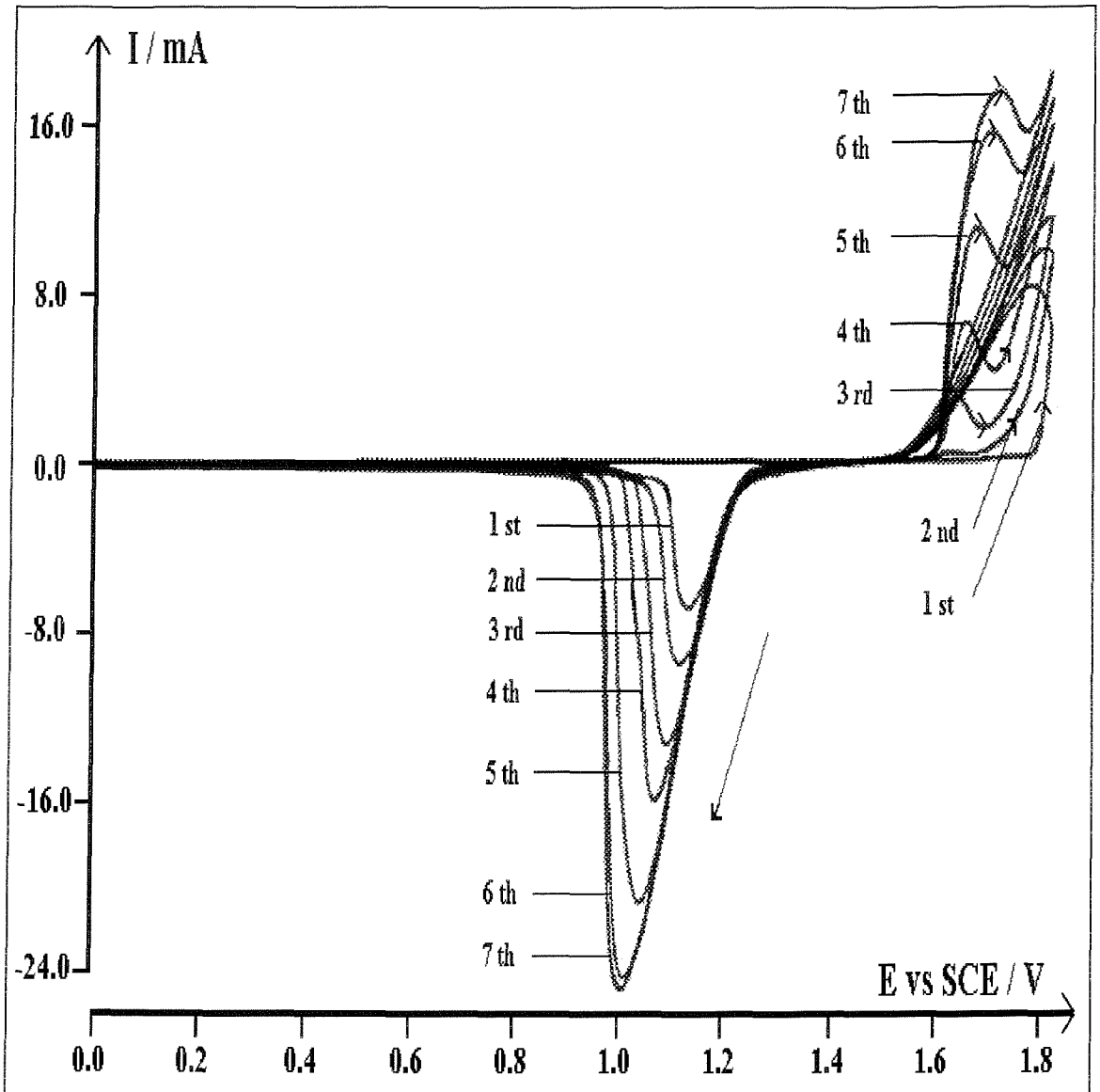

Figure (31) Multiple cyclic voltammograms recorded on vitreous carbon rotating disc electrode (0.126 cm^2) from 0.4 M Pb(II) in 1.2 M methanesulfonic acid at a rotation speed of 1600 rpm.

It can be concluded that

- lead dioxide deposits on gold and vitreous carbon electrodes.
- the deposit does not have any dendrites rather, it is relatively smooth but brittle.
- gas bubbles are associated with the deposition of the lead dioxide.
- the adhesion is poor even with low current densities.
- titanium and graphite electrodes corrode in methanesulfonic acid solutions.
- deposition of lead dioxide is not associated with dendrites therefore it may be possible to plate thick deposit.

4-12 Substrates for PbO_2 deposition

In the literature, there are reports of PbO_2 deposition on Pt, Au, C, Ti and steel from alkaline, neutral and acidic (other than methanesulfonic acid) solutions. In some cases these deposits have been used for commercial anodes and have given satisfactory lifetimes. It is clear that pre-treatment of the substrates has a large influence on the characteristics of the deposit and the adhesion between the deposited PbO_2 and the substrate. In most cases, the deposition is carried out with low current densities [34].

Cyclic voltammograms showed that for Ti and steel, corrosion was an obvious problem but Ni might be possible. Au, C (and probably Pt) have been shown to be satisfactory.

During the voltammetry experiments, it was felt that on vitreous carbon, the deposit was always brittle and adhered poorly to the surface. From the experiments with Au , the impression was that the deposits were more adherent.

A series of depositions were carried out from 0.4 M Pb(II) in 2 M methanesulfonic acid solution at several current densities and the results are summarised in table (2).

Electrode	J / mA cm^{-2}	Remarks
Au	1 60 min	Shiny deposit. Flat with very little gas bubbles under the surface. Poor adhesion. The deposit is brittle. See figure (32)
Au	5 44 min	Shiny deposit. Flat with little bulb on the surface. Adhesion is poor
Au	8 30 min	PbO_2 deposits. Brittle. Gas bubbles. The adhesion is poor
Au	10 22 min	Like the above. More expansion of the deposit on the surface.
Au	16 45 min	As the above.
Au	20 11 min	Shiny deposit. The edge is detached from the surface. Adhesion is poor.
Au	40 5.5 min	Like the above. Some bubbles within the deposit. There are more than one layer of lead dioxide.
Vitreous carbon	16 45 min	Shiny PbO_2 deposit. Brittle. Not flat. Flakes are on the electrode surface. Not adhered to the surface.
Vitreous carbon	32 22 min	As above. See figure (33)
Vitreous carbon	63 11 min	As above. Very lose and a whole disc of PbO_2 falls off the electrode during the rotation.
Graphite	16, 64 45 min	Little deposition even at high current densities. The electrode is corroding.
Ti	8, 16, 32 40 min each	No deposition has noticed and the electrode has corroded.
Ni	8 40 min	Shiny PbO_2 deposit. Porous and flaked
Ni	16 40 min	Shiny PbO_2 deposit. Porous and flaked see figure (34)
Ni	32 22 min	As the above Gas bubbles are implanted in the deposit.

RDE at 200 rpm and room temp.

Table (2) Lead dioxide electroplating on various materials from 0.4 M Pb(II) in 2 M CH_3SO_3H solution.

It can be seen from the table above, that the deposits were not satisfactory and the adhesion is always poor especially with the vitreous carbon electrode. However,

the deposits are smooth and shine hence the thickness of the deposit can be increased to high values.

When lead dioxide is deposited on nickel, it has been noted that the PbO_2 adhered to the edge of the electrode which means that the adhesion in this case is due to a mechanical means. Therefore, maybe it is appropriate to use electrodes with rough surfaces in order to enhance the mechanical attachment between the deposited PbO_2 and the substrate. Moreover, Johnson and Feng suggest the addition of NaF into the plating solution to enhance the adhesion between PbO_2 and Au electrode [49].

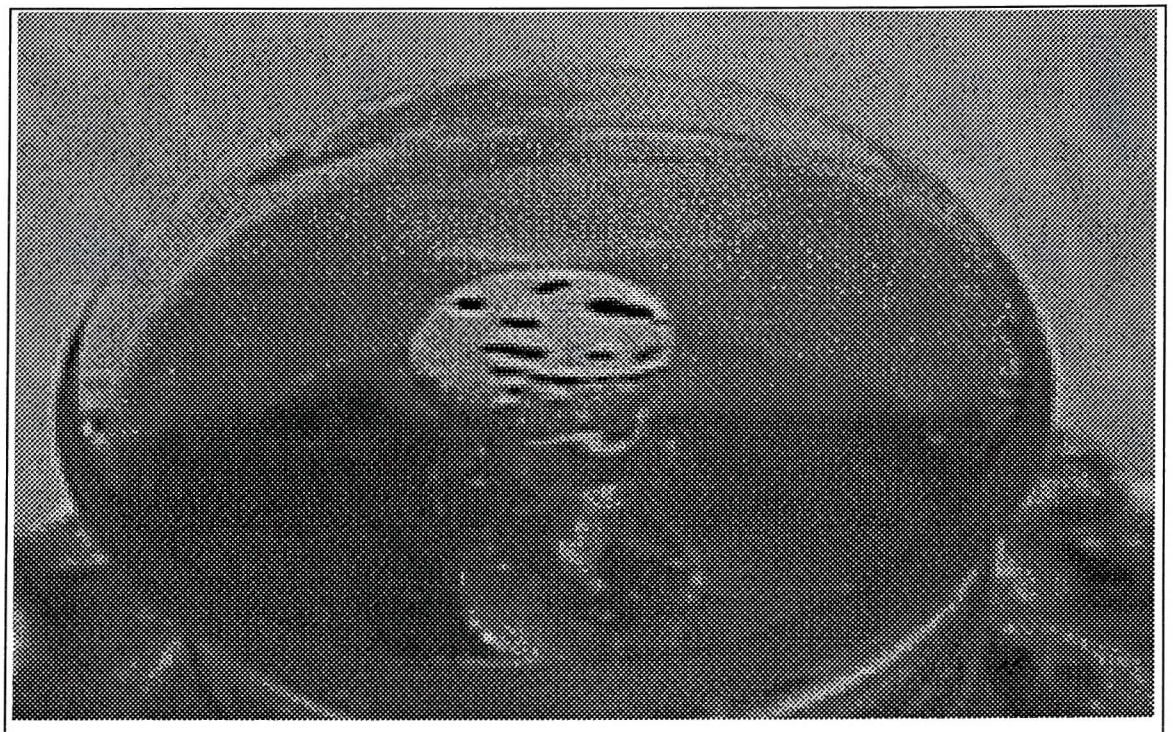

Figure (32) PbO_2 deposited on gold rotating disc electrode (0.03 cm^2) from 0.4 M Pb(II) in 2 M CH_3SO_3H acid solution at a rotation speed of 200 rpm. Current density is 1 mA cm^{-2}.

It is possible that titanium does not resist corrosion in methanesulfonic acid solution as seen in table (2). This was supported by cyclic voltammetry where the titanium was corroded to some extent and no lead dioxide was deposited from 0.4 M

Pb(II) and 2 M methanesulfonic acid. Even with pre-treatment process to titanium electrodes, the oxidation process is still possible since oxygen penetrates the lead dioxide layers and reaches the substrate surface to form an oxide layer[72].

Table (3) shows plating experiments on vitreous carbon and gold disc electrodes from solution of 0.4 mM Pb(II) in methanesulfonic acid with lignin sulfonate.

Electrode	**J / mA cm^{-2}**	**Remarks**
Vitreous carbon	1 60 min	Thin lead dioxide deposit. Some of the deposit is adhered to the surface and some went off with the adhesive tape.
Vitreous carbon	8 45 min	Lead dioxide deposited on the surface. Shiny, brittle and cracked. No adhesion except on the edges by means of mechanical adhesion. There is a gap between the deposit and the surface. A lot of small gas bubbles are covering the lead dioxide surface.
Au	1 60 min	Lead dioxide deposited evenly on the surface. No gas bubbles are seen on the surface. The adhesion is very poor and the deposit fall off the electrode during washing.
Au	8 45 min	Lead dioxide deposited on the electrode with some gas bubbles covering the surface. Shine and brittle. Adhesion is poor but better than the above experiment.

RDE at 200 rpm and room temp.

Table (3) lead dioxide plating on vitreous carbon and gold electrodes from 0.4 Pb(II) in 2 M methanesulfonic acid solution + 1 g/l lignin sulfonate.

Clearly seen from table (3), that lead dioxide deposits are associated with gas bubbles covering the surface due to the presence of lignin sulfonate. The adhesion is poor in both cases except for very low current densities where the adhesion can be noticed. Lead dioxide adhere to the edges of the electrode which suggests that rough surfaces may improve the adhesion.

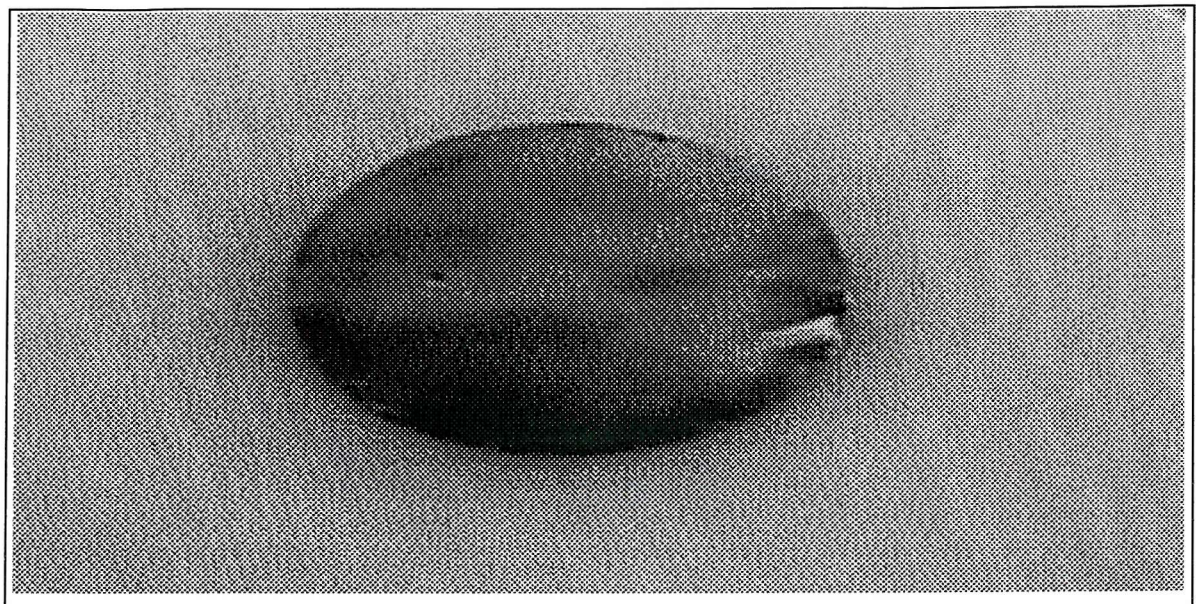

Figure (33) PbO_2 deposited on vitreous carbon rotating disc electrode (0.126 cm^2) from 0.4 M Pb(II) in 2 M CH_3SO_3H acid solution at a rotation speed of 200 rpm. Current density is 32 mA cm^{-2}.

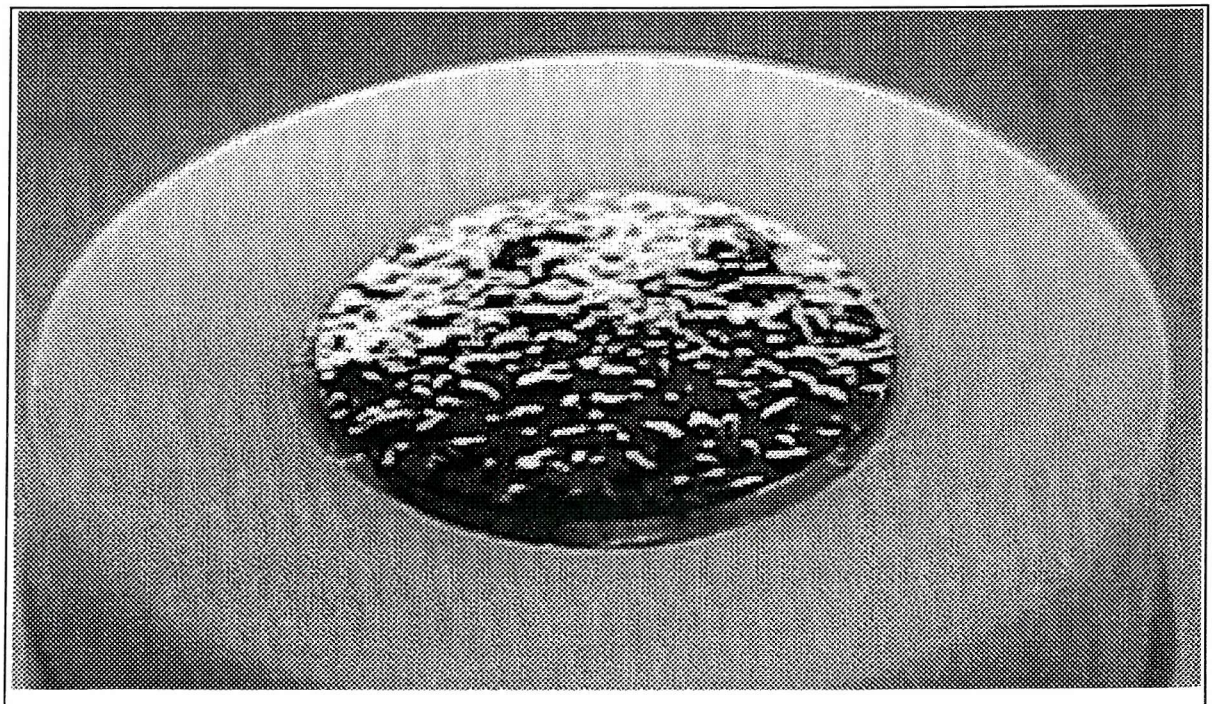

Figure (34) PbO_2 deposited on nickel rotating disc electrode (0.2 cm^2) from 0.4 M Pb(II) in 2 M CH_3SO_3H acid solution at a rotation speed of 200 rpm. Current density is 16 mA cm^{-2}.

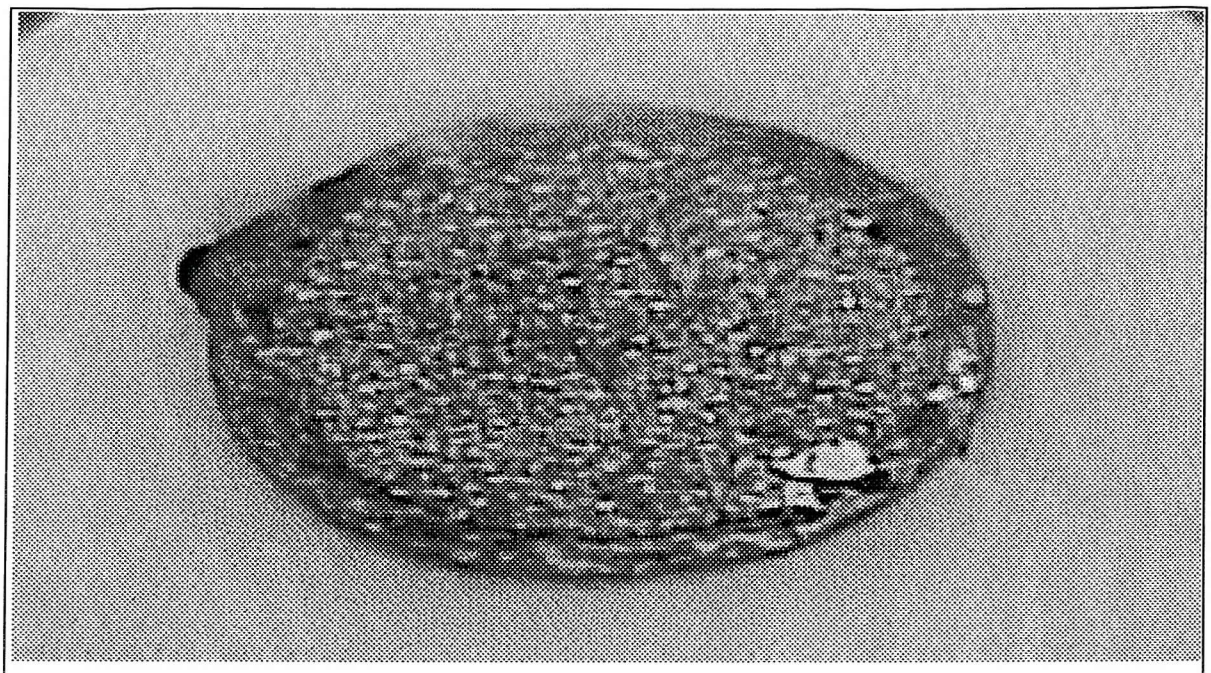

Figure (35) PbO_2 deposited on nickel rotating disc electrode (0.2 cm^2) from 0.4 M Pb(II) in 2 M CH_3SO_3H acid + 1 g/l lignin sulfonate solution at a rotation speed of 200 rpm. Current density is 8 mA cm^{-2}.

From the tables and figures above, it is seen that lead dioxide is easily deposited on vitreous carbon and gold electrodes within the conditions mentioned above. Gold however is slightly better than vitreous carbon with respect to adhesion with the deposit. However, the adhesion is not yet satisfactory.

Increase of current density increases the gas evolution and hence, the deposit becomes porous and expanded hence, a high rotation speed is needed to remove the bubbles away from the electrode or even use some appropriate wetting agents. It is possible also to try other additives instead of lignin sulfonate that do not create foam in the solution. The gas bubbles couple with the deposit and separate the deposit from the substrate material.

Chapter (V)

Conclusion

In this thesis, a preliminary study of the electrode reactions in a novel battery for load levelling applications is reported. The negative electrode involves the deposition and dissolution of lead from aqueous methanesulfonic acid, solutions where lead (II) is highly soluble. The positive electrode reaction involves the deposition and dissolution of lead dioxide from the same solution. It is envisaged that the battery would be operated as an undivided flow cell with the electrolyte stored external to the cell. During charging, the electrolyte would be depleted in lead (II) and the solution would become more acidic. At the same time, lead metal and lead dioxide would deposit as layers on inert electrodes; clearly, one requirement is that thick, uniform and adherent deposits are formed on both electrodes. During discharge, the reverse chemistry should occur and a further requirement for a successful battery is that the battery may be cycled many times without significant decay in performance.

In this initial stage in the battery development, the work has focused on defining conditions where the electrode reactions occur at high rate without significant overpotentials and commencing the study of the deposit properties/morphology. Hence, voltammetry has been used to study the electrode reactions under a range of conditions and thick layers have been deposited and studied.

Carbon and nickel have been identified as possible substrates for the negative electrode. Voltammetry at both stationary and rotating electrodes demonstrated that in aqueous methanesulfonic acid the Pb/Pb(II) couple has relatively straightforward characteristics. With a solution containing 0.4 M Pb(II) in 2 M methanesulfonic acid, the equilibrium potential for the couple is $\sim$ - 0.45 V vs SCE for a solution and it is possible to both deposit and dissolve lead at very high rates (> 100 mA cm^{-2}) with very small overpotentials. Moreover, there are no significant competing electrode reactions. This indicates that the couple has great promise for application in the battery.

When electroplating experiments were carried out it became clear that in the absence of an additive, the deposit quality was poor. The coatings were not uniform and they peeled off the substrate. After examining the literature, lignin sulfonate was selected as an additive and, fortunately, this additive was found to improve substantially the quality of the deposits. Indeed, good quality deposits could be achieved with a current density of 256 mA cm^{-2} with additive concentrations of below 1 g l^{-1}. The layers consist of overlapping, small crystallites and the layers > 10 μm thick appeared uniform and free from dendrites. The lignin sulfonate was stable and further voltammetry showed that although the lignin sulfonate slowed the kinetics of the Pb/Pb(II) couple, the changes were relatively small.

The chemistry at the positive electrode is more complex. Voltammetry showed that it was possible to deposit and redissolve lead dioxide at high rates (again, > 100 mA cm^{-2}) from 0.4 M Pb(II) in 2 M methanesulfonic acid. The equilibrium potential is ~ + 1.45 V vs SCE but there is an overpotential associated with both deposition and dissolution. The deposition process is complicated by oxygen evolution that occurs on the PbO_2 and minimising this process requires careful control of the conditions. Dissolution is complicated by the formation of some solid Pb(II) species on the substrate surface that dissolves into the acid only slowly. Even so, the charge ratio during cyclic voltammetry can approach 100 % and this is promising for further work. The presence of lignin sulfonate had only a small influence on the positive electrode and certainly did not appear to oxidise on the electrode.

Attempts to prepare satisfactory thick lead dioxide layers were not entirely successful. The deposits appeared fragile and poorly adherent to the substrate. Gold was the best substrate but data was also obtained for carbon. This is an area requiring further development.

Overall, this preliminary study has not identified any insurmountable problems with the development of a battery although further work is necessary to improve the control of the positive electrode chemistry. It is also clearly essential to set up a flow

cell and to examine the electrode reactions in conditions that relate more closely to a battery environment. It would also be interesting to extend the study to other additives.

References

1. D. Pletcher, F. C. Walsh, *Industrial Electrochemistry.* 2nd edition (1990), Chapman and Hall, London
2. V. S. Bagotzky, A. M. Skundin, *Chemical Power Sources*, 1st edition (1980), Academic Press Inc., London Ltd.
3. S. Male, P. Mitchell, *An introduction to the Regenesys^R energy storage system*, paper presented at the Royal Institute of Great Britain (2000)1
4. A Price, G. Thijssen, P. Symons, Electricity Storage, A Solution in Network Operation, paper presented at *Distributech Europe* (2000).
5. F. Beck, P. Ruetschi, *Electrochim. Acta.*, **45** (2000) 2467
6. H. Bode, *Lead-Acid Batteries*, John Wiley & Sons (1977)
7. J. Burbank, A. C. Simon, E. Willihnganz, *Advances in Electrochemistry and Electrochemical Engineering*, P. Delahay, C.W. Tobias, (ed.), Willy Interscience, New York, Vol. **8** (1971) 157 .
8. S. M Caulder, A. C. Simon, *Materials for advanced Batteries*, D. W Murphy, H. Broadhead, (ed.), Plenum, New York, (1980) 199
9. R. P. Clark, J. L. Chamberlin, H. J. Saxton, P. C. Symons, *Power Sources*, **9,** J. Thompson, (ed.), Academic Press, New York, (1983) 271
10. H. Binder, R. Knodler, A. Kohling, G. Sandstede, G. Walter, Power Sources, **6** , D. H. Collins (ed.) (1976) 643.
11. C. Menictas, D. R. Hong, Z. H. Yan, J. Wilson, M. Kazacos, M. Skyllas-Kazacos, *Status of the Vanadium Redox Battery Development Program*, paper downloaded at The Vanadium Redox Battery Web site; http://www.ceic.unsw.edu.au/centers/vrb/ (1998).
12. M. Skyllas-Kazacos, C. Menictas, The Vanadium Redox Battery for Emergency Back-Up Applications, paper downloaded at The Vanadium Redox Battery Web site; http://www.ceic.unsw.edu.au/centers/vrb/ (1998).
13. A. Czerwinski, M. Zelazowska, *J. Electroanal. Chem.*, **410** (1996) 55

14. J. Wang, *Electrochim. Acta.*, **26** (1981) 1721
15. P. Faber, *Power Sources*, **6**, J. Thompson, (ed.), Academic Press, New York, (1976) 45
16. N. E. Bagshaw, *Power Sources*, **7,** J. Thompson, (ed.), Academic Press, New York, (1979) 677
17. M. D. Gernon, T. Buszta, P. Janney, Personal communication.
18. W. J. Tuszynski, *Special. Chem.*, **9** (1989) 409.
19. C. Rosenstien, *Met. Finish.*, **88** (1990) 17.
20. J. Horkans, *IBM J RES DEV* **42** (1998) 621.
21. Printed Wiring Board Case Study 3, *Design For The Environment*, EPA USA, (1996)
22. Southampton Electrochemistry Group, *Instrumental Methods in Electrochemistry*, 1st edition (1985), Ellis Horwood Ltd., Chichester
23. E. B Budevski, *Comprehensive Treatise of Electrochemistry*, 7, B.E. Conway, J. O'M. Bockris, E. Yeager, S. U. M. Khan, R. E. White, (ed.), Plenum, New York, (1983) 399.
24. M. Fleischmann, H. R. Thirsk, *Advances in Electrochemistry and Electrochemical Engineering*, P. Delahay, C.W. Tobias, (ed.), Willy Interscience, New York, Vol. **3** (1963) 123
25. J. O'M. Bockris, A. Danjanovics, *Modern Aspects of Electrochemistry*, J.O'M. Bockris, B.E. Conway, (ed.), Butterworth, London, **3** (1964) 224.
26. J. O'M. Bockris, G. A. Razumney, *Fundamental Aspects of electrocrystallisation*, Plenum, New York, (1967)
27. A. R. Despic, *Comprehensive Treatise of Electrochemistry*, 7, B.E. Conway, J. O'M. Bockris, E. Yeager, S. U.M. Khan, R. E. White, (ed.), Plenum, New York, (1983) 451
28. D. Pletcher, *A First Course in Electrode Process*, 1st edition (1991), The Electrochemical Consultancy, Romsey
29. C. Brett, O. Brett, *Electrochemistry Principles, Methods and Applications* (1993), Oxford University Press , Oxford

30. Gonzalez-Garcia, F. Gallud, J. Iniesta, V. Montiel, A Aldaz, A. Lasia, *J. Electrochem. Soc.*, **147** (2000) 2969

31. F. A. Lowenheim - *Modern Electroplating*, 3rd edition, Wiley Interscinece, New York, (1974)

32. C. J Raub,- *Comprehensive Treatise of electrochemistry,* **2**, J. O'M Bockris, B. E. Conway, E. Yeager, R. E. White (eds.), Plenum Press, New York, (1981) 381

33. D. A. Vermilyea, *Advances in Electrochemistry and Electrochemical Engineering*, P. Delahay, C.W. Tobias, (ed.), Willy Interscience, New York, Vol. **3** (1963) 211.

34. *Electrodes of Conductive Metallic Oxides, Part A.* S. Trasatti, (ed.), Elesevier, Amsterdam, (1980).

35. W. C. Wake, *Adhesion and the Formulation of Adhesives*, Applied Science Publitiers Limited, London, (1976)

36. A. C. Ramamurthy, T. Kuwana, *J. Electroanal. Chem.*, 135, (1982) 243

37. J. A. Gonzalez-Dominguez, E. Peters, D. B. Dreisinger, *J. Appl. Electrochem.* **21** (1991) 189

38. L. Muresan, L. Oniciu, M. Froment, G. Maurin, *Electrochem. Acta.*, **37** (1992) 2249

39. T. M. Tam, *J. Electrochem. Soc.*, **133** (1986) 1792.

40. J. A. Bard, (ed.) *Encyclopaedia of Electrochemistry. of the Elements*, Marcel Dekker, Inc. New York, **1** (1973) 235

41. I. A. Carlos, M. A. Malaquias, M. M. Oizumi, T. T. Matsuo, *J. Power Sources*, **92** (2001) 56.

42. L. Ghergari, L. Oniciu, L. Muresan, A. Pantea, V.A. Topan, D. Ghertoiu, *J. Electroanal. Chem.*, **313** (1991) 303.

43. I. Petersson, E. Ahlberg, B. Berghult, *Journal of Power sources*, **76** (1998) 98

44. H. Chang, D.C. Johnson, *J. Electrochem. Soc.*, **136** (1989) 17

45. I. H. Yeo, Y. S. Lee, D. C. Johnson, *Electrochim Acta,* **37** (1992) 1811

46. H. Chang, D.C. Johnson, *J. Electrochem. Soc.*, **136** (1989) 23

47. H. Chang, D. C. Johnson, *J. Electrochem. Soc.*, **137** (1990) 3108

48. L. A. Larew, J. S. Gordon, Y. L. Hsiao, D. C. Johnson, *J. Electrochem. Soc.*, **137** (1990) 3071

49. J. Feng, D. C. Johnson, *J. Electrochem. Soc.*, **138** (1991) 3328

50. J. Feng, D. C. Johnson, *J. Appl. Electrochem.*, **20** (1990) 116

51. D. C. Johnson, H. Chang, J. Feng, W. Wang, *Electrochemistry for a Cleaner Environment*, D. Genders, N. Weinberg, (ed.), Electrosynthesis Company, New York, (1992) 334

52. J. P. Carr, N. A. Hampson, *Chem. Rev.*, **72** (1972) 679

53. J. Lee, H. Varela, S. Uhm, Y. Tak, *Electrochem. Commun.*, **2** (2000) 646

54. *The Electrochemistry of Lead*, A.T. Kuhn, (ed.), Academic Press, London (1979).

55. E. Herron, D. Pletcher, F. C. Walsh, *J. Electroanal. Chem.*, **332** (1992) 183..

56. A. B. Velichenko, D. V. Girenko, S. V. Kovalev, F. I. Danilov, *Russian Journal of Electrochemistry*, **35** (1999) 1250

57. S. A. Campbell, L. M. Peter, *J. of Electroanal. Chem.*, **306** (1991) 185

58. A. Brenner, Electrodeposition of Alloys Principles and practice, Acadimic Press, New York, (1963)

59. *Canning Handbook of Electroplating*, 21st edition, W. Canning & Co. Ltd., Birmingham (1970)

60. T. C. Wen, M. G. Wei, K. L. Lin, *J. Electrochem. Soc.*, **137** (1990) 2700

61. C. N. Ho, B. J. Hwang, *Electrochim Acta,* **38** (1993) 2749

62. L. Oniciu, L. Muresan, *J. Appl. Electrochem.*, **21** (1991)

63. D. P. Woodruff, *The Solid-Liquid Interface*, Cambridge University Press, London, (1973)

64. E. C. Potter, *Electrochemistry Principles and applications*, Cleaver-Hume Press Ltd., London, (1956)

65. M. G. Semeneko, *Russian Journal of Electrochemistry*, **35** (1999) 1276.

66. H. Reid, W. Goldie, *Gold Plating Technology*, Electrochemical Publications Ltd., Scotland, (1974) 422

67. I. Peterson, E. Ahlberg, *J. of Electroanal. Chem.*, **485** (2000) 166.

68. L. Muresan, L. Oniciu, R. Wiart, *J. Appl. Electrochem.*, **23** (1993) 66

69. M. D. Capelato, J. A. Nobrega, E. F. A. Neves, *J. Appl. Electrochem.*, **25** (1995) 408

70. Gaur, H. S. Srinivasan, *British Corrosion Journal*, **34** (1999) 63

71. L. Muresan, L. Oniciu, R. Wiart, *J. Appl. Electrochem.*, **24** (1994) 332

72. N. Munichandraiah, S. Sathyanarayana, *J. Appl. Electrochem.*, **17** (1987) 22